March 1993
(Distributed: August. 1993)

ANNUAL TECHNICAL REPORT

to

US AIR FORCE OFFICE OF SCIENTIFIC RESEARCH

110 Duncan Avenue, Suite B115
Bolling Air Force Base
Washington DC 20332-0001

AFOSR Grant No. 91-0170

TRANSPORT PHENOMENA AND INTERFACIAL KINETICS IN MULTIPHASE COMBUSTION SYSTEMS

Principal Investigator: **Daniel E. Rosner**

Period Covered: 15 February 1992 to 14 February 1993

Yale University
High Temperature Chemical Reaction Engineering Laboratory
Department of Chemical Engineering
PO Box 2159 YS, New Haven CT 06520 USA

REPORT DOCUMENTATION PAGE

Form Approved
OMB No. 0704-0188

1. AGENCY USE ONLY (Leave blank)	2. REPORT DATE	3. REPORT TYPE AND DATES COVERED
	MARCH 1993	Annual Tech. Rep. 2/15/92 - 2/14/93

4. TITLE AND SUBTITLE

TRANSPORT PHENOMENA AND INTERFACIAL KINETICS IN MULTIPHASE COMBUSTION SYSTEMS

5. FUNDING NUMBERS

PE - 6110ZF
PR - 2308
SA - BS
G - 91-0170 (AFOSR)

6. AUTHOR(S)

Principal Investigator: Daniel E. Rosner

7. PERFORMING ORGANIZATION NAME(S) AND ADDRESS(ES)

HIGH TEMPERATURE CHEMICAL REACTION
ENGINEERING LABORATORY
YALE UNIVERSITY
BOX 2159, YALE STATION
NEW HAVEN, CONNECTICUT 06520 U.S.A.

8. PERFORMING ORGANIZATION REPORT NUMBER

9. SPONSORING/MONITORING AGENCY NAME(S) AND ADDRESS(ES)

AFOSR/NA
Building 410
Bolling AFB DC 20332-6448

10. SPONSORING/MONITORING AGENCY REPORT NUMBER

11. SUPPLEMENTARY NOTES

12a. DISTRIBUTION/AVAILABILITY STATEMENT

Approved for public release; distribution is unlimited

12b. DISTRIBUTION CODE

13. ABSTRACT (Maximum 200 words)

This *annual technical report* summarizes Yale High Temperature Chemical Reaction Engineering Laboratory research activities (under Grant AFOSR 91-0170) for the one-year period ending 14 February 1993. Among our research *results* described in detail in the cited references (Section 5), perhaps the most noteworthy are the development/reporting of:

R1 rational methods to predict the *accessible surface area* of aggregated 'soot' particles in high pressure combustion gases

R2 experimental inference of particle thermophoretic diffusivities for titania aggregates in laminar counterflow laminar diffusion flames; consequences of particle thermophoresis for flame radiation , flame synthesis, and particle-based diagnostics

R3 quantitative methods for predicting/correlating the effects vapor phase chemical reactions on the rate and quality of vapor-deposited metal oxide thin films

Eight presentations and 4 publications have resulted from this research program. Copies of the principal reprints appearing during this period are included in the Appendices (Section 6) of this report.

14. SUBJECT TERMS

Key Words: Soot, aggregated particles, mass transport, thermophoresis, Brownian diffusion, chemical vapor deposition

15. NUMBER OF PAGES 55

16. PRICE CODE

17. SECURITY CLASSIFICATION OF REPORT	18. SECURITY CLASSIFICATION OF THIS PAGE	19. SECURITY CLASSIFICATION OF ABSTRACT	20. LIMITATION OF ABSTRACT
Unclassified	Unclassified	Unclassified	UL

TRANSPORT PHENOMENA AND INTERFACIAL KINETICS IN MULTIPHASE COMBUSTION SYSTEMS

1. INTRODUCTION

The performance of ramjets burning slurry fuels (leading to condensed oxide aerosols and liquid film deposits), gas turbine engines in dusty atmospheres, or when using fuels from non-traditional sources, depends upon the formation and transport of small particles across non-isothermal combustion gas boundary layers (BLs). Even airbreathing engines burning "clean" hydrocarbon fuels can experience *soot* formation/deposition problems (*e.g.*, combustor liner burnout, accelerated turbine blade erosion and "hot" corrosion). Moreover, particle formation and transport are important in many chemical reactors used to synthesize or process aerospace materials (turbine blade coatings, optical waveguides, ceramic precursor powders,...). Accordingly, our research is directed toward providing chemical propulsion systems engineers and materials-oriented engineers with new techniques and quantitative information on important particle- and vapor-mass transport mechanisms and rates.

The purpose of this report is to summarize our research methods and accomplishments under AFOSR Grant 91-0170 (Technical Monitor: J.M.Tishkoff) during the 1-year period: 15 February '92-14 February '93. Readers interested in greater detail than contained in Section 2 are advised to consult the published papers explicitly cited in Sections 2 and 5. Copies of any of these published papers (Section 5.2) or preprints (Section 5.3) can be obtained by writing to the PI: Prof. Daniel E. Rosner, at the Department of Chemical Engineering, Yale University, Box 2159 Yale Station, New Haven CT 06520-2159 USA. Comments on, or examples of, the applications of our research (Section 3.4) will be especially welcome.

An interactive experimental/theoretical approach has been used to gain understanding of performance-limiting chemical-, and mass/energy transfer-phenomena at or near interfaces. This included the development and exploitation of seeded laboratory burners (Section 2.1), and new optical diagnostic techniques (Section 2.2, Fig. 5). Resulting experimental rate data (Fig.8), together with the predictions of asymptotic theories (Section 2), were used as the basis for proposing and verifying simple viewpoints and effective engineering correlations for future design/optimization studies.

2. RESEARCH ACCOMPLISHMENTS

Most of the results we have obtained under Grant AFOSR 91-0170 during 1992 can be divided into the subsections below:

2.1. TRANSPORT AND STABILITY OF AGGREGATED PARTICLES: THEORY

The ability to reliably predict the transport properties and stability of *aggregated* flame-generated *particles* (carbonaceous soot, Al_2O_3, SiO_2,...) is important to many technologies, including chemical propulsion and refractory materials fabrication.

The *Brownian diffusion-*, inertial-, and optical-properties of *aggregated* particles, as formed in sooting diffusion flames, are quite *sensitive* to size (*e.g.* number N of "primary" particles; see Fig. 1) and morphology (geometrical arrangement of the primary particles). Needed are methods to anticipate coagulation and deposition rates of suspended populations of such particles, especially in combustion systems. Toward this end we have recently devloped improved and efficient methods for predicting the Stokes drag of large 'fractal' aggregates *via* a spatially variable porous sphere model (Figs. 1, 2). Using the Stokes-Einstein equation, the results of Fig. 2 can now be used to predict the Brownian diffusivity of such aggregates in the high pressure (near continuum-) limit (proportional to the product of the reciprocal of the ordinate of Fig. 2 and N^{-1/D_f}). This approach is currently being extended to predict the *thermophoretic diffusivity* of such aggregates, an important quantity we have recently found to be much less sensitive to size and morphology than the translational Brownian diffusivity (Rosner *et.al.* 1992). Indeed, this provides the theoretical basis for the *thermophoretic sampling* technique being employed in our current experimental studies (Section 2.2). These new methods/results, together with recent

results on the *spread* of aggregate sizes in coagulating populations, will be used to predict wall *capture rates* by the mechanisms of convective-diffusion, turbulent eddy-impaction, and thermophoresis (Rosner, Tassopoulos and Tandon,1993). Also needed are methods to predict interactions between aggregates and their surrounding *vapor* environment---interactions which can lead to primary particle growth, or burn-out. Toward this end we have also developed new and efficient methods to predict the "accessible surface area" of aggregates (expressed as a fraction , η, of the true surface area in Fig. 3), including its dependence on size (N), structure (fractal dimension, D_f), probing molecule reaction probability α, and pressure level (*via* Knudsen number based on primary particle diameter). Figure 4 shows the test of our "effective Damkohler number" correlation approach when compared with exact results of many numerical integrations (Rosner and Tandon,1993).

Also recently initiated are studies of the *restructuring kinetics* of aggregates — *ie.* those factors which determine the observed size of the apparent "primary particles" comprising soot particles, and the "collapse" of surface area observed in some high temperature systems (Cohen and Rosner,1993).

2.2. FORMATION, TRANSPORT AND STABILITY OF COMBUSTION-GENERATED PARTICLES: LAMINAR COUNTERFLOW DIFFUSION FLAME EXPERIMENTS

A manuscript describing our measurements of the *thermophoretic diffusivity* of flame-generated submicron "soot" particles using a ($TiCl_4$(g)-)seeded low strain-rate counterflow laminar diffusion flame (CDF-) technique has just appeared (Gomez and Rosner, 1993). A knowledge of the relative positions of the gas and particle stagnation planes and the associated chemical environments, can be used to control the composition and morphology of flame-synthesized particles. These factors should also influence particle production and *radiation* from *turbulent* non-premixed "sooting" flames, as discussed further in Gomez and Rosner, 1993.

To extend this work to obtain fundamental information on nucleation, growth and aggregate restructuring, during this past year we have developed an improved "slot-type" burner (Fig. 5) and introduced instruments to carry out *in situ* measurements of particle Brownian motion ("dynamic light scattering"). We have also developed a thermophoretic sampler (Fig. 6) to extract aggregates from various positions in the seeded-CDF for morphological analysis using electron microscope images. Aggregate data obtained from CH_4 flames seeded with titanium tetra-isopropoxide (TTIP-) vapor are now being obtained and will be analyzed using the theoretical methods briefly outlined in Sections 2.1, 2.3.

2.3. MULTIPHASE BOUNDARY LAYER THEORY: NUCLEATION, GROWTH, THERMOPHORESIS AND INERTIA

Our *IJHMT J* paper giving comprehensive results of Seeded micro-combustor experiments, and ancillary theoretical calculations on the interesting competition between particle *inertia* and particle *thermophoresis* for the case of laminar gaseous boundary layers on surfaces with streamwise curvature (*e.g.*, turbine blades), should appear this Fall (Konstandopoulos and Rosner, 1993).

We are now carrying out theoretical studies on the structure of thin reaction-nucleation-coagulation 'sublayers' within laminar boundary layers, including stagnation flows similar to those achieved in our counterflow burner (Fig. 5) and CVD-impingement reactor (see Fig. 7 below).

An account of our recent studies of the *unusual population dynamics* of coagulating absorbing-emitting particles in strong *radiation fields* is about to appear in *Aerosol Sci. Tech.* (Mackowski *et.al.*, 1993). For a useful overview of our recent work on these and other effects of energy transfer on suspended particle dynamics, see Rosner, *et. al.*, 1992, which was included as an Appendix to our last OSR Annual Report.

2.4. KINETICS AND MORPHOLOGY OF CVD-MATERIALS IN MULTI-PHASE ENVIRONMENTS

A small impinging jet (stagnation flow) reactor (Fig. 7) is being used to study the chemical vapor deposition (CVD-)-rates of refractory layers on inductively (over-)heated substrates (Collins, Rosner and Castillo,1992,1993). These measurements, initiated with the co-sponsorship of NASA-Lewis Labs, are being used to understand deposition rates and associated

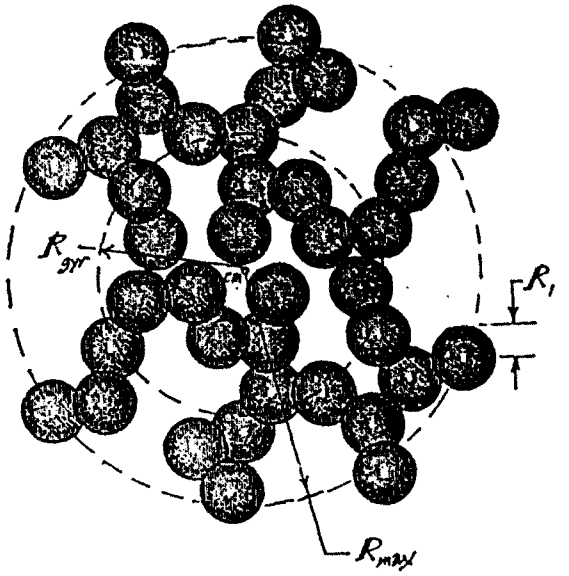

Fig.1 "Porous sphere" model of large fractal aggregate suspended in a background gas; basis for the calculation of translational and rotational Brownian diffusion coefficients, thermophoretic diffusivity, "stopping time", accessible area, and restructuring kinetics (after Rosner and Tandon, 1993, Rosner, Cohen and Tandon, 1993)

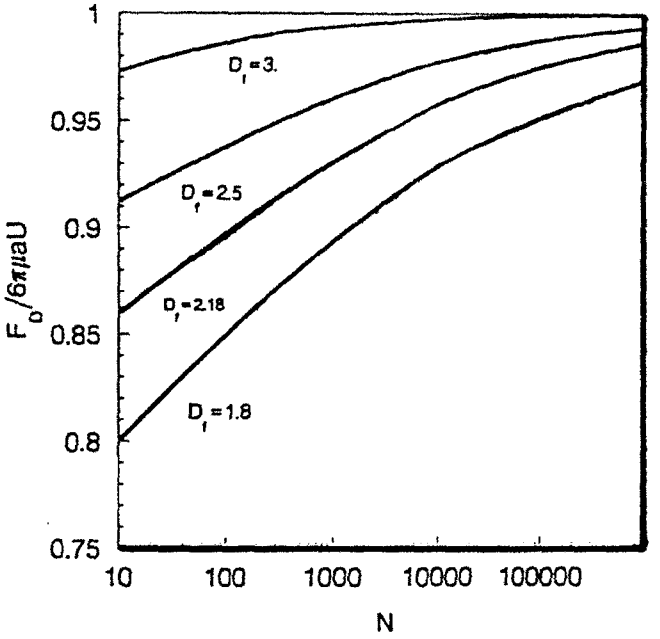

Fig. 2 Drag reduction associated with effective permeability for quasi-spherical "fractal" aggregates comprised of N primary spheres in the continuum regime ($a = R_{max} = \{(3/2) \cdot [D_f+2)/D_f]\}^{1/2} R_{gyration}$) (after Rosner and Tandon, 1993)

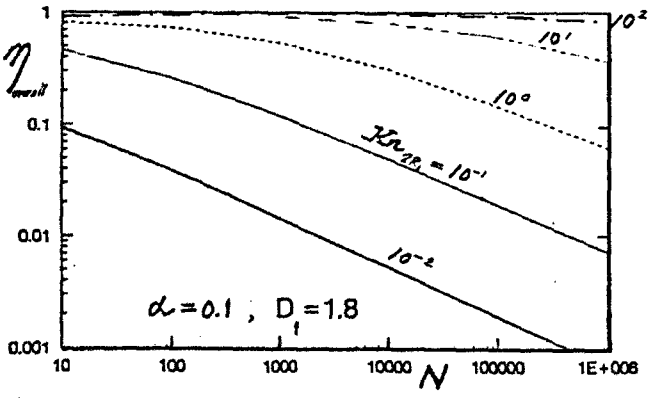

Fig. 3 Pressure dependence (*via* the Knudsen number based on primary sphere diameter) of the *accessible surface area* of large "open" (D_f=1.8) aggregates; reaction probability, α, of probing molecule 0.1; (after Rosner and Tandon, 1993)

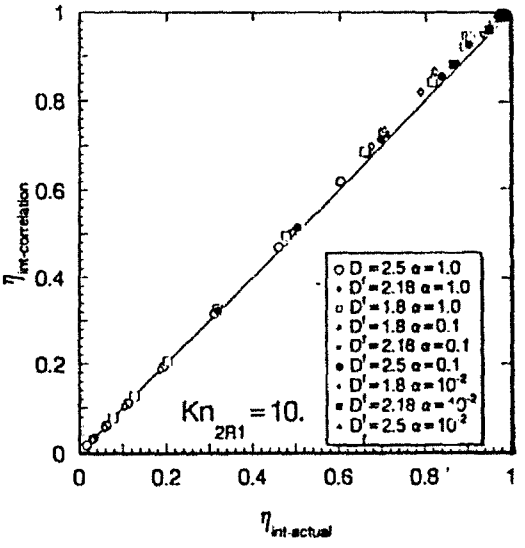

Fig. 4 Test of an "effective Damköhler number" correlation for the *accessible surface area* of a large fractal aggregate (after Rosner and Tandon,1993); success makes possible the efficient calculation of the accessible area evolution of polydispersed *populations* of aggregated particles in combustion gases.

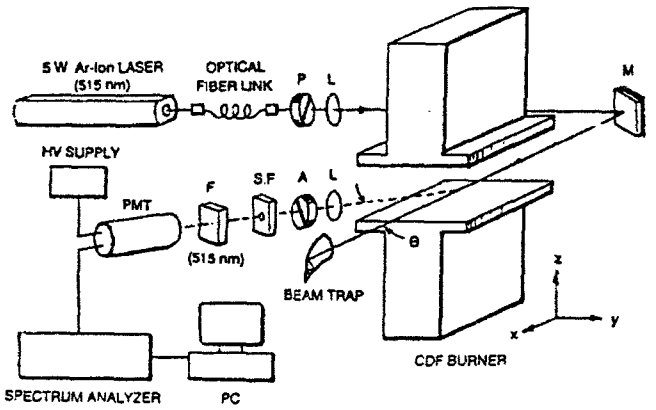

Fig.5 "Slot"-type counterflow diffusion flame (CDF-) burner set-up for *in situ* and extractive experimental studies of the nucleation, growth, transport and restructuring of aggregates in flames (after Albagli and Rosner, 1993; see, also,Gomez and Rosner, 1993)

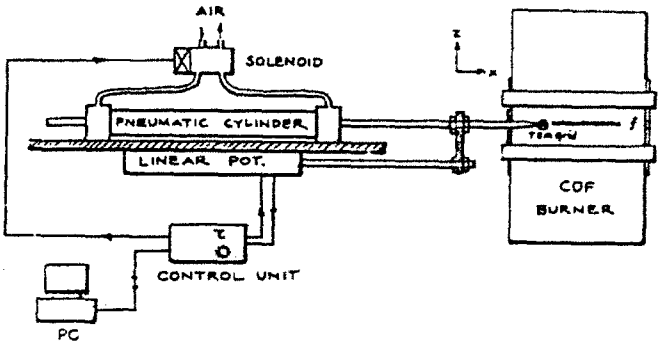

Fig.6 Probe for rapid local extraction (exploiting thermophoretic transport) of aggregates formed in a laminar counterflow diffusion flame (after Albagli and Rosner,1993; see, also: Rosner *et.al.* 1991)

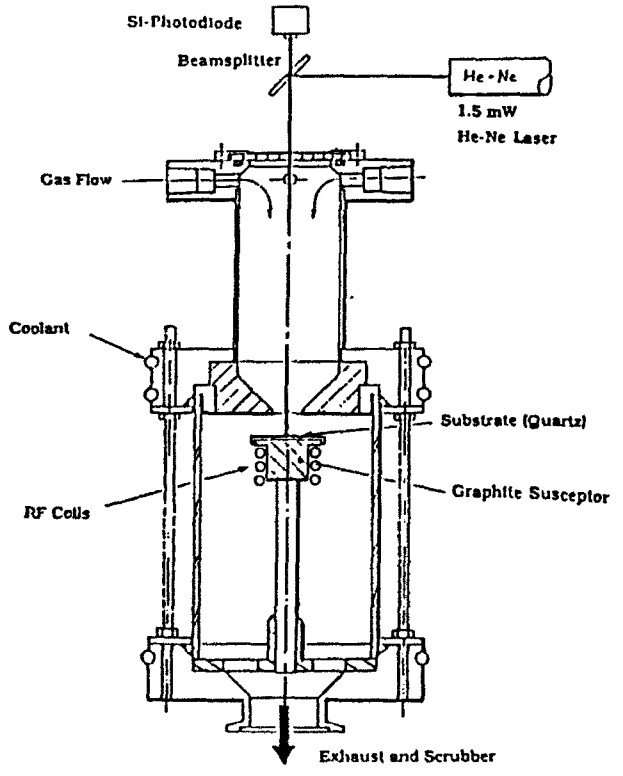

Fig. 7 Axisymmetric impinging jet CVD-reactor with inductively heated "pedestal" (after Rosner, Collins and Castillo, 1993)

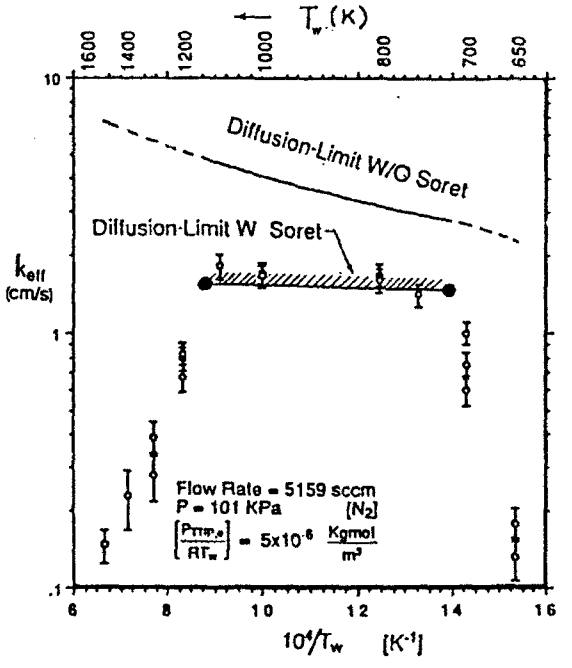

Fig.8 TiO_2(s) deposition rate data (reported as an apparent first order heterogeneous rate constant) from TTIP/O_2/N_2 mainstream showing calculated limiting surface temperatures and associated deposition rates (after Rosner, Collins and Castillo, 1993)

sponsorship of NASA-Lewis Labs, are being used to understand deposition rates and associated deposit microstructures observed in highly non-isothermal, often particle-containing local CVD environments. Figure 8 shows (logarithmic ordinate) our apparent first order deposition rate constants *vs.* reciprocal surface temperature for TiO_2(s) obtained from TTIP(g). The dark points show our predicted surface temperatures for the onset of vapor phase reactions ("vapor phase ignition"(VPI)) within the boundary layer and the onset of vapor phase diffusion control of the heterogeneous reaction(Castillo and Rosner,1993).

****

In our OSR-sponsored Yale HTCRE Lab research during the past year, briefly reviewed here, we have shown that new methods for rapidly measuring particle transport rates, combined with recent advances in boundary layer theory, provide useful means to identify and incorporate important, but previously neglected, mass transport phenomena in many propulsion engineering and materials engineering design/optimization calculations.

Despite the formidable complexities to be overcome in the design and operation of air-breathing propulsion power plants utilizing a broad spectrum energetic fuels these particular techniques and results are indicative of the potentially useful simplifications and generalizations which have emerged from our present fundamental AFOSR-funded research studies of combustion-generated particle transport mechanisms. It is hoped that this Annual Report and its supporting (cited) papers will facilitate the refinement and/or incorporation of some of the present ideas into engineering design procedures of much greater generality and reliability. This work has already helped identify new directions where research results would have a significant impact on engineering practice in both the defense and civilian sectors of the US economy (Section 3.4).

3. ADMINISTRATIVE INFORMATION: PERSONNEL, PRESENTATIONS, APPLICATIONS, "COUPLING' ACTIVITIES

The following sections summarize some pertinent 'non-technical' facets of the abovementioned Yale HTCRE Lab/AFOSR research program:

3.1 Personnel

The present results (Sections 2 and 5) are due to the contributions of the individuals listed in Table 3.1-1, which also indicates the role of each researcher and the relevant time interval of the activity. It will be noted that, in addition to the results themselves, this program has simultaneously contributed to the research training of a number of students and recent PhDs, who will now be in an excellent position to make future contributions to technologies oriented toward air-breathing chemical propulsion, and high-tech materials processing.

Table 3.1-1 Summary of *Research Participants*[a] on AFOSR Grant :
TRANSPORT PHENOMENA AND INTERFACIAL KINETICS IN MULTIPHASE COMBUSTION SYSTEMS

Name	Status[a]	Date(s)	Principal Research Activity[b]
Albagli, D.	PDRA	4/92-	particle production in CDFs
Cohen, R. D.	VS	1,2/93	aggregate restructuring theory
Collins, J.	GRA	'92,'93	CVD of ceramic coatings
Gomez, A.	Asst.Prof.	'92	Ms. on particle transp. props.(CDFs)
Kho,T.	GRA	'92,'93	chemical vapor infiltration (coatings)
Papadopoulos, D	GRA	'92	transport phenomena in CVD reactors
Rosner, D.E.	PI	'92-'93	program direction-dep. theory/exp
Silverman, I.	PDRA	'92-'93	spray evap/comb. at high pressures
Tandon, P.	GRA	'92-'93	transport phenomena in BLs and CDFs

[a] PDRA=Post-doctoral Research Asst GRA= Graduate Research Assistant
PI = Principal Investigator VS = Visiting Scholar

[b] See Section 5 for specific references cited in text (Section 2)

3.2 Cooperation with US Industry

The research summarized here was supported by AFOSR under Grant 91-0170 (2/15/92-2/14/93). The Yale HTCRE Laboratory has also been the beneficiary of continuing smaller grants from U.S. industrial corporations, including GE-Schenectady, DuPont, and Shell as well as the feedback and advice of principal scientists/engineers from each of these corporations and Combustion Engineering-ABB and Textron. We appreciate this level of collaboration, and expect that it will accelerate inevitable applications of our results in areas relevant to their technological objectives (see, also, Section 3.4, below).

3.3 Presentations and Research Training

Apart from the publications itemized in Section 5 and our verbal presentation (of progress) at the regular AFOSR Contractors Meeting (6/18/92, La Jolla), our results have also been presented at annual or topical conferences of the following professional organizations:

Int. Fine Particle Res. Inst. (6/2/92; Harrogate England))
AIChE (11/3/92; Miami FL)

In addition, during the period: 2/15/92 -2/14/93, the PI presented seminars at the following Universities:

U Manchester Inst.Sci.Tech. 5/28/92 Leeds 5/29/92 Penn State (7/28/92)

Brown (9/22/92) Notre Dame (10/27/92)

In all, a total of 8 external talks were given based in part on the results of this AFOSR research program.

This program involved the PhD dissertation research of two Yale graduate students (J. Collins and P. Tandon; *cf.*Table 3.1-1). Indeed, J. Collins is expected to complete his PhD degree requirements in Fall '93.

3.4 Some Known *Applications* of Yale-HTCRE Lab Research Results

It has been particularly gratifying to see direct applications of some of this generic AFOSR-supported particle and vapor mass transfer research in more applications-oriented investigations reported in recent years. Indeed, the writer would appreciate it if further examples known to the reader can be brought to his attention.

In the area of multicomponent vapor deposition in combustion systems additional applications of our predictive methods (for "chemically frozen" (Rosner *et.al.*, 1979) and LTCE multicomponent laminar boundary layers) continue to be made by British Coal Corporation-Power Generation Branch (I. Fantom, contact) in connection with their topping cycles which run gas turbines on the products of fluidized bed coal combustors/gasifiers. The writer has also proposed applications of our computational methods to Aerojet Propulsion Div. (D.M. Jassowski) in connection with predicting the chemical stability of iridium rocket nozzle coatings. Our Poster in the 1988 Combustion Symposium (Seattle) appears to have motivated Prof. Takeno (Nagoya) to initiate experiments using a laminar counterflow diffusion flame to estimate the thermophoretic diffusivity of LDV seed particles. Our paper on the experimental determination of smaller aggregated particle thermophoretic diffusivities using laminar CDF/LDV/Laser Light Scattering techniques is nearing completion, and will be submitted to *Combustion Science and Technology* early in our next year's program. Also, in combustion research many groups (*eg.* Dobbins *et.al.* (Brown U.), Faeth *et.al.* (U. Mich.), Katz *et al.* (J.Hopkins U.)) are now utilizing "thermophoretic sampling" techniques to exploit the size- and morphology-insensitive capture efficiency characteristics that we have proven in our AFOSR research (Section 2.1).

Explicit examples are provided in ongoing work at MIT (Walsh *et.al.* 1992), and Sandia CRF, both groups having incorporated our rational correlation of *inertial particle impaction* (*e.g.* a cylinder in cross-flow) in terms of an effective Stokes number. This PI was also pleased to confirm recent applications of our AFOSR and DOE-supported research (on the correlation of inertial impaction by cylinders in crossflow) by the National Engineering Laboratory (NEL) of Glasgow Scotland (Contact: Dr. Andrew Jenkins). NEL is apparently collaborating with

Marchwood Labs-CEGB on developing mass-transfer prediction methods applicable to waste-heat recovery systems in incinerators, as well as pulverized coal-fired boilers. These applications are somewhat similar to those reported by the Combustion Lab R&D group at MIT and Penn State U.

As mentioned last year, explicit use of our studies of self-regulated "capture" of incident impacting particles (Rosner and Nagaragan, 1987) is being made in current work on impact separators and ceramic heat exchangers for coal-fired turbine systems in high performance stationary power plants. Other potential applications arise in connection with "candle filters" used to remove fines (sorbent particles,...) upstream of the turbines. A useful summary of work in these interrelated areas (Solar Turbines, Textron Defense Systems, Hague International,...) was presented at the Engineering Foundation Conference *Inorganic Transformations and Ash Deposition During Combustion.*, the proceedings of which appeared during this past year.

Clearly, fruitful *opportunities* for the application of our recent "non-Brownian" convective mass transfer research now exist in many of the programs currently supported by the US Air Force, as well as civilian sector R&D.

4. CONCLUSIONS

In the OSR-sponsored Yale HTCRE Lab research during the period: 2/15/92-2/14/93, briefly described above, we have shown that new methods for rapidly measuring particle-mass transfer rates , combined with our recent advances in mass transport theory, provide useful means to identify and incorporate important, but previously neglected, mass transport phenomena in many propulsion engineering and materials engineering design/optimization calculations. One important class of examples involve our treatment of aggregated particle transport phenomena (Section 2.1)

Despite formidable complexities to be overcome in the design and operation of mobile and stationary power plants utilizing a broad spectrum of energetic fuels the abovementioned techniques and results (Section 2) are indicative of the potentially useful simplifications and generalizations emerging from our present fundamental AFOSR-funded research studies of combustion-generated particle transport mechanisms and interfacial reactions relevant to the synthesis of refractory materials. It is hoped that this Annual Report and its supporting papers (Section 5) will facilitate the incorporation of many of the present ideas into design and test procedures of greater generality and reliability. This work has also helped identify new directions where it is anticipated that research results will have a significant impact on future DOD and civilian sector engineering practice.

5. REFERENCES

5.1 CITED BACKGROUND PUBLICATIONS (Predecessor OSR, DOE- Grants)

Castillo, J.L., Garcia-Ybarra, P., and Rosner, D.E.,"Morphological Instability of a Thermophoretically Growing Deposit", *J. Crystal Growth* **116**, 105-126, (1992)

Eisner, A.D. and Rosner, D.E., Experimental Studies of Soot Particle Thermophoresis in Non Isothermal Combustion Gases Using Thermocouple Response Techniques", *Combustion and Flame* **61**, 153-166(1985); see, also: *J PhysicoChemical Hydrodynamics* (Pergamon) **7** , 91-100 (1986)

Rosner, D.E. and Kim,S.S., "Optical Experiments on Thermophoretically Augmented Submicron Particle Deposition From 'Dusty' High Temperature Gas Flows", *The Chemical Engrg. J.*(Elsevier) **29**,[3], 147-157 (1984)

Rosner, D.E. and Nagarajan. R.,"Toward a Mechanistic Theory of Net Deposit Growth from Ash-Laden Flowing Combustion Gases: Self-Regulated Sticking of Impacting Particles and Deposit Erosion in the Presence of Vapor 'Glue'", *Proc. 24th National Heat Transfer Conf.*, AIChE Symposium Series, Vol. **83** [257], pp. 289-296, (1987)

Rosner, D.E., Mackowski, D.W,. Tassopoulos,M., Castillo,J.L., and Garcia-Ybarra, P., "Effects of Heat Transfer on the Dynamics and Transport of Small Particles in Gases", *I/EC - Research (ACS)* **31**,760-769 (1992)

Rosner, D. E. , Chen B.K., Fryburg G.C. and Kohl F.J., Chemically Frozen Multicomponent Boundary Layer Theory of Salt and/or Ash Deposition Rates from Combustion Gases", *Combustion Science and Technology* **20**, 87-106 (1979)

Rosner, D.E., **Transport Processes in Chemically Reacting Flow Systems**, Butterworth-Heinemann, Stoneham MA, 1986; 3d Printing 1990.

Sung, C.J., Law, C.K., and Axelbaum, R.L., "Thermophoretic Effects on Seeding Particles in LDV Measurements of Flames", *Combustion Science and Technology* (submitted, 1993)

Walsh, P.M., Sarofim, A. F., and Beer, J.M., "Fouling of Convection Heat Exchangers by Lignitic Coal Ash", *Energy and Fuels* (ACS) **6** (6) 709-715 (1992)

5.2 PUBLICATIONS WHICH APPEARED* BASED IN PART ON AFOSR 91-0170

Collins, J., Rosner , D. E. and Castillo, J.L., "Onset Conditions for Gas Phase Reaction and Nucleation in the CVD of Transition Metal Oxides", *Materials Research Soc. Symposium Proceedings* Vol. **250**, MRS (Pittsburgh PA) (1992), pp. 53-58

Gomez, A., and Rosner, D.E.*, "Thermophoretic Effects on Particles in Counterflow Laminar Diffusion Flames " *Combustion Science and Technology* **89**, 335-362 (1993)

Gomez, A., Rosner, D.E. and Zvuloni, R., "Recent Studies of the Kinetics of Solid Boron Gasification by $B_2O_3(g)$ and Their Chemical Propulsion Implications", *Proc. 2d Int. Sympos. on Special Topics in Chemical Propulsion*: **Combustion of Boron-Based Solid Propellants and Solid Fuels**, (1993), pp 113-132.

Rosner, D.E., Konstandopoulos, A.G., Tassopoulos, M., and Mackowski, D.W, "Deposition Dynamics of Combustion-Generated Particles: Summary of Recent Studies of Particle Transport Mechanisms, Capture Rates, and Resulting Deposit Microstructure/Properties", *Proc. Engineering Foundation Conference*: **Inorganic Transformations and Ash Deposition During Combustion**, Engineering Foundation/ASME, New York (1992); pp. 585-606

5.3 PAPERS IN PREPARATION OR SUBMITTED FOR PUBLICATION

Albagli, D., and Rosner, D.E., "Factors Governing the Accessible Surface Area of Combustion-Generated Ultrafine Particles" (in preparation, 1993)

Cohen, R. D., and Rosner, D. E. , "Kinetics of Restructuring of Large Multiparticle Aggregates" (in preparation 1993)

Castillo, J. L. and Rosner, D.E., Role of High Activation Energy Homogeneous Chemical Reactions in Affecting CVD-Rates and Deposit Quality for Heated Surfaces", in preparation, 1993)

Konstandopoulos, A.G. and Rosner, D.E.,"Inertial Effects on Thermophoretic Transport of Small Particles to Walls With Streamwise Curvature---I. Experiment, II. Theory", Accepted 1993 *Int. J. Heat Mass Transfer* (Pergamon)

Konstandopoulos, A.G., Labowsky, M J., and Rosner, D.E., "Inertial Deposition of Particles From Potential Flows Past Cylinder Arrays", *J. Aerosol Sci* (Pergamon Press) **24** (4) 471-483 (1993)

Mackowski, D.W., Tassopoulos, M. and Rosner, D.E.,"Effect of Radiative Heat Transfer on the Coagulation Dynamics of Combustion-Generated Particles", (Accepted 1992; Revision submitted to *Aerosol Sci. Technol.(AAAR)* (1993))

*During this reporting period; Full papers are reproduced in Section 6 (with Forms 298)

Park, H.M., and Rosner, D.E., "Thermophoretically Induced Phase Separation in Highly-Loaded 'Dusty' Gas Mixtures"(Revised version of HTCRE #162, in preparation 1993)

Rosner, D. E., Collins, J. and Castillo, J.L., "Onset Conditions for Gas Phase Reactions and Particle Nucleation/Growth in CVD Boundary Layers", submitted for *Int. Conf. on CVD (XII)*, 1993.

Rosner, D.E. and Tandon, P., "Diffusion and Heterogeneous Reaction in Large Multi-particle Aggregates; Calculation and Correlation of 'Accessible' Surface Area", (accepted; to appear *AIChE J.* Winter '93-'94)

Rosner, D.E., Tassopoulos M., and Tandon, P. , "Sensitivity of Total Mass Deposition Rate and Resulting Deposit Microstructure to Morphology of Coagulation-Aged Aerosol Populations of Aggregated Primary Particles", in preparation, 1993)

Zavuloni, R., Rosner, D.E., and Gomez, A., "High Temperature Kinetics of Solid Boron Gasification By its Higher Oxide $B_2O_3(g)$: Flow Reactor Techniques, Rate Measurements and Their Chemical Implications", *J. Phys. Chem.* (to be submitted, 1993)

LIST OF ABBREVIATIONS

BL	Boundary layer	CDF	Counterflow diffusion flame
CVD	Chemical vapor deposition	CRF	Combustion Research Facility
LDV	Laser Doppler Velocimetry	LTCE	local thermochemical equilibrium
MRS	Materials Research Society	TTIP	Titanium tetra-isopropoxide

6. APPENDICES (Complete Papers Published During 2/15/92-2/14/93 Period; including Form 298 for each)

HIGH TEMPERATURE CHEMICAL REACTION ENGINEERING LABORATORY
YALE UNIVERSITY
BOX 2159, YALE STATION
NEW HAVEN, CONNECTICUT 06520 U.S.A.

REPORT DOCUMENTATION PAGE

Form Approved
OMB No. 0704-0188

1. AGENCY USE ONLY (Leave blank)	2. REPORT DATE	3. REPORT TYPE AND DATES COVERED
	1992	Reprint: Sympos. Proc.-MRS

4. TITLE AND SUBTITLE

ONSET CONDITIONS FOR GAS PHASE REACTION AND NUCLEATION IN THE CVD OF TRANSITION METAL OXIDES

5. FUNDING NUMBERS

PE - 61102F
PR - 2308
SA - BS
G - AFOSR 91-0170

6. AUTHOR(S)

J. Collins, D.E. Rosner and J. Castillo

7. PERFORMING ORGANIZATION NAME(S) AND ADDRESS(ES)

HIGH TEMPERATURE CHEMICAL REACTION ENGINEERING LABORATORY
YALE UNIVERSITY
BOX 2159, YALE STATION
NEW HAVEN, CONNECTICUT 06520 U.S.A.

8. PERFORMING ORGANIZATION REPORT NUMBER

9. SPONSORING/MONITORING AGENCY NAME(S) AND ADDRESS(ES)

AFOSR/NA
110 Duncan Avenue, Suite B115
Bolling AFB DC 20332-0001

10. SPONSORING/MONITORING AGENCY REPORT NUMBER

11. SUPPLEMENTARY NOTES

12a. DISTRIBUTION/AVAILABILITY STATEMENT

Approved for public release; distribution is unlimited

12b. DISTRIBUTION CODE

13. ABSTRACT (Maximum 200 words)

A combined experimental/theoretical study is presented of the onset conditions for gas phase reaction and particle nucleation in hot substrate/cold gas CVD of transition metal oxides. Homogeneous reaction onset conditions are predicted using a simple high activation energy reacting gas film theory. Experimental tests of the basic theory are underway using an axisymmetric impinging jet CVD reactor. No "vapor phase ignition" has yet been observed in the $TiCl_4/O_2$ system under accessible operating conditions (below substrate temperature T_w=1700 K) and further experiments are planned using more reactive feed materials. The goal of this research is to provide CVD reactor design and operation guidelines for achieving acceptable deposit microstructures at the maximum deposition rate while simultaneously avoiding homogeneous reaction/nucleation and diffusional limitations.

14. SUBJECT TERMS

chemical vapor deposition, vapor phase ignition, metal oxide films
chemical reaction engineering, convective-diffusion, Soret mass transport

15. NUMBER OF PAGES

4

16. PRICE CODE

17. SECURITY CLASSIFICATION OF REPORT	18. SECURITY CLASSIFICATION OF THIS PAGE	19. SECURITY CLASSIFICATION OF ABSTRACT	20. LIMITATION OF ABSTRACT
Unclassified	Unclassified	Unclassified	UL

MATERIALS RESEARCH SOCIETY SYMPOSIUM PROCEEDINGS VOLUME 250

Chemical Vapor Deposition of Refractory Metals and Ceramics II

Symposium held December 4-6, 1991, Boston, Massachusetts, U.S.A.

EDITORS:

Theodore M. Besmann
Oak Ridge National Laboratory, Oak Ridge, Tennessee, U.S.A.

Bernard M. Gallois
Stevens Institute of Technology, Hoboken, New Jersey, U.S.A.

James W. Warren
Composite Innovation Corporation, Woodland Hills, California, U.S.A.

MRS MATERIALS RESEARCH SOCIETY
Pittsburgh, Pennsylvania

ONSET CONDITIONS FOR GAS PHASE REACTION AND NUCLEATION IN THE CVD OF TRANSITION METAL OXIDES

J. Collins[a], D.E. Rosner[a] and J. Castillo[b]
[a]Yale Univ., Chem. Engrg. Dept., HTCRE Lab., New Haven CT 06520-2159, USA
[b]U.N.E.D., Dept. Física Fundamental, Apdo 60141, Madrid 28080, Spain

ABSTRACT

A combined experimental/theoretical study is presented of the onset conditions for gas phase reaction and particle nucleation in hot substrate/cold gas CVD of transition metal oxides. Homogeneous reaction onset conditions are predicted using a simple high activation energy reacting gas film theory. Experimental tests of the basic theory are underway using an axisymmetric impinging jet CVD reactor. No "vapor phase ignition" has yet been observed in the $TiCl_4/O_2$ system under accessible operating conditions (below substrate temperature T_w=1700 K) and further experiments are planned using more reactive feed materials. The goal of this research is to provide CVD reactor design and operation guidelines for achieving acceptable deposit microstructures at the maximum deposition rate while simultaneously avoiding homogeneous reaction/nucleation and diffusional limitations.

INTRODUCTION

The onset of gas phase reaction and particle nucleation is a common problem in the CVD of transition metal oxides, often resulting in decreased deposition rates and reduced film quality [1-3]. This is particularly true in cold gas/hot substrate CVD systems in which homogeneous reactions in the thermal boundary layer adjacent to the hot substrate produce particles which are thermophoretically repelled from the surface and, for the most part, do not deposit [4]. We call the sudden onset of significant reagent consumption by homogeneous reactions which result in non-depositing products (*e.g.* TiO_2 particles) "*vapor phase ignition*" (VPI). Since the onset of homogeneous reactions can effectively starve the growing surface of reagent, it is often possible to detect vapor phase ignition by a sharp drop in deposition rates with increasing surface temperature. On the other hand, in hot gas/cool substrate systems the onset of homogeneous particle nucleation can lead to increased film growth rates due to interface roughening associated with thermophoretically driven particle/vapor co-deposition [5,6]. It must also be mentioned that high temperature deposition rate decreases may be due to other causes, such as reaction product thermodynamic instability [7]. Dramatic rate decreases attributed to VPI were first reported by Ghoshtagore [4] for titania deposition from $TiCl_4$ in O_2, and his early experimental studies may still be the most thorough. Unfortunately, it difficult to use his data to predict conditions under which vapor phase ignition will occur in other reactors (let alone other chemical systems) because the transport conditions in his experiments were not well characterized.

We developed and are using an impinging-jet stagnation point reactor to experimentally study vapor phase ignition under well-defined transport conditions. In particular, we are inferring the onset of VPI in the thermal boundary adjacent to a hot substrate from observable decreases in deposition rates and changes in deposit microstructures. Future experiments will also include light scattering from particles nucleated in the boundary layer and non-intrusive measurements of local vapor phase species concentration. Experimental results are being used to assist in the development and eventual verification of a quantitative theory to predict the onset of vapor phase ignition in systems where high activation energy confines homogeneous reactions to a thin chemically reacting sublayer embedded within the thermal boundary layer adjacent to the hot deposition surface. Our objective is to develop a general theory which can be used with available homogeneous and heterogeneous chemical kinetics data to establish reactor design criteria and select optimal operating conditions which maximize deposition rates while just avoiding both VPI and vapor reagent diffusional limitations. A potentially useful byproduct of the theory will be the ability to extract global homogeneous reaction kinetic parameters from deposition rate data taken under well-defined transport conditions - *i.e.* just as it is now common practice to extract heterogeneous kinetic parameters from exponentially increasing deposition rate data using an Arrhenius plot, with a more complete analysis of the type outlined here it should also be possible to

extract useful *homogeneous kinetic parameters* using deposition rate data in the fall-off region beyond VPI.

HIGH ACTIVATION ENERGY REACTING FILM THEORY

The basic theory is intended to predict the effect of homogeneous reaction on vapor deposition rates when homogeneous reactions result in non-depositing products for the typical typical case of cold gas/hot substrate CVD systems [8]. If the homogeneous reactions are controlled by some high activation energy process with an apparent overall activation energy E_{hom} and $(E_{hom}/RT_w) >> 1$ (where R is the gas constant), then at sufficiently high wall temperatures there should be a chemically "frozen" outer region and a thin chemically reacting sublayer adjacent to the hot substrate. By exploiting the thinness of this reacting sublayer (to which all homogeneous reactions are confined), it is possible to generate a simple asymptotic solution for one-dimensional species mass transport and obtain expressions for the reagent mass fraction profile $\omega(y)$ normal to the substrate and the deposition flux which account for Soret as well as Fick diffusion everywhere, and reagent losses in the reacting sublayer.

The key assumptions in our present simplified model are: 1) a cold reagent gas stream at inlet temperature T_e impinging on a hot deposition surface at T_w 2) transport to the deposition surface through a one-dimensional stagnant gas film of thickness δ representing a stagnation point boundary layer 3) high activation energy homogeneous chemical kinetics ($E_{hom}/RT_w >> 1$) and 4) simple global homogeneous and heterogeneous chemical reaction rates $\dot{r}'''_{hom}$ and $\dot{r}''_{het}$ for a single limiting reagent, of the form:

$$\dot{r}'''_{hom} = A\cdot(\rho\cdot\omega(y))^m\cdot e^{(-E_{hom}/RT)}$$

$$\dot{r}''_{het} = B\cdot(\rho\cdot\omega(y))^n\cdot e^{(-E_{het}/RT)}$$

where ρ is the gas density, A and B are the homogeneous and heterogeneous reaction pre-exponential factors, and E_{hom} and E_{het} are their activation energies. Besides T_w/T_e, our solution involves the following key dimensionless parameters:

$$Dam_{hom} \equiv \frac{A\delta^2}{D}\cdot(\rho\omega_e)^{m-1} \quad , \quad \left(\frac{E_{hom}}{RT_w}\right)$$

$$Dam_{het} \equiv \frac{B\delta}{D}\cdot(\rho\omega_e)^{n-1} \quad , \quad \left(\frac{E_{het}}{RT_w}\right)$$

where D is the limiting species Fick diffusivity and Dam_{hom} and Dam_{het} are Damkohler numbers for the homogeneous and heterogeneous reactions. For the case of first order homogeneous and heterogeneous reactions ($m=n=1$), we obtain a simple closed form expression for the surface flux of the limiting reagent which displays the expected high temperature fall-off when $E_{hom} > E_{het}$, as shown in figure (1). Note that when the heterogeneous reaction is sufficiently fast (i.e. when Dam_{het} is sufficiently large) there is a transition from heterogeneous kinetic control to diffusion control and finally to VPI and the high temperature deposition rate fall-off region. Slower surface kinetics result in a transition from heterogeneous kinetic control directly to VPI and the fall-off region (presumably the sequence of events in Ghoshtagore's experiments). It is also evident that to maximize deposition rates, optimal operating conditions would result in incipient vapor phase ignition. However, to obtain acceptable deposit microstructures it may be necessary to operate at surface temperatures below both VPI and the onset of appreciable diffusional limitations. Since a primary goal of this work is to guide CVD reactor design and operation, experimental correlation of deposit microstructures with deposition conditions in the vicinity of VPI is currently underway to complement our CVD-rate measurements.

EXPERIMENTAL

To verify or guide improvements of our theoretical model we are now investigating the onset of VPI under well-defined transport conditions using an axisymmetric impinging jet CVD reactor. The reactor is shown schematically in figure (2). Cold reagent and carrier gas enter the reactor from the top, flow through a converging cast alumina nozzle and impinge on a polished quartz disk substrate which rests on an RF-heated graphite susceptor ($r_{substrate} = r_{jet}$). Preliminary experiments have been for titania deposition from $TiCl_4/O_2/Ar$ and $TiCl_4/N_2O/Ar$ at .1 MPa pressure using excess oxidizer. The $TiCl_4$ source is a constant temperature liquid bubbler and all lines carrying the $TiCl_4$ are teflon with stainless steel fittings and valves. To avoid water contamination the reactor is pumped down to 10 Pa for several hours before each run and only dry gasses are used (ultra high purity Ar, H_2O < .5 ppm). Our intention was to measure deposition rates with effectively no water, since it reacts violently with $TiCl_4$ even at room temperature. In some of our experiments water contamination was inferred from the presence of TiO_2 particles in the cold (300 K) reagent mixing chamber above the nozzle. Deposition rate data from these experiments were thrown out and gas handling was improved to eliminate the problem, although future experiments with controlled water addition are planned. Deposition rate measurements are by *in situ* interferometry (at a wavelength of 633 nm) and *ex situ* weight gain.

Our current range of accessible operating conditions (with well defined fluid flow) are: T_w up to 1600 K, pressure P between 0.01 and 0.1 MPa, and impinging jet Reynolds number Re_{jet} between roughly 100 and 600 (based on nozzle radius r_{jet}). Under these conditions natural convection is not expected in the primary reagent jet since $Re_{jet}^2/Gr >> 1$, (Gr is the Grashof number for the impinging jet - there may be buoyancy-driven flows away from the jet). Indeed, flow visualization of the jet using argon seeded with fine titania particles showed no flow distortions when the susceptor was hot or cold. Standard operating conditions used in our preliminary experiments are:

T_w:	900 - 1700 K	Ar	99%
P:	0.1 MPa	O_2 or N_2O	1%
Re_{jet}:	200 (nozzle velocity ≈ 1 m/s)	Oxidizer/$TiCl_4$	20/1 to 200/1

PRELIMINARY RESULTS AND DISCUSSION

The most striking preliminary result we have obtained is that under the abovementioned reactor conditions, no VPI has been observed for substrate temperatures up to 1700 K in the $TiCl_4/O_2/Ar$ system. This is very different from Ghoshtagore's experimental results, which indicated VPI at only 1125 K for the same chemical system but under rather different flow conditions [4]. As shown in figure (3), our results for titania deposition from $TiCl_4/O_2$ in Ar show a transition from heterogeneous kinetic control to diffusion control at roughly 1300 K with no high temperature rate fall-off. The relatively temperature insensitive region of our deposition rate data above 1300 K approaches the $TiCl_4$ convection-diffusion limit calculated assuming local thermochemical equilibrium at the gas/solid interface and Fick and Soret diffusion through a variable property mass transfer boundary layer [9,10].

The absence of VPI in our reactor is consistent with preliminary light scattering experiments in which a 10mW He-Ne laser was used to produce a 12 mm laser sheet which was passed through the reactor between the nozzle exit and the substrate planes. Visual inspection revealed a particle-free primary jet impinging on the substrate at all temperatures†. The results of our basic reacting film theory are also not inconsistent with our experimental results when rate calculations are made using heterogeneous kinetic parameters from Ghoshtagore [4] and homogeneous kinetic parameters from a recent independent (isothermal flow reactor) study of global $TiCl_4$ oxidation kinetics [11], as can be seen in figure (3). However, reacting film theory deposition rate calculations using these kinetic parameters and the approximate flow conditions in Ghoshtagore's experiments do not show a fall-off in deposition rate due to VPI until 2100 K (off scale on figure 3), and then it very gradual. In order to explain Ghoshtagore's observed VPI at 1125 K using our basic theory, it would be necessary to assume a homogeneous activation energy

† Particles were seen in the corners of the reactor where the reagent gases recirculate, but a negligible fraction of these gases can reach the substrate.

Figure 1.
Representative Film Theory Predictions

j_w = dep. flux at substrate

$j_{diff-ref}$ = reference diffusion flux

α_T = thermal diffusion factor

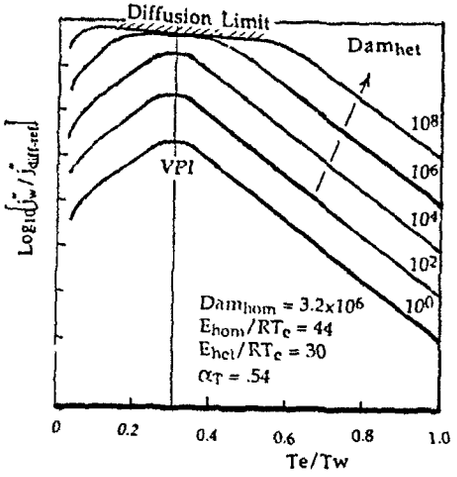

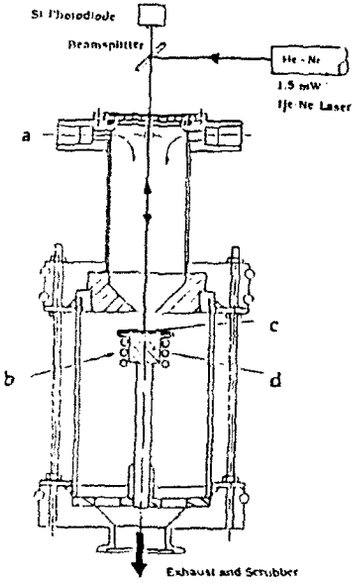

Figure 2.
Axisymmetric Impinging Jet CVD Reactor
a) reagent inlet, b) RF coils c) substrate
d) graphite susceptor

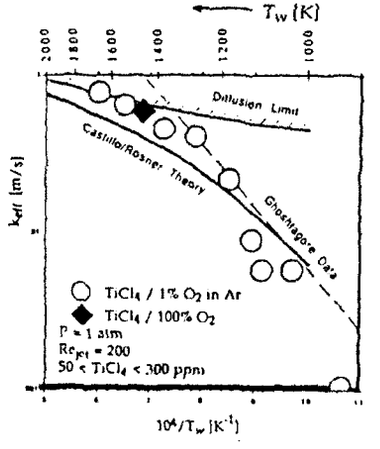

Figure 3.
Arrhenius Plot of Normalized TiO_2 Deposition Rates from $TiCl_4 + O_2$
$k_{eff} \equiv r''_{het} / [P_{TiCl4}/RT_w]$

of roughly 345 kJ/mole as opposed to the published 89 kJ/mole. Furthermore, using the high activation energy estimated in this way from Ghoshtagore's data, our basic theory would predict VPI at only 1300 K under our reactor conditions, which was not observed. These inconsistencies have not yet been resolved. To do so may require a more sophisticated treatment of homogeneous chemical reactions than is now incorporated in our theory. However, there are uncertainties in the transport conditions in Ghoshtagore's experiments, including the possibility for buoyancy-driven recirculation around his deposition substrate. Recall that in our experiments no particles are observed in the primary reagent jet, but they are plainly visible in recirculating zones in the reactor. Trace water contamination in Ghoshtagore's (or our) experiments may also contribute to the discrepancy in VPI conditions.

Avoiding VPI would be good news if our goal was simply to produce high quality TiO_2 films, but our goal is to study VPI and its sensitivity to reactor operating parameters. To force VPI to occur at lower temperatures in our jet impingement reactor we have tried halving the total gas flow rate (i.e. doubling the reagent residence time in the thermal boundary layer), but this did not yield a clear VPI. Increasing the O_2 partial pressure from .001 to .1 MPa (as in the Ghoshtagore experiments) had no measurable effect on deposition rates at 1500 K (with $O_2/TiCl_4$ always > 30). Another approach we considered was using N_2O as an oxidizer, since N_2O begins to dissociate to N_2 and atomic O at roughly 1300 - 1400 K under our standard operating conditions (residence time in thermal boundary layer ≈ 17 ms). O atom attack of $TiCl_4$(g) should be much faster than O_2 attack, and should lower the VPI temperature [12]. Preliminary experiments for $N_2O/TiCl_4$ = 20, 40 and 200 have not yet given conclusive evidence of VPI at accessible surface temperatures, but still higher N_2O concentrations may finally give the anticipated effects. Future experiments may also include more reactive metal sources and organometallics known to react in the gas phase at lower temperatures [3].

CONCLUSIONS AND FUTURE WORK

While we have not yet been able to observe $TiCl_4$ vapor phase ignition in our impinging jet reactor (fig. 2), we are confident that our basic model of high activation energy reacting gas films will prove to be useful for many CVD applications once the theory has been experimentally verified for some prototypical chemical system. The most obvious reason for our difficulty in achieving VPI below 1700 K in our reactor at atmospheric pressure is the very short reagent residence time in the thermal boundary layer adjacent to the substrate. The sensitivity of the system to trace amounts of water has not yet been determined by experiments with controlled water addition.

We must also acknowledge that the current version of our theory is unable to reconcile recent isothermal flow reactor data on global homogeneous $TiCl_4$ oxidation kinetics [11] with the deposition rate data of Ghoshtagore - nor are the homogeneous oxidation kinetics estimated using the present theory and Ghoshtagore's CVD rate data consistent with our own preliminary deposition experiments. However, it would be premature to conclude that any useful theory for VPI in CVD reactors requires a more complex description of the relevant homogeneous reaction kinetics. Other more straight-forward enhancements to the basic theory under consideration are treating real viscous flow, as opposed to an equivalent stagnant gas film (including Stefan flow for non-dilute systems), and accounting for variable thermophysical properties.

Once our high activation energy reacting gas film theory, with any necessary modifications, is experimentally verified it will provide rational criteria to reactor designers and process engineers on how to achieve the maximum possible deposition rates while still avoiding VPI and diffusional limitations. Coupling the prediction of VPI onset conditions with semi-empirical correlations of deposit microstructures in the vicinity of VPI will then help find the operating conditions needed to produce films of desired microstructure at the maximum rate.

ACKNOWLEDGEMENTS

This work (carried out in the Yale High Temperature Chemical Reaction Engineering (HTCRE) Laboratory) was supported by NASA Lewis Research Center under Grants NTG-5037 and NAG 3-884, the US Air Force under Grant 89-0223 and the Yale HTCRE Lab. Industrial Affiliates (Shell, GE, DuPont, and Union Carbide). Thanks are also due to Tony Macini of the student machine shop and Dick Downing from Gibbs machine shop for their help in the design and construction of our CVD reactor.

REFERENCES

1. Y. Takashi *et al.*, J. Cryst. Growth, **74**, 409 (1986).
2. H. Yamane and T. Hirai, J. Mat. Sci. Let., **6**(10), 1229, (1987).
3. M. Balog *et al.*, J. Electrochem. Soc., **126**(7), 1203 (1979).
4. R.N Ghoshtagore, J. Electrochem. Soc., **117**(4), 529 (1970); R.N. Ghoshtagore and A.J. Noreika, *ibid*, **117**(10), 1310 (1970).
5. H. Komiyama *et al.*, in Chemical Vapor Deposition X, edited by G.W. Cullen (Electrochem. Soc. *Proc. 87-8. Pennington NJ 1987) pp. 1119-1128.*
6. H. Komiyama and T. Osawa, Jap. J. Appl. Phys., 24(10), L795 (1985).
7. M. Tirtowidjojo and R. Pollard, J. Cryst. Growth, **98**, 420 (1989).
8. J. Castillo and D.E. Rosner, presented at the 1990 AIChE Meeting, paper no. 55d; J. Electrochem. Soc. *publication in preparation.*
9. D.E. Rosner and J. Collins in Chemical Vapor Deposition XI, edited by K.E. Spear and G.W. Cullen (Electrochem. Soc. Proc. **90**-12, Pennington NJ 1990) pp. 49-60.
10. D.E Rosner, Transport Processes in Chemically Reacting Flow Systems, (Butterworths, Boston, 1986), pp. 307-404 (3rd Printing 1990).
11. S.E. Pratsinis *et al.*, J. Am. Ceram. Soc., 73(7), 2158 (1990).
12. J.D. Chapple-Sokol *et al.*, J. Electrochem. Soc., 136(10), 2993 (1989).

REPORT DOCUMENTATION PAGE

Form Approved
OMB No. 0704-0188

1. AGENCY USE ONLY (Leave blank)	2. REPORT DATE	3. REPORT TYPE AND DATES COVERED
	1993	Reprint: Comb. Sci Tech. 89 335-362

4. TITLE AND SUBTITLE

Thermophoretic Effects on Particles in Counterflow Laminar Diffusion Flames

5. FUNDING NUMBERS

PE - 61102F
PR - 2308
SA - BS
G - AFOSR 91-0170

6. AUTHOR(S)

ALESSANDRO GOMEZ and DANIEL E. ROSNER

7. PERFORMING ORGANIZATION NAME(S) AND ADDRESS(ES)

HIGH TEMPERATURE CHEMICAL REACTION ENGINEERING LABORATORY
YALE UNIVERSITY
BOX 2159, YALE STATION
NEW HAVEN, CONNECTICUT 06520 U.S.A.

8. PERFORMING ORGANIZATION REPORT NUMBER

9. SPONSORING/MONITORING AGENCY NAME(S) AND ADDRESS(ES)

AFOSR/NA
110 Duncan Avenue, Suite E115
Bolling AFB DC 20332-0001

10. SPONSORING/MONITORING AGENCY REPORT NUMBER

11. SUPPLEMENTARY NOTES

12a. DISTRIBUTION/AVAILABILITY STATEMENT

Approved for public release; distribution is unlimited

12b. DISTRIBUTION CODE

13. ABSTRACT (Maximum 200 words)

Abstract—*Thermophoresis*, meaning particle drift down a local gas temperature gradient, is now known to be important to many combustion-related technologies. Until now, however, no direct experimental determinations of primary and aggregated particle thermophoretic diffusivities, $(\alpha_T D)_p$, in high temperature combustion environments have been reported. To perform such measurements, we selected a seeded laminar counterflow diffusion flame (CDF) operated at low strain-rate as a well-defined combustion system, offering at the same time a low velocity and high temperature gradient environment. We established a CH_4, O_2-Inert opposed jet diffusion flame in which the gaseous fuel:oxygen ratio, and the diluent flow rates were adjusted to obtain a flat, stable flame, approximately coincident with the *gas* stagnation plane (GSP). Particles fed to or formed on either or both sides of the GSP move toward this plane until the local axial velocity is exactly counterbalanced by the thermophoretic velocity. As a result of this dynamic "equilibrium" condition, a *particle* stagnation plane (PSP) is established on one or both sides of the GSP, resulting in the formation of a readily observable "dust-free" zone. Dramatic confirmation of this phenomenon is offered by using laser-sheet visualization of the region, which reveals a thick dark zone, the dust-free volume, that contrasts with the bright particle-laden regions. This "phase separation" phenomenon allowed us to determine TiO_2 particle thermophoretic diffusivities by: i) measuring the temperature field using fine thermocouples, ii) measuring the thickness of the dark zone (*i.e.* PSP-positions) using laser light scattering, and iii) measuring/computing the axial gaseous convective velocity at the particle stagnation plane(s). Experiments and calculations indicate quantitative agreement between these measurements and kinetic theory predictions for isolated spheres at $Kn_p \gg 1$ in the case of $CH_4/O_2/N_2$ diffusion flames. Replacement of N_2 with He as diluent resulted in a much thicker and more readily measurable particle-free layer, but yielded only qualitative agreement with the theory, because of uncertainties in the gas composition in the flame, as well as possible contributions from simultaneous *diffusiophoretic* mechanisms. In some 'sooting' diffusion flames, and in 'synthesis' flames in which particles are the desired products, both laminar and turbulent, it is shown that thermophoresis can influence particle residence times in the decisive region where nucleation, growth, coagulation, sintering and oxidation occur, as well as particle temperatures, which influence particle morphology and radiative heat loads. We briefly discuss the non-premixed combustion conditions under which these thermophoretically-induced effects are likely to be appreciable.

14. SUBJECT TERMS

Key Words: Aerosols, Soot, Aggregated Particles, Gaseous Diffusion Flames, Thermophoresis, Brownian Diffusion, Flame Synthesis of Fine Particles, Aerosol Reaction Engineering

15. NUMBER OF PAGES

15

16. PRICE CODE

17. SECURITY CLASSIFICATION OF REPORT	18. SECURITY CLASSIFICATION OF THIS PAGE	19. SECURITY CLASSIFICATION OF ABSTRACT	20. LIMITATION OF ABSTRACT
Unclassified	Unclassified	Unclassified	UL

Combust. Sci. and Tech., 1993, Vol. 90, pp. 135-362
Photocopying permitted by license only

Thermophoretic Effects on Particles in Counterflow Laminar Diffusion Flames

ALESSANDRO GOMEZ and DANIEL E. ROSNER *High Temperature Chemical Reaction Engineering (HTCRE) Laboratory, Yale University, New Haven CT 06520-2159 USA*

(Received May 8, 1992, in final form July 23, 1992)

Abstract—*Thermophoresis*, meaning particle *drift down a local gas temperature gradient* is now known to be important to many combustion-related technologies. Until now, however, no direct experimental determinations of primary and aggregated particle thermophoretic diffusivities, $(\rho_p D)_{th}$, in high temperature combustion environments have been reported. To perform such measurements, we selected a seeded laminar counterflow diffusion flame (CDF) operated at *low strain-rate as a well-defined combustion system*, offering at the same time a low velocity and high temperature gradient environment. We established a CH_4, O_2, Inert opposed jet diffusion flame in which the gaseous fuel/oxygen ratio, and the dilu[illegible] flow rates were adjusted to obtain a flat, stable flame, approximately coincident with the *gas* stagnation plane (GSP). Particles fed to or formed on either or both sides of the GSP move toward *this plane until the local axial velocity is exactly counterbalanced by the thermophoretic velocity*. As a *result of this dynamic "equilibrium" condition*, a *particle* stagnation plane (PSP) is established on one or both sides of the GSP, resulting in the formation of a readily observable "dust-free" zone. Dramatic confirmation of this phenomenon is offered by using laser-sheet visualization of the region, which reveals a thick dark zone, *the dust-free volume, that contrasts with the* bright particle-laden regions. This "phase separation" phenomenon allowed us to determine TiO_2 particle *thermophoretic diffusivities* by: i) *measuring* the temperature field using fine thermocouples; ii) measuring the thickness of the dark zone (*i.e.* PSP-positions) using laser light scattering; and iii) measuring/computing the axial gaseous convective velocity at the particle stagnation plane(s). Experiments and calculations indicate quantitative agreement between these measurements and kinetic theory predictions for isolated spheres at $Kn_p \gg 1$ in the case of CH_4, O_2, N_2 diffusion flames. Replacement of N_2 with He as diluent resulted in a much thicker and more readily measurable particle-free layer, but yielded only qualitative agreement with the theory, because of uncertainties in the gas composition in the flame, as well as possible *contributions from* simultaneous *diffusiophoretic* mechanisms. In some 'sooting' diffusion flames, and in 'synthesis' flames in which particles are the desired products, both laminar and turbulent, it is shown that thermophoresis can influence particle residence times in the decisive region where nucleation, growth, coagulation, sintering and oxidation occur, as well as particle temperatures, which influence particle morphology and radiative heat loads. We briefly discuss the non-premixed combustion conditions under which these thermophoretically-induced effects are likely to be appreciable.

Key Words: Aerosols, Soot, Aggregated Particles, Gaseous Diffusion Flames, Thermophoresis, Brownian Diffusion, Flame Synthesis of Fine Particles, Aerosol Reaction Engineering

ABBREVIATIONS

BSL	Brownian sublayer (Fig. 4b)
CDF	counterflow diffusion flame (Fig. 1b)
CVD	chemical vapor deposition
f	flame (where T-maximizes)
GSP	gas stagnation plane (or point)
LDV	laser-Doppler velocimetry
LHS	left hand side (of equation or inequality)
PDF	probability density function
PMT	photomultiplier tube
PSP	particle stagnation plane (or point)
rms	root-mean-square
rxn	reaction
RHS	right hand side (of equation or inequality)
stoich	stoichiometric

NOMENCLATURE

a	strain rate parameter, $(1/2)(dV_z/dz)_{GSP}$
D_{i-mix}	Fick diffusion coefficient for species i
r	cylindrical radial variable
T	local absolute temperature
V_c	convective (mass-averaged) velocity
U	axial velocity of feed stream (Eqs.15,16)
y_i	mole fraction of species i
z	axial variable (Fig.1b)
α_T	thermophoretic (Soret-like) factor (Eqs. 3,6)
ζ	dimensionless axial position (Eqs.15,16)
ν	momentum diffusivity of local gas mixture
ν_{stoich}	stoichiometric fuel/oxidizer molar ratio
ρ	density
Φ	equivalence ratio (Eqs.2,13)

Subscripts

f	evaluated at flame
F	pertaining to fuel
O	pertaining to oxidizer
p	pertaining to suspended particles
T	pertaining to thermophoresis

1. INTRODUCTION

Thermophoresis is the phenomenon whereby small spherical particles suspended in a gas characterized by a temperature gradient, **grad** T, drift in the direction opposite to that of **grad** T. The significant role of thermophoresis in many nonisothermal 'dusty gas' flow systems has been demonstrated in the recent engineering literature (for a recent summary, see Rosner *et al.*, 1992). Most attention has been focused on the enhancement of particle deposition from hot, lightly loaded gas streams onto actively cooled solid surfaces. However, there are also situations of both theoretical and industrial importance where the surface is hotter than the mainstream (Gökoğlu and Rosner, 1986; Friedlander *et al.*, 1990), and thermophoretic repulsion results in a dust-free layer adjacent to the hot surface which can be exploited to reduce its contamination, as in applications of high purity chemical vapor deposition and in the catalytic combustion of ash-containing fuels. As discussed in this paper, a somewhat similar situation can arise near a high temperature gaseous diffusion flame "sheet", even when there is some gas flow through it.

The thermophoretic diffusivity $(\alpha_T D)_p$ can be defined by the local particle drift velocity expression:

$$V_T = (\alpha_T D)_p \cdot \left(-\frac{\mathbf{grad}\ T}{T} \right) \tag{1}$$

where α_T is the (dimensionless) thermophoretic diffusion factor, D_p is the particle Brownian diffusivity, T is the local temperature and **grad** T its local spatial gradient. A knowledge of the thermophoretic diffusivity of combustion-generated aerosols such as carbonaceous soot, TiO_2, Al_2O_3, SiO_2, is important to a variety of deposition experiments (Eisner and Rosner, 1985 and 1986; Rosner and Kim, 1986; Makel and Kennedy, 1990; Konstandopoulos and Rosner, 1992), in many technologies (*e.g.*, production of optical fibers (Rosner and Park, 1988), high temperature gas filtration, electric power generation and combustion turbine operation with ash-containing fuels, energy recovery from stack gases, solid propellant rocketry,...), and in combustion research (see, *e.g.*, Eisner and Rosner, 1985; Dobbins and Megaridis, 1987; Rosner *et al.*, 1991). Until now, no experimental values of this property in high temperature combustion environments have been reported, perhaps for the following reason. Experimental difficulties arise from the fact that even the highest obtainable thermophoretic velocities are of the order of only a few centimeters per second. Thus, a rather careful characterization of the velocity field in which thermophoresis occurs is necessary to be able to discriminate the thermophoretic velocity from the host gas convective flow on which it is superimposed. A counterflow diffusion flame (Tsuji, 1982), hereafter abbreviated CDF, is a prototypical laboratory scale combustion environment recently used in several aerosol formation studies (Katz *et al.*, 1985, 1986 and 1990; Zachariah *et al.*, 1989, 1990 and 1991), as well as for studies of single-phase diffusion flames displaying chemical kinetic effects (see, *e.g.*, Sick, 1990, Smooke, 1991). Typically, these latter experiments have been performed under high strain-rate conditions to approach the flame extinction limit, with particular relevance to turbulent combustion which taxes so-called "flamelet" conditions (Bilger, 1988; Peters, 1991). But low strain-rate flames, characterized by low velocity gradients shown here to be desirable for the present purposes, have also been successfully stabilized (Pandya and Weinberg, 1964; Hahn *et al.*, 1981). In this paper we demonstrate the feasibility of exploiting low strain rate, seeded, laminar gas counterflow diffusion flames for experimentally determining the high temperature thermophoretic diffusivity of inorganic aerosols present at negligible mass loadings. We also discuss the possible importance of thermophoresis in some naturally sooting, luminous diffusion flames, and flames used to synthesize fine particles of desired composition, size (distribution) and morphology. Because of its possible application to 'gas cleaning', a theoretical investigation of the rather similar situation of a dust-free layer adjacent to a hot solid wall is treated elsewhere (Park and Rosner, 1987), including the industrially important case of appreciable particle mass loading. For a review of the use of the thermophoretic diffusivity to predict thermophoretically-modified submicron particle *deposition* rates across laminar or turbulent boundary layers, the reader is directed to Gökoğlu and Rosner (1984), Rosner *et al.* (1992), and the extensive references cited therein.

2. EXPERIMENTAL ARRANGEMENT AND PROCEDURES

Figure 1a shows a schematic of the burner consisting of two brass ducts (25.7 mm I.D.) mounted coaxially. The top duct was held in place by three brass rods with threaded ends screwed into the support base of the bottom duct. Turning the rods allowed both a fine adjustment of the burner separation and minor tilting to obtain a horizontal flame. Five wire screens (40 mesh) were placed in each duct to reduce turbulence and ensure sufficiently flat velocity profiles at the duct exits. Two diffusion flames were studied in greatest detail: gaseous methane and oxygen were diluted with either nitrogen or helium for reasons explained below. When N_2 was used as the diluent, oxygen was admitted to the lower tube whereas methane flowed downward through the upper duct. When He replaced N_2 as inert, fuel and oxidizer feeds were switched to yield a more stable flame configuration. Since the burner was operated under low strain-rate conditions, the flame was extremely sensitive to room drafts; it was therefore necessary to shield it using a pyrex 'chimney' (Fig. 1a) with two small openings for optical access. The whole burner assembly was mounted on a xyz translational stage to allow for scanning of the combustion region by thermocouples and a laser beam. Part of the pre-dried inert flow was bubbled through a $TiCl_4$ evaporator/saturator and carried into the combustion zone where the titanium chloride vapor reacted with the flame-generated $H_2O(g)$ to form an

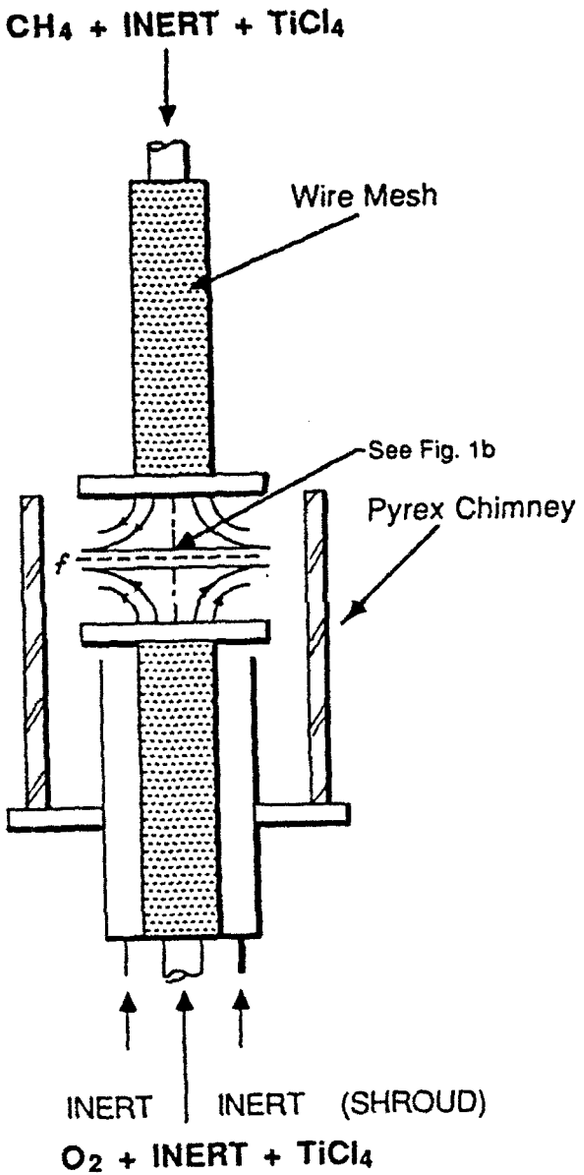

FIGURE 1 a) Schematic of the counterflow diffusion flame (CDF) burner

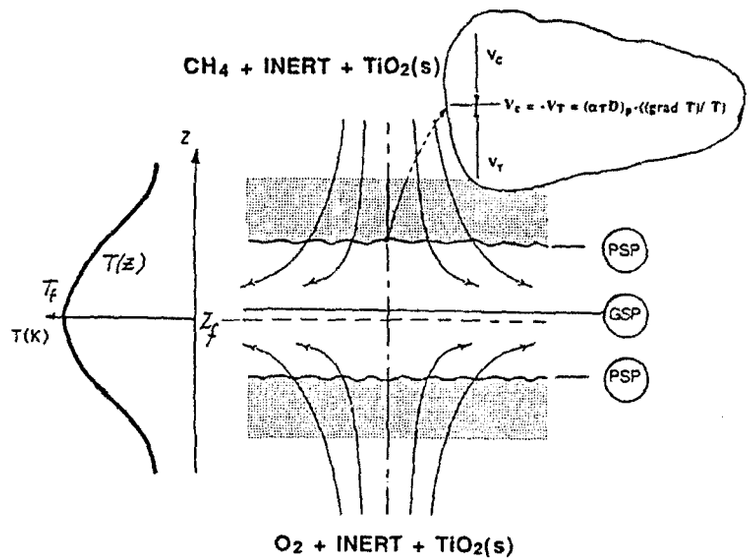

FIGURE 1 b) Principle underlying the experimental procedure to determine the "soot" particle thermophoretic diffusivity, $(\alpha_T D)_p$ in gaseous combustion products (Eq.1).

aerosol of submicron TiO_2 particles (Ulrich, 1984; Roquemore *et al.*, 1986). A high flow rate, inert gaseous shroud flow prevented particle deposition on the pyrex chimney.

Flow rate conditions were adjusted to obtain a flat, stable flame, approximately coincident with the *gas stagnation plane* established in the impingement region of the two opposed jets (Fig. 1b). This corresponds to a situation of high temperature gradients in very low speed convective flows, the most advantageous condition to emphasize thermophoretic effects. As recognized by Pandya and Weinberg (1964), this condition is achieved when fuel and oxidizer are fed in approximately stoichiometric proportions. On the basis of the now-classical theory of non-premixed gaseous combustion in nearly-equal diffusivity systems (see, *e.g.*, Liñan, 1974, and the review of Rosner, 1986, Chapter 6), it can be expressed in terms of an *equivalence ratio parameter*[3], Φ, defined as

$$\Phi \equiv \frac{(y_F)_{feed}/(y_O)_{feed}}{\nu_{stoich}} \tag{2}$$

where $(y_F)_{feed}$ is the fuel mole fraction in the "fuel" feed stream, $(y_O)_{feed}$ is the oxygen mole fraction in the "oxidizer" feed stream and ν_{stoich} is the stoichiometric number of moles of fuel associated with one mole of oxidizer. In near-equal diffusivity systems Φ is clearly the most important parameter determining the relative positions of the flame and the gas stagnation plane, that are in principle coincident when this parameter equals

[3] The reader is cautioned that most authors of CDF-studies report an "overall equivalence ratio" defined in terms of molar *flow rates* directed toward the flame.

unity. In practice, favorable conditions from a thermophoretic vantage point are achieved over a range of effective Φ-values near unity, as discussed in detail in Section 3.4.

Thus, conditions were selected so that the diffusion flame "sheet" would stabilize sufficiently close to the gas stagnation plane (GSP) that the axial gas velocities at the flame were not much larger than the maximum absolute particle thermophoretic velocities. Particles added or formed upstream on either side of the GSP move toward this plane until the condition is met at which the convective velocity towards the GSP is exactly counterbalanced by the thermophoretic velocity in the opposite direction. As a result of this equilibrium condition, an effective *particle stagnation plane* (PSP) can be established on both sides of the GSP, in the case of titanium chloride feeding from both fuel and oxidizer side, which results in the formation of a dynamic dust-free zone 'sandwiched' between the particle-laden regions of the flow. Smallness of the Brownian diffusivity of such particles ensures the sharpness of these "fronts", certainly on the scale of the reported dust-free zone thickness (> 1 mm). Illumination of the combustion region by a He-Ne laser sheet allowed visualization of this dust-free zone, which, since it could not be penetrated by the light scattering particles, appeared as a dark zone (Fig. 1b). Thus, even without *a priori* knowledge of the gas stagnation plane location, it was relatively easy to adjust gas flow rates and choose optimal conditions resulting in maximum separation of the two particle stagnation planes. It appears that Pandya and Weinberg (1964) first observed this phenomenon; however, they did not attribute it to thermophoresis. Kim *et al.* (1984) also reported similar behavior for carbonaceous soot particles in an opposed jet polymer diffusion flame. They recognized the role of thermophoresis but extracting the transport properties of such particles was not their purpose. Here we demonstrate that it is possible to exploit this phenomenon to extract experimental values of $(\alpha_T D)_p$, the particle thermophoretic diffusivity, for aggregated submicron aerosol particles in high temperature combustion products, and to compare results with the predictions of gas-kinetic theory.

At a steady particle stagnation plane (PSP) the viscous drag force and thermophoretic force acting on the particles counterbalance each other. This balance can be re-expressed as the kinematic condition $V_T = -V_c$, where V_T is the thermophoretic 'drift' velocity and V_c is the z-component of the local gaseous mass-averaged convective velocity. Then, using Eq.(1), $(\alpha_T D)_p$ can be obtained from:

$$(\alpha_T D)_p = \left(\frac{|V_c|}{\left| \frac{dT/dz}{T} \right|} \right)_{PSP} \tag{3}$$

Thus, to determine $(\alpha_T D)_p$ we first measured the temperature in the vicinity of the flame as a function of axial position z using fine Pt/Pt-10% Rh silica coated thermocouples (bead typical dimension ≈ 75 μm). These measurements were corrected for radiative losses by a standard convective-radiative balance performed for either cylindrical or spherical geometry, depending on the bead shape, and for an assumed bead emissivity equal to 0.22. We then needed to determine the local axial gas velocity V_c at the observed PSP position(s). Preliminary calculations were performed by utilizing the predictions of a numerical code previously validated against extensive experimental data (Smooke *et al.*, 1986). Although reasonably good agreement between experiments and calculations was obtained for the shape of the temperature profiles, the predicted absolute position of the flame (*e.g.*, the axial location z_f of T_{max}) was systematically shifted towards the lower burner, which made unreliable the quantitative use of this prediction. The discrepancy between experiments and predictions may be due to either buoyancy effects, a phenomenon not accounted for in the one-dimensional computational model in which

the momentum equation in the axial direction is replaced by an isobaric condition, or to sensitivity to the velocity boundary conditions (plug flow versus parabolic flow). Both effects may be quite important at the low strain rates of these flames (Smooke, 1992). For this reason, it became necessary to independently measure V_c using Laser Doppler Velocimetry (LDV). To circumvent the inevitable thermophoretic effects we wish to ultimately quantify, we actually measured the *radial* velocity at a fixed radial position as a function of axial coordinate, z. This measurement is not influenced by seed particle thermophoresis since one of the simplifying features of the flat counterflow flame is that sufficiently near the axis both temperature and concentrations are functions only of the axial coordinate z; *i.e.* there are no radial temperature gradients, as we experimentally verified[4]. Then, by knowing the local temperature and estimating the local mixture molecular weight, we computed the local mixture density, ρ. Finally, the axial gaseous velocity $V_z(z)$ could be constructed by applying mass conservation to a pill-box control volume centered on the burner axis and with one end coincident with either burner mouth where boundary conditions (to begin the spatial integration) are known. Accordingly, from a total mass balance:

$$\pi r^2 \{\rho V_z|_{z=0} - \rho V_z|_{psp}\} = 2\pi r \int_{z=0}^{PSP} (\rho V_r)|_r \, dz \tag{4}$$

which yields

$$V_z|_{psp} = \frac{1}{\rho_{psp}} \left[\rho V_z|_{z=0} - \frac{2}{r} \int_{z=0}^{PSP} (\rho V_r)|_r \, dz \right] \tag{5}$$

for any convenient choice of r (=const) within the abovementioned "one-dimensional" core. The radial velocity of the gas was measured by a lab-assembled LDV optical system based on the same He-Ne laser used for visualization purposes. The beam was split by a prism into two beams 16 mm apart and focused down by a 160 mm f.1 achromatic lens, which determined a fringe spacing of 6.3 μm. Since TiO_2 particles are not suitable for LDV measurements in high temperature environments because of a reduction in light scattering efficiency (Kennedy, 1982; Witze and Baritaud, 1986), Al_2O_3 particles of 1.4 μm nominal diameter were introduced in the flame by aerodynamic entrainment into the gaseous streams forced through two cyclone-type feeders. Such particles are small enough to accurately track the acceleration of radial gas flow since their estimated local stopping time is less than 0.02 percent of the inverse strain rate. To prevent particle aggregation, the feeders were shaken by small vibrators. The modulated signal scattered off the alumina particles was collected in the forward scattering lobe by a lens centered at 14 degrees and imaged on a spatial filter mounted on the window of a photomultiplier tube. The PMT signal was then processed by a counter (Model 1980B, TSI, MN).

Care was taken to measure temperature, velocity and TiO_2 particle stagnation plane at the same axial position in the flame by checking burner and probe positioning with a vertical cathetometer. The generation of titania particles inevitably results also in the byproduct hydrochloric acid. Consequent problems of burner corrosion and clogging were minimized by forming these particles only when it was necessary to measure with the cathetometer the dark zone position. Temperature and radial velocity were measured in the absence of these particles, based on the assumption that the generation of trace amounts of this aerosol does not significantly affect either the velocity field or the thermal

[4] Nor is the *radial* velocity affected by gravitational effects on the injected particles since the burner oriented with its axis parallel to the direction along which gravity acts (z-coordinate).

field. Since the $TiCl_4$(g) mole fraction in the feed stream(s) was estimated at less than 0.015, this assumption is seen to be valid.

Experiments were performed on two flames. For each of them the following information is provided in Table I: the volumetric flow rates of fuel and inert on the fuel side, oxygen and inert on the oxidizer side, respectively; the equivalence ratio parameter, Φ, defined in Eq. 2; the adiabatic flame temperature, T_{ad}; the burner separation, BS, and a nominal strain rate, a_{ref}, defined as the ratio of the velocity of the oxidizer at the burner mouth and the burner gap.

3. RESULTS AND DISCUSSION

3.1 N_2-diluted Flame

Figure 2 presents thermocouple measurements in the N_2-diluted flame corrected for radiation loss, as a function of the axial coordinate, z, computed from the bottom burner exit. As expected, the peak temperature of 1769 K is somewhat lower than the adiabatic flame temperature of 1933 K corresponding to the feed stream compositions[5]. The position of the observed particle stagnation planes is also indicated on opposite sides of the rather sharp temperature peak. The corresponding total dark zone thickness was about 1.25 mm, an easily measured and significant thermophoretic separation effect at the chosen flow rate conditions. Also shown in the same figure are the *radial* velocity measurements at a fixed radial location, $r = 3.55$ mm, and various axial positions. As anticipated, measurements were not obtainable near the temperature peak itself because the thermophoretic repulsion acting on the injected alumina particles produce a "dust-free" zone and cause the data rate of the Doppler counter to drop to zero. Also, for reasons related to optical access, no scanning in the vicinity of the lower burner was possible. The radial velocity grows monotonically from either burner to the flame front, as a consequence of the stagnation flow configuration and the gas expansion near the flame. Figure 3 shows the axial velocity component profile, reconstructed on the basis of the procedure outlined in the previous section, as a function of the axial coordinate z. Since several velocity data points were missing on the oxidizer side and the uncertainty associated with data extrapolation was significant, only one half of the flame region, the one on the fuel side, is shown. Errors associated with estimates of molecular weight for the determination of the local density and viscosity are deemed negligible because the total molecular weight change from burner mouth to flame location, the latter evaluated by chemical equilibrium calculations, is only about 5%. In correspondence of the particle stagnation plane on the fuel side the gaseous velocity measured is 1.8 cm/s; inserting these experimental data in the RHS term in Eq. 3, we obtain a value of 1.3 cm^2/s for the thermophoretic diffusivity of TiO_2 particles at the PSP.

We can now compare this value with the relevant predictions of kinetic theory (Waldmann, 1966) in the free molecular regime ($Kn_p \gg 1$, where Kn_p is the Knudsen number based on particle diameter). According to Waldmann's calculation the thermophoretic diffusivity of a spherical particle in this regime can be expressed

[5] The adiabatic flame temperature was calculated by assuming that the reactant input temperatures were 298K. Our measurements indicate otherwise, as shown in Fig. 2, because of two effects: one was the conductive heat loss from the flame to the burners; the other is heat transfer from the exhaust gases to the top burner around which they flow. By assuming room temperature at reactant inlets, we essentially compensated for the first effect, whereas the second one is still unaccounted for. Therefore this calculation somewhat underestimates the adiabatic flame temperature (probably by less than 100K).

TABLE I

CH_4	$(Inert)_F$	O_2	$(Inert)_{Ox}$	Φ	T_{ad}	BS	a_{ref}
(cc/s)	(cc/s)	(cc/s)	(cc/s)		(K)	(mm)	(s^{-1})
3.38	20.2	8.2	18.6	0.935	1933	13.8	4.6
4.74	36.7	13.3	13.9	0.466	2371	12.6	18

$$(\alpha_T D)_p = \left(\frac{3}{4}\right)\cdot\left[1 + \left(\frac{\pi}{8}\alpha\right)\right]^{-1}\cdot\nu \tag{6}$$

where α is the (tangential) momentum accommodation coefficient, equivalent to the fraction of incident gas molecules that 'accommodate' upon impingement with the particle, *i.e.* leave the surface 'diffusely' as opposed to reflecting specularly, and ν is the momentum diffusivity of the prevailing gas mixture. We can then calculate the thermophoretic velocity at every axial position in the flame by setting the momentum accommodation coefficient equal to unity, a plausible assumption (Talbot *et al.*, 1980), calculating the function $(1/T)(dT/dz)$ after smoothing somewhat the experimental temperature measurements, and the corresponding momentum diffusivity at the prevailing gas temperatures[6]. Accordingly, we show in Fig. 3 the negative of V_T superimposed on the experimentally inferred axial gas velocity profile. Intersection of the two curves corresponds to the expected location of the particle stagnation plane based on this kinetic theory prediction. As is apparent from the figure, agreement between experimental measurements and this hybrid theoretical/experimental prediction is very good, indicating that in the present situation isolated single sphere, size independent kinetic theory predictions are rather accurate, even though our "soot" particles are aggregated and distributed in size. The explanation for this morphology and size insensitivity can be found in theoretical studies motivated in part by these experiments, in which we have shown that the orientation-averaged thermophoretic diffusion $<\alpha_T D>$ for aggregated particles is remarkably close to that of the much smaller primary particles themselves, especially in the free-molecule limit (Rosner *et al.*, 1991). We also note that even though the theory used applies strictly to single particles in the free-molecular limit ($Kn \gg 1$), it is also approximately valid down to $Kn_p \cong 0.7$ (Talbot *et al.*, 1980), which corresponds to a particle diameter of 0.39 μm, a size certainly larger than those typical of the TiO_2 aggregated particles generated here.

It remains for us to estimate the *smallest* size particle at which Eq.(6) might be expected to apply. This will establish the range of validity of the present type of analysis, especially with regard to the transport of particles undergoing homogeneous or heterogeneous nucleation in the presence of flame-produced large temperature gradients. This question has been explicitly considered by Garcia-Ybarra and Rosner (1989), who derived a condition for the "particle" to be large enough to be considered effectively motionless when calculating net momentum transfer from impacting gas molecules. They showed that particle displacements between successive gas impacts will be negligible on the scale of the particle dimension, d_p, provided that

$$m_p d_p^3 > (8\pi\sqrt{2})\cdot m_g \sigma_g^2 l_g \tag{7}$$

[6] Equilibrium calculations indicate that at the flame the mole fraction of N_2, H_2O and CO_2 are approximately 0.77, 0.13 and 0.07, respectively. Our momentum diffusivity calculations are based on the assumption that N_2 was the only present species, since some cancellation occurs for the contribution of H_2O and CO_2 having, respectively, lower and higher diffusivity than N_2.

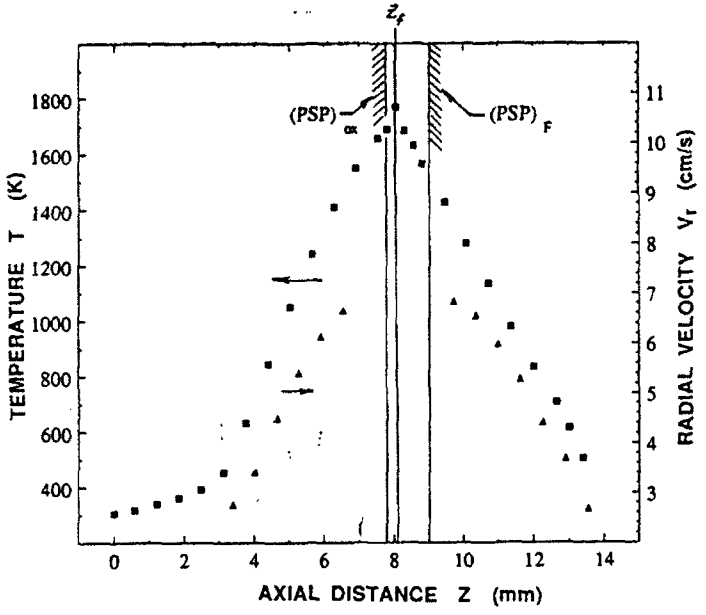

FIGURE 2 N_2-diluted $CH_4(g)/O_2(g)$ flame—Measured temperature and *radial* velocity at a fixed radial position (r = 3.55 mm) as function of the axial distance z from the lower burner mouth.

where σ_g is the effective gas molecule diameter and l_g the corresponding gas mean-free-path. In our N_2-diluted CH_4/O_2 flame we find that this criterion would be satisfied for all dense TiO_2 particles larger than about 2 nm diameter, *i.e.* for particles containing more than about 100 TiO_2 "monomer" units. We conclude that in our flame the free-molecule expression, Eq. (6), for $(\alpha_T D)_p$ should apply to particle sizes covering a diameter range of over two decades between about 2 nm and about 0.4 μm, an impressive domain of validity. For particle sizes below the 2 nm threshold the relevant value of the coefficient $(\alpha_T D)_p$ should be estimated from the theory of thermal (Soret) diffusion in gas mixtures, as summarized by Rosner (1980, 1987). Additionally, it would no longer be valid to neglect the Brownian diffusion of such small "particles" in determining the two-phase flame structure. In principle, this precludes a simple "residence time" analysis for such particles (*cf, e.g.* Zachariah and Semerjian (1989)).

Since, as mentioned above, a loss in light scattering efficiency of TiO_2 particles at high temperatures had been reported (Kennedy, 1982; Witze and Baritaud, 1986), we decided to verify the existence of this particle-free region near the flame by an independent experimental technique to confirm that it was not an artifact of the optical experimental method. For this purpose we rapidly inserted a fine (125 μm diameter) platinum wire into the TiO_2-laden flame and positioned it parallel to the flame axis. After letting a deposit grow on the wire for less than a minute, the probe was quickly withdrawn. Figure 4a is a picture of the deposit grown as seen under an optical microscope. Two regions of relatively thick deposit appear, corresponding to the particle-laden regions; in

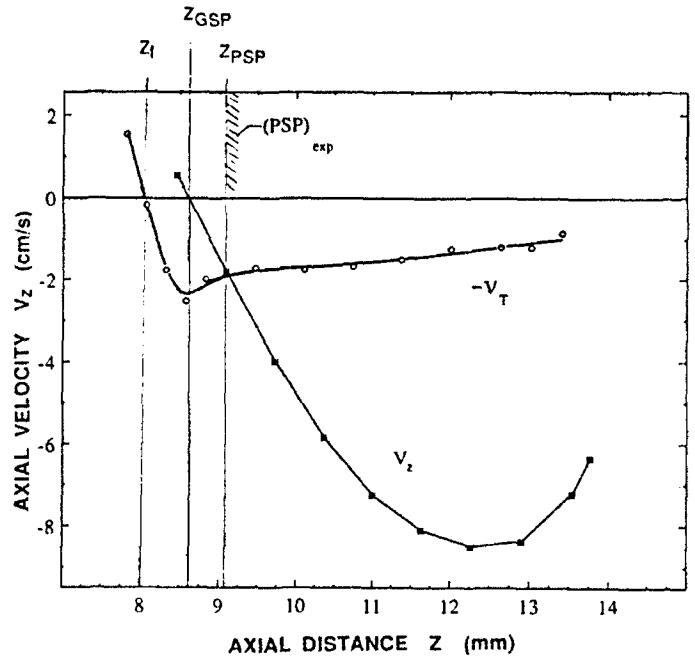

FIGURE 3 N_2-diluted $CH_4(g)/O_2(g)$ flame—Experimentally inferred axial velocity, V_z, and negative of the calculated thermophoretic velocity, $-V_T$, as function of axial distance (from the lower burner mouth).

between one can observe a region with no apparent deposit growth, corresponding to the particle-free region straddling the flame. One can also notice that the deposits grown on the wire do not have sharp boundaries, which is indicative of a "smearing" of the particle stagnation plane, due partly to Brownian motion of the suspended particles, partly to minor fluctuations of the flame during the time over which particles were deposited. It is clear from Fig. 4a that the "smearing" does not seriously compromise the accuracy of our determinations of PSP-locations: for this particular flame, half the smear thickness appears to be on the order of 8% of $|z_{PSP} - z_f|$. These observations and interpretations are summarized in the sketch in Figure 4b.

3.2 He-diluted flame

Encouraged by these results, we decided to verify another aspect of the kinetic theory by dramatically changing the momentum diffusivity of the host gas. To this end, we replaced N_2 with He as diluent and repeated the same set of experiments/calculations. Flow rate conditions needed to be modified because of the very poor stability of the He-diluted flame and, consequently, the flame was operated at a nominal strain rate three times larger than in the nitrogen diluted case. Figure 5 shows corrected temperature measurements as a function of the axial coordinate z, computed from the bottom burner exit. The flame appears much thicker than in the N_2-diluted case (Fig. 2) despite the higher strain rate

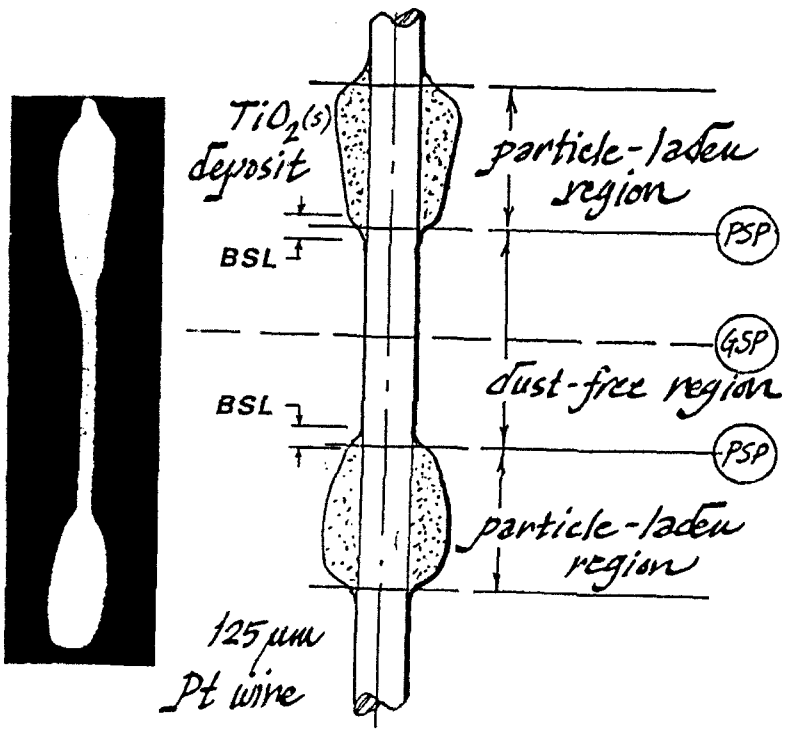

FIGURE 4 a) Shape of TiO_2 particle deposit collected on a 125 μm diam. Pt wire inserted along the axis in the particle-laden flame; b) Interpretation of deposit shape.

of the present case, largely because of the high thermal conductivity of the diluent. The PSP locations are also shown: the corresponding dark zone thickness is 2.9 mm, which results in a repulsion effect even more dramatic than the one observed in the N_2-diluted flame. In the same plot we also show the radial velocity profile, with extrapolated data points at the burner mouths. The radial velocity seems to grow monotonically starting from each burner mouth and moving towards the flame, and peak on the fuel side in agreement with numerical predictions for similar flames (Smooke and Seshadri, 1986). When we attempted to reconstruct the corresponding axial velocity profiles we were confronted with a significant source of error associated with gas composition effects. In fact, for such flames, the molecular weight from burner end to burner end varies by a factor of three and the consequences of gas composition uncertainties on local density and, also, momentum diffusivity calculations are dramatic. Nevertheless, we calculated V_t according to the procedure discussed in Section 2, by relying on the species profiles

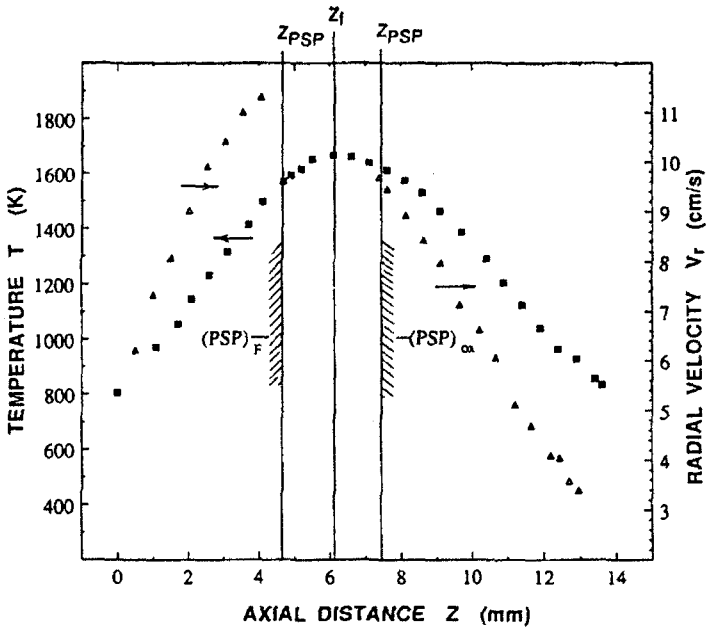

FIGURE 5 He-diluted $CH_4(g)/O_2(g)$ flame—Measured temperature and radial velocity as function of axial distance (from the lower burner mouth).

obtained in numerical calculations on a one-dimensional counterflow flame with the same input conditions as the present one in the limit of infinitely fast chemical kinetics (flame sheet) (Smooke, 1992). Results, here shown again for half the flame region in correspondence of the fuel side, are presented in Fig. 6; notice that the sign of the velocity has been changed with respect to Fig. 3, since in this case the fuel was fed into the lower burner. The intersection of the reconstructed axial velocity profile and the curve of $-V_T$ determined by a procedure analogous to the one described in the nitrogen diluted flame discussion, indicate a PSP-prediction at approximately 4.1 mm above the bottom burner mouth, to be compared with the experimentally measured position of 4.6 mm. The discrepancy may be due not only to the uncertainties mentioned above but also to additional phoretic effects that we shall now address.

3.3 Role of Other Phoretic Mechanisms

Other phoretic effects in addition to thermophoresis can *in principle* act on the particles and complicate the interpretation of the results. They are: diffusiophoresis, electrophoresis and photophoresis. In the first approximation, we shall discuss each of these effects sequentially and independently, i.e. without accounting for "coupling" terms that should be calculated when two or more phoretic effects are acting simultaneously (see, for ex-

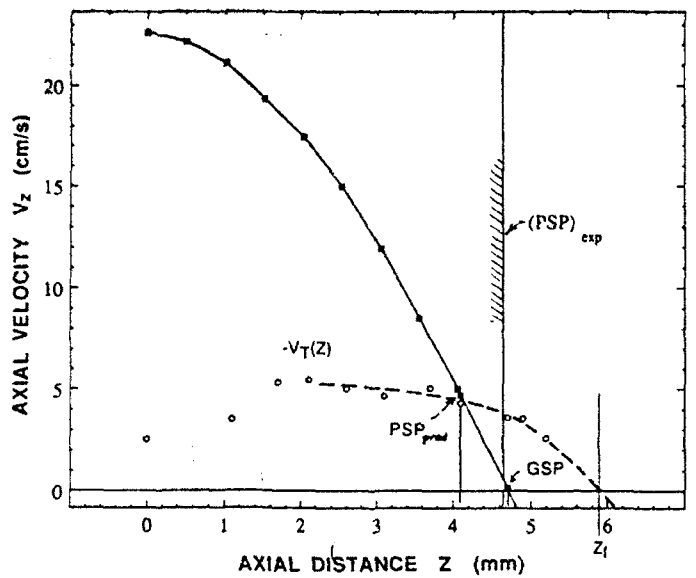

FIGURE 6 He-diluted $CH_4(g)/O_2(g)$ flame—Axial velocity, V_z, and negative of the calculated thermophoretic velocity, $-V_T$, as function of axial distance (from the lower burner mouth).

ample, Annis and Mason, 1975). We conclude that for our N_2-diluted flame experiments these supplementary particle drift mechanisms are indeed negligible.

A particle suspended in an *isothermal* vapor mixture with local species mole fractions y_i and local species diffusion velocities V_i will tend to drift relative to the mean mass motion of the mixture with a velocity (called the "diffusiophoretic velocity"). In the free-molecule limit Waldmann (1966) has shown that this velocity can be expressed as

$$(\mathbf{V}_p)_{diffusioph} = \sum_{i=1}^{N} Y_i \mathbf{V}_i \tag{8}$$

where

$$Y_i \equiv \frac{\left(1+\frac{\pi}{8}\alpha_i\right) M_i^{1/2} y_i}{\sum_j \left(1+\frac{\pi}{8}\alpha_j\right) M_j^{1/2} y_j} \tag{9}$$

can be interpreted as a "pseudo-composition" variable (different from either the local mole fraction or mass fraction), α_i is the momentum accomodation coefficient (defined as in Eq. 6), M_i is the molecular weight. Our previous data analysis has clearly been based on the assumption that the diffusiophoretic velocity at PSP is negligible compared to the *thermophoretic* velocity there, *i.e.*

$$\left|\left(\sum_{i=1}^{N} Y_i V_{i,z}\right)_{PSP}\right| \ll |(V_T)_{PSP}| \tag{10}$$

But, since the RHS is "known" at PSP (see Figs. 3 and 6) to evaluate the possible importance of diffusiophoresis it remains for us to estimate the LHS for both the N_2-diluted and He-diluted flames, using the individual estimates:

$$V_{i,z} \approx \left\{ D_{i-inert} \left(\frac{-1}{y_i} \cdot \frac{dy_i}{dz} \right) \right\}_{PSP} \tag{11}$$

and, say, $\alpha_i \cong 1$ for each species i. Concentration estimates were based on flame "sheet" numerical calculations for the input conditions specified in Table I (Smooke, 1992). The diffusion coefficient appearing in Eq. 10 is the binary diffusion coefficient of species i diffusing in the inert gas as estimated from kinetic theory (Rosner, 1986). This approximation is applicable if the concentration of the inert is much larger than any other species, as verified in the present situation where the inert mole fraction at the PSP was estimated to be larger than 0.8. The characteristic net diffusiophoretic particle velocity calculated in this way (LHS in eq. 10) was found to be less than about 5% of $|V_T|_{PSP}$ (RHS) in the N_2-diluted flame. For the He-diluted flame, on the other hand, the corresponding value is of the same order of magnitude as the thermophoretic velocity. Consequently, diffusiophoretic effects are evidently non-negligible in the latter case.

Electrophoresis is another possible phoretic effect and is here associated with electrical charging of the particles and their drift in the presence of an electrostatic field. Since no external fields were applied to our flames, the only driving force for this phoretic effect is the self-field due to separation of bipolar charges naturally present in any hydrocarbon flame because of chemi-ionization. This charge separation is induced by the thermal motion of charge carriers of disparate molecular mass. An estimate of the importance of this effect can be obtained by comparing the Debye length, the characteristic distance over which charge separation can occur, and the characteristic length scale (O(mm)) over which the discussed particle separation phenomenon is observed. The Debye length, L_D, can be estimated to be:

$$L_D = \sqrt{\frac{\varepsilon_0 k_B T}{2ne^2}} \tag{12}$$

where ε_0 is the vacuum permittivity, k_B is the Boltzmann constant, T is the temperature, n is the ion concentration and e is the elementary charge. For a typical temperature of 1600 K and a maximum ion concentration of $10^{17} m^{-3}$ typical of hydrocarbon flames (Bradley, 1986), the Debye length is estimated at only 6.2 μm, a value over two orders of magnitude smaller than the thickness of the dust-free zone observed in these flames. Thus, electrophoretic effects are expected to be negligible.

With respect to *photophoresis*, associated with particle drift due to gas molecule impacts on a particle that experiences asymmetric radiative heating, Castillo *et al.* (1990) have shown that absorbing supermicron particles can be appreciably influenced by radiating fluxes when the latter are comparable to Fourier fluxes. In the present case this photophoretic contribution is negligible compared to thermophoresis because: a) the particles are too small; b) radiative-to-Fourier energy flux ratios are too small and c) the particles are non-absorbing at the wavelengths of interest.

We conclude that the thermophoretic PSP-analysis of the N_2-diluted flame neglecting other phoretic effects is defensible, but this simplification is unjustified in the He-diluted case where diffusiophoretic effects may be as important as those due to thermophoresis. This situation, combined with the associated concentration uncertainties which influence our calculations of $(V_i)_{PSP}$ and of the local kinematic viscosity, probably account for the poorer agreement between "predicted" and observed PSP-locations in the latter case. Thus, while He dilution indeed increases the displacement $|z_{PSP} - z_f|$ (and the distance

between the two stable PSPs), such flames are evidently less suitable for quantitative experimental determinations of the *thermophoretic* diffusivity.

3.4 Comparisons with Related Studies of Particle Transport in Counterflow Diffusion Flames

After several preliminary reports on this study (*e.g.*, Gomez *et al.*, 1987a, b, 1988) and while this paper was being prepared for publication, we became aware of a parallel investigation of TiO_2-particle-seeded laminar counterflow diffusion flames by Nishioka *et al.* (1991). Motivated by the implications of thermophoresis for flame imaging using micron-size TiO_2 particles, these authors have studied near-stoichiometric N_2-diluted CH_4/O_2 laminar counterflow diffusion flames using a direct particle seeding device in each feed stream. In the absence of direct measurements of gas temperatures or velocities, they relied on computed flow fields, including the effects of finite-rate combustion chemistry. Based on a best-fit to their axial distributions of laser light scattering intensity measurements, they inferred a value of $(\alpha_T D)_p/\nu \approx 0.3$, below the one found in our PSP measurements ($(\alpha_T D)_p/\nu \approx 0.5$). One possible explanation for the discrepancy is the average size of their particles (estimated at about 1 μm diam.) that might have been large enough for a systematic reduction below the free-molecule limit. But, perhaps, a more likely reason might be found in the systematic disagreement between experiments and such buoyancy-free calculations that we observed in our initial approach, as discussed in Section 2, and to which these authors also allude in their report. Indeed, this was the reason why we ultimately chose the more tedious, but more reliable, strictly experimental approach.

Also relevant to our discussion are the recent measurements and ancillary calculations of Zachariah and Semerjian (1989), who studied silane-seeded Ar-diluted hydrogen-oxygen CDFs to produce fine silica particles. While extensive measurements of local temperature, vapor species and particle concentration profiles were reported, evidently no gas or particle *velocity* measurements were made. Accordingly, these authors computed the corresponding axial gas and submicron particle velocities in their flames using a code developed by Smooke (1986). Apart from the aforementioned "bouyancy-induced shift", in effect, our present experiments show that the particle thermophoretic velocity relation used by these authors to interpret their data is reasonably accurate, even for aggregated particles, except that *diffusiophoresis* (Section 3.3) may simultaneously contribute.

3.5 Criteria for the Importance of Thermophoresis on Two-Phase CDF Structure

A number of detailed laboratory studies have been reported on the structure of sooty diffusion flames of pure hydrocarbons burning in air in the vicinity of a porous solid cylinder through which fuel (e.g., C_2H_4) is forced (see, *e.g.* Vandsburger *et al.*, 1984; Axelbaum *et al.*, 1988). These studies, and ancillary numerical computations, reveal that for such systems the diffusion flame sheet is stabilized well out into the O_2-containing stream where the convective velocities through the flame are more than one decade larger than typical thermophoretic velocities. In such a system soot particle thermophoresis, therefore, only begins to make a significant (local) contribution as one approaches the *gas stagnation point*, GSP, and thermophoresis will cause the soot particles to only slightly overshoot GSP on the fuel side. On the other hand, in the seeded and diluted CH_4/O_2 CDFs we have studied and in the seeded, diluted, H_2/O_2 CDFs studied by Katz *et al.* (1990), and Zachariah *et al.* (1989), one can easily show that gas velocities through the flame are *not* large compared to the maximum particle thermophoretic velocities. Indeed, in our N_2-diluted flame the ratio of $|(V_T)_{max}|$ to $|(V_c)_f|$ is seen (Fig. 3) to be about 1.35 and in Flame #1 of Katz and Hung (1990) this ratio is estimated to be about 3. In fact,

in this latter case we estimate that $V_{T,p,max}$ is no less than *ca.* 6.5 cm/s, which should be compared with the H_2-*feed* stream velocity of only 7.1 cm/s! In what follows we identify in terms of a modification of the equivalence ratio parameter, Φ, introduced in Section 2, useful conditions under which non-premixed systems will inevitably display significant thermophoretic effects on the soot-laden flame structure[7], with practical consequences discussed in Sections 3.6 and 3.7. We conclude with comments about the possible relevance of these laboratory steady laminar CDF-studies to applications in which there is turbulent, non-premixed gaseous fuel combustion in the presence of desired or undesired "soot".

Since we will be discussing disparate molecular weight laminar flame systems (*e.g.* H_2/O_2 with Ar dilution in the case of Katz and Hung (1990) and Zachariah and Semerjian (1989)) it is necessary to approximately account for the obvious inequality between the molecular diffusivities D_{F-mix}, D_{O-mix}, $k/(\rho c_p)$ ($\equiv \alpha_{mix}$) and ν_{mix}. To accomplish this, at least insofar as flame position with respect to GSP, for the remainder of this discussion we will therefore define and use the following *effective equivalence ratio parameter*, Φ_{eff}:

$$\Phi_{eff} \equiv \Phi \cdot \left(\frac{D_{F-mix}}{D_{O-mix}}\right)^{2/3} = \frac{(y_F)_{feed}/(y_O)_{feed}}{\nu_{stoich}} \cdot \left(\frac{D_{F-mix}}{D_{O-mix}}\right)^{2/3} \tag{13}$$

We introduce the diffusivity ratio to the 2/3 power exponent to account approximately for the convective laminar flows normal to the stagnation plane. (In ordinary laminar boundary layer flows this is known to reduce the sensitivity of the diffusion fluxes (evaluated, say, at a solid wall) to the molecular diffusivity itself (see, *e.g.*, Section 6.5 of Rosner, 1986)). The indicated Fick diffusivity-ratio correction factor is modest for the present CH_4/O_2 system (estimated to be *ca.* 1.03) and previously studied C_2H_4/O_2 systems (*e.g.* Axelbaum, *et al.*, 1988), but quite appreciable for the Ar-diluted H_2/O_2 system (*e.g.*, factor of *ca.* 2.3 for Flame #1 of Katz and Hung, 1990). On this basis we see that previous studies of soot dynamics in counterflow C_2H_4/air systems were carried out at Φ_{eff}-values between about 7.4 (N_2-diluted C_2H_4) and 14.8, whereas our seeded N_2-diluted CH_4/O_2-CDF measurements, and those of, say, Katz and Hung (Flame #1) were carried out at Φ_{eff}-values of 0.95 and 0.83, respectively. Zachariah (1991) has reported extensive measurements in a SiH_4(g)-seeded, Ar-diluted H_2/O_2 flame with $\Phi_{eff} \approx 1.4$. It is interesting to also note that for the combustion of pure C_2H_2 and C_2H_4 in *pure* O_2 the respective values of Φ_{eff} would be close to the corresponding values of ν_{stoich}^{-1}, *i.e.*, "only" 2.5 and 3.

We are now in a position to evaluate the conditions under which particle thermophoretic velocities in "sooting" CDFs will be appreciable compared to convective gas velocities at the flame location, as well as to qualitatively map out the eligible PSP locations. In Figs. 7a, b we sketch two qualitatively different situations for the structure of CDFs with effective equivalence ratio, Φ_{eff}, not very far from unity. Figure 7a corresponds to the case of a "sharp" flame with modest strain rate parameter, (case A), whereas Fig. 7b corresponds to the converse case of broad flame-large strain rate (case B). Here "sharpness" is defined not in terms of overall width of the temperature profile but in terms of the curvature of the temperature profile at z_f. A criterion for the occurrence of either one of these two regimes can be based on the relative magnitude of the spatial gradient of thermophoretic velocity and gas convective velocity at the flame "surface". For flames without appreciable molecular weight variations the temperature dependence

[7] When T_f is much greater than T_{feed} then a rough criterion for when $|V_{T,max}|$ will not be negligible compared to $|V_c|_f$ is provided by $|V_c|_f \delta_h/\nu_g(T_f) < 1/2$ – i.e. where the indicated Reynolds number based on the velocity $|V_c|_f \approx 2a|z_{GSP} - z_f|$ and slope thickness, δ_h, of the temperature profile is less than about 1/2.

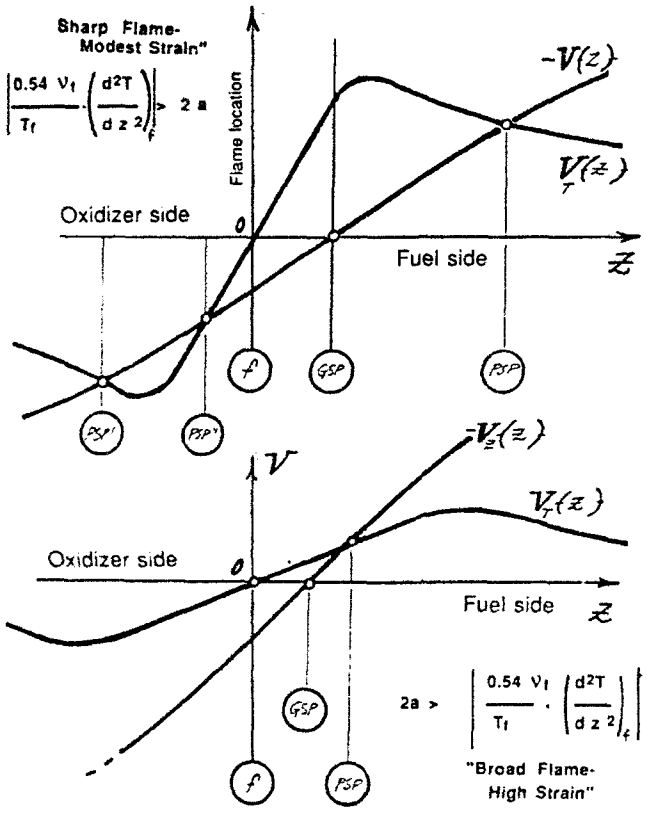

FIGURE 7 Gas velocity and particle thermophoretic velocity profiles in near-stoichiometric (Φ_{eff} near-unity) counterflow diffusion flames. a) "Sharp flame-modest strain" case (Eq(14) with RHS>LHS) with *three* eligible particle stagnation planes. "Broad flame-high strain" case with *one* eligible PSP.

of $\nu(\equiv \mu/\rho)$ appearing in Eq. 6 dominates and one can show that Cases A or B are obtained, depending upon:

$$\left|\frac{0.54\nu_f}{T_f}\left(\frac{d^2T}{dz^2}\right)_f\right| \begin{matrix} ? \\ > \\ < \end{matrix} 2a \tag{14}$$

where $2a = (dV_z/dz)_{GSP}$ and the subscript f denotes the location of the flame—*i.e.* the value of z at which T maximizes (and, of course, $(dT/dz)_f = 0$). One notices that in Case A the $V_T(z)$ locus, calculated from Eq. 6, can exhibit *three* intersections with $V_z(z)$, each corresponding to an eligible particle stagnation plane. Note also that in the flame "sheet" limit $-d^2T/dz^2 \to \infty$ at z_f and the $V_T(z)$-curve locally has the

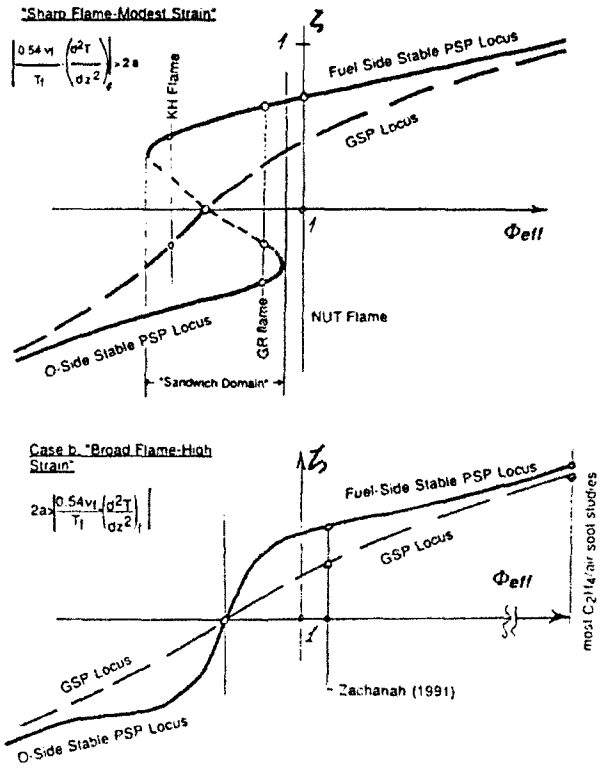

FIGURE 8 Behavior of the locus of dimensionless axial positions of *particle stagnation plane(s)* (PSP) and *gas stagnation plane* (GSP) for laminar counterflow diffusion flames as a function of the effective fuel vapor equivalence ratio, Φ_{eff} (Eq.(13). NUT ≡ Nishioka, Uchida, and Takeno (1991), GR ≡ Gomez and Rosner (1992)

appearance of the Heaviside function, with PSP'' moving to z_f. In contrast, in Fig. 7b only *one* such intersection is possible.

Considering first Case A ("sharp flame-modest strain"), in Fig. 8a we qualitatively[8] sketch the corresponding loci of the dimensionless positions of PSP and GSP with respect to the flame—*i.e.* the values of, say:

$$\zeta_{PSP} \equiv (z_{PSP} - z_f)(2a)/U_F \tag{15}$$

[8] A rigorously calculated diagram for, say, N_2-diluted CH_4/O_2 flames at atmospheric pressure is being constructed and will be discussed in a follow-on paper.

and:

$$\zeta_{GSP} \equiv (z_{GSP} - z_f)(2a)/U_F \tag{16}$$

over a range of effective equivalence ratios, Φ_{eff}, including the singular value of Φ_{eff} (not exactly unity since additional parameters will influence the exact location of the flame relative to GSP) at which ζ_{GSP} goes to zero, *i.e.*, when the flame and GSP are coincident. Note that about this value there is a Φ_{eff}-band within which ζ_{PSP} is multivalued, with the outermost solutions corresponding to the PSP "sandwich" structure we experimentally observed when seeding both streams with $TiCl_4$(g). The dashed locus of PSP locations is found to be *unstable* in the sense that a small particle finding itself at such a point will tend to be displaced, ultimately all the way to either of the extreme PSPs, by the slightest disturbance. Far to either side of the "sandwich structure" Φ_{eff}-band there is only one stable PSP location and this location becomes rather close to the GSP location. Such a diagram will immediately betray the domain in which $|(V_c)_f|$ is not large compared to $|(V_T)|$ since, if ζ is not too large, it is easy to prove that (at any constant Φ_{eff} of interest):

$$\frac{|(V_T)_{PSP}|}{|(V_c)_f|} \approx \frac{|\zeta_{PSP} - \zeta_{GSP}|}{|\zeta_{GSP}|} \tag{17}$$

The previously mentioned criterion that this ratio not be negligibly small is clearly satisfied within the "sandwich"-region, but also for a domain of Φ_{eff}-values on either side of it. Also roughly identified on this qualitative sketch are four typical experimental conditions: the first corresponds to our N_2-diluted CH_4/O_2 system with a stable PSP on the fuel-side and the GSP also on the fuel-side (cf. Fig. 3). The second condition corresponds to that of Ar-diluted H_2/O_2 Flame #1 of Katz and Hung *(1990)* in which there is a stable PSP on the fuel side of the flame, but the GSP is calculated to be on the oxidizer feed side. In both of these flames the RHS of Eq. (17) is clearly $\geq$ O(1). The third condition corresponds to the near-stoichiometric N_2-diluted CH_4/O_2 flame of Nishioka *et al.* (1991) who by running their experiments at an effective fuel equivalence ratio Φ_{eff} of 1.03 reported on only *one* stable PSP, rather than the *two* stable PSP locations we observed at $\Phi_{eff} \cong 0.95$. Also shown is the situation for previous C_2H_4/air CDFs in which Φ_{eff} (even for the diluted C_2H_4 case) is so large that the LHS of Eq. (17) is small (typically $ca.10^{-1}$ in the experiments of Axelbaum *et al.*, 1988).

Figure 8b is a schematic of the "broad flame-high strain rate" situation in which there is no Φ_{eff}-domain of eligible "sandwich" structures and there is only *one* (stable) PSP at all Φ_{eff}-values. Again, there is a domain of Φ_{eff} (on each side of the singular Φ_{eff} corresponding to ζ_{GSP}=0) for which the ratios on either side of Eq. (17) are not small, but outside of this Φ_{eff} interval, for $\Phi_{eff} >> 1$ or $\Phi_{eff} << 1$, thermophoretic effects on the two phase flame structure will be negligible.

In applying these notions to particular engineering situations it should be realized that flame broadening (corresponding to reductions in $(-d^2T/dz^2)_f$) can be due to either reaction "reversibility" or finite-rate chemical kinetics of the heat releasing fuel/oxidizer reaction. In the latter case at any pressure level this broadening would itself be influenced by the prevailing value of the strain rate a (see, *e.g.*: Law, 1988; and Dixon-Lewis, 1990). Indeed, it is well known that above some threshold strain rate the flame can be extinguished altogether.

In *turbulent* diffusion flames the local time-average strain rate, $\bar{a}$, is set by the prevailing value of $(1/2)(\bar{\varepsilon}/\nu)^{1/2}$, where $\bar{\varepsilon}$ is the local time average rate at which the mechanical kinetic energy of turbulence is dissipated by viscous action per unit mass of mixture. In the case of combustion reaction times which are very small compared to the characteristic time $(\bar{a})^{-1}$ (normally itself smaller than the turbulent mixing time $\kappa/\bar{\varepsilon}$) there will be "flamelets"

at a-values on either side of $\bar{a}$ in accord with the prevailing probability density function for the instantaneous $(\bar{\varepsilon}/\nu)^{1/2}$. Thus, when the kinetic processes responsible for particle formation are also sufficiently fast on the time scale of $(\bar{a})^{-1}$ and actual instantaneous PSP-displacements from the flame are sufficiently small[9] on the length scale of, say, $(D/2\bar{a}))^{1/2}$ our laminar CDF flame-structure discussion would carry over to *turbulent* diffusion flames. In other cases the connections are far less direct, but thermophoretic effects on particle transport and their consequences discussed below may still prove to be appreciable at near-unity Φ_{eff}-values.

3.6 Effects of Thermophoresis on the Continuum Radiation From Particle-Laden Flames

One potentially important consequence of the repelling action of high temperature diffusion flame zones is that the peak particle temperatures are inevitably lower than T_f or T_{GSP} as a result of their exclusion from the immediate vicinity of the reaction zone. In accord with the discussion of Section 3.5, this should particularly influence the continuum *radiating power* of particle-laden diffusion-flames operated with an effective equivalence ratio Φ_{eff} not very far from unity, especially when Φ_{eff} is sufficiently below unity to cause the flame to be on the fuel side of the GSP. This is obviously the case in the present experiments whose conditions were deliberately chosen to emphasize thermophoretic effects. For example, in the N_2-diluted CH_4/O_2 flame, operating with $\Phi_{eff} \approx 0.95$, we see that the measured fuel-side PSP temperature is only about 1530K, whereas the measured peak gas temperature T_f, is about 1760K. The associated reduction factor in black-body emissive power at these two temperatures is seen to be about[10] $(1530/1760)^4$=0.57. Other recent laboratory investigations of particle formation in laminar diffusion flames provide an even *more extreme* example, as in the abovementioned $GeCl_4$-seeded H_2/O_2 CDF experiments of Katz and Hung (1990), in which the measured temperature at the estimated PSP was about 1760K (Flame #1 with $\Phi_{eff} \approx 0.8$), compared to a maximum gas temperature T_f of 2750K, with a corresponding 83% reduction in emissive power. Perhaps more importantly from a practical standpoint, the effective equivalence ratio for $TiCl_4$(g) "combustion" in O_2-rich combustion products in the commercial production of TiO_2(s)-pigment (see, *e.g.*, Ulrich (1984)) is also not very far from unity, again suggesting that in such particle synthesis systems phoretic effects on the structure of turbulent "flamelets" should be investigated further. As discussed in Section 3.7 below, additional thermophoretic effects on continuum radiation from particles can also result from alterations of the conditions of particle nucleation, growth, coagulation and/or sintering, as well as other temperature-sensitive phenomena such as NO_x-production. We should also note that our comments on the likely need to include thermophoretic particle "displacement" effects in *turbulent* sooting diffusion flames operating at near-unity Φ_{eff}-values are not necessarily confined to the range of validity of "flamelet" models, although such models certainly provide the

[9] This should be true in systems and at locations in the turbulent flow for which

$$\frac{|\Omega_{PSP} - \Omega_f|}{\left(\overline{\Omega'\Omega'}\right)^{1/2}} \ll \frac{1}{2}\left(\frac{\nu}{\nu_t}\right)^{1/4}$$

where Ω_{PSP} is the mixture fraction associated with the PSP location in a steady *laminar* diffusion flame, ν_t is the local *turbulent* momentum diffusivity and $\left(\overline{\Omega'\Omega'}\right)^{1/2}$ the local *rms* mixture fraction fluctuation.

[10] This fourth power-law would, of course, not apply to submicron ceramics. For example, owing to a temperature dependent emittance, continuum radiation for most macroscopic *ceramics* increase with temperature with an exponent less than 4. Nevertheless, the associated reduction in emissive power is still appreciable

most direct conceptual linkage between laboratory laminar CDF investigations and local conditions in industrial turbulent combustors. If such particle-laden flames are dealt with using probability density function methods (see, *e.g.*, Metternich *et al.*, 1991; Pope, 1985 and 1990; Fox, 1991), as may be necessary due to the comparative slowness of particle synthesis precursor reactions, thermophoretic effects may have to be explicitly included in future "micro-mixing" models.

For ordinary sooty hydrocarbon/air diffusion flames, that operate with Φ_{eff}-values much larger than unity, thermophoretic effects on particle velocities and temperatures are negligible, except for some specific cases of diluted fuel burning in, say, *pure* O_2. For example, we note that Φ_{eff} for an equimolar $C_2H_2 + N_2$ (or combustion products) mixture burning in pure O_2 is only about 1.5, for which thermophoretic effects are likely to be significant.

In closing this section on the consequences of thermophoresis for particle radiation we also note that related studies initiated at this laboratory have shown that since not all soot particles in a population will achieve the same local particle temperatures even the coagulation rate process itself will be modified by the gaseous thermal boundary layer adjacent to each particle, especially in the high pressure ($Kn \ll 1$) limit (Mackowski *et. al.* 1991, 1992, Rosner, *et. al.* 1992). This can lead to significant departures from the more familiar coagulation-aged (self-preserving) soot size distributions that have been observed in low pressure-and/or isothermal-systems.

3.7 Implications of Thermophoresis for Controlled Particle Flame-Synthesis

The broad area of interesting physicochemical processes determining the number, size, composition and morphology of flame-synthesized particles is clearly beyond the scope of this paper; but, in the light of specific experimental studies of seeded-fuel CDF-synthesized particles by Chung and Katz (1985), Katz and Hung (1990), Zachariah and Semerjian (1989), and Zachariah (1991), some potentially useful remarks can be made by exploiting the perspective of Section 3.5.

Particle precursor vapor ("monomer") production by homogeneous pyrolysis and oxidative attack of the vapor "seed" compound are not *directly* influenced by the phenomenon of *particle* thermophoresis. However, peak particle precursor concentrations (*e.g.* SiO(g) monomer), and hence peak supersaturation levels, can be limited by the sink associated with embryonic particle formation and growth itself. Thus, to the extent that embryonic particles are 'retarded' in this nucleation zone, more time is available for them to grow by scavenging vapors and by colliding with one another. Moreover, in CDFs such particles are ultimately provided a rather long dwell time in the local thermal/species environment prevailing at the PSP[11].

While Zachariah (1990, 1991) and other seeded-fuel CDF investigators have demonstrated the penetration of "monomer" *vapor* past PSP, and commented upon the ability of oxidizing species (*e.g.* OH(g) in flames) to diffuse upstream to and even survive beyond PSP, evidently the possibility of some ultrafine particle formation on the flame side of PSP has not been explicitly considered, perhaps in view of the available measurements. We note here that such particles would be driven to the same "stable" PSP, but arrive from the *flame side*, to be ultimately ejected radially outward. Thus, not all particles emerging from a PSP region will have necessarily experienced similar "histories". In particular, those "born and raised" on the flame side would tend to be far less numerous, much smaller, and more highly oxidized than those on the fuel-feed side of PSP.

[11] Zachariah and Semerjian (1989) make the interesting comment that, in some of the flames they investigated in detail, thermophoresis *doubled* the residence time of the particles in the nucleation/coagulation/growth zone.

Another factor expected to influence the particle oxidation state is the position of GSP compared to the PSP and flame. Thus, if Φ_{eff} is large enough to interpose GSP between PSP and the flame, but still not too large compared to unity, then oxidizing species (*e.g.* OH(g)) will be able to reach PSP much more readily—*i.e.*, with the help of *convection* for at least a portion of the journey.

Regarding particle morphology, in many systems particle formation will occur in a region hot enough to pyrolyze and/or oxidize the seed vapor, but not hot enough to give the small particles that nucleate enough "fluidity" (low enough viscosity) to permit their rapid coalescence upon inevitable Brownian coagulation. However, if the level of Φ_{eff} and dilution are suitably chosen, then the temperature at the PSP will be large enough to lead to the strengthening, densification and even spheroidization of such initially "aggregated" particles[12] due to rapid sintering/coalescence near T_{PSP}. Thus, depending upon whether one is interested in high ("specific") surface area, low density possibly branched-chain aggregates, or, instead, low specific area and dense spherical smooth particles, one can establish:

$$T_{PSP} \begin{matrix} ? \\ > \\ < \end{matrix} T_{sint} \tag{18}$$

where T_{sint} is the nominal temperature level required for sufficiently rapid sintering of the particles (of the type and size) of interest. By using multiple "seed" compounds the aggregated particles can be comprised of two (or more) distinct substances (*e.g.* TiO_2 and SiO_2) of limited miscibility, which can exhibit unusual phoretic behavior (see, *e.g.*, Mackowski, 1990). In their H_2-O_2-Ar CDF studies, Hung and Katz (1992) have recently shown that under suitable conditions the *fusion* of such (heterogeneous) aggregates can lead to spherical, *coated* particles (*e.g.* TiO_2 "core" with an outer shell of SiO_2).

Although the emphasis above has clearly been on *fuel*-seeded laminar CDF systems, in many cases (and in our present "double PSP" experiments) "seed" vapor compounds can be added to the *oxidizer* feed stream. Apart from increasing the relative importance of seed vapor oxidation compared to pyrolysis, our previous comments on the importance of the thermophoretically dictated PSP location(s), and associated temperature(s), carry over (*ceteris paribus*) to such "inverse" cases. Moreover, the particle precursor could be a solute (*e.g.* sulfate or nitrate salt(s)) in a solvent (*e.g.* $H_2O(l)$) which is "nebulized" and entrained with the carrier gas or oxidizer (see, *e.g.*, Rosner and Liang, 1988; Matsoukas and Friedlander, 1991). For example, Zachariah and Huzarewicz (1991) recently used this technique, a form of "spray precipitation or pyrolysis", to deliver the precursors of superconducting $Y_1Ba_2Cu_3O_{7-x}$ particles to a laminar (but not counterflow) H_2/O_2 diffusion flame *via* 0.5 μm diameter droplets. To control the exposure of such precursors to both high temperatures and H_2O-vapor an understanding of thermophoretic phenomena and CDF-structure will clearly be essential[13].

Finally, as noted before, some of these ideas will also carry over to *turbulent* diffusion flame reactors, usually of much greater industrial interest, albeit with considerable

[12] A specific example of this kind has, in fact, been reported by Zachariah and Semerjian (1989). These authors have also reported an apparent instance of localized aggregate *breakup*, but the mechanism is, as yet, unclear.

[13] Note that the stopping time, t_p of droplets in this size range is very small on the time scale of $(2a)^{-1}$ so that inertial penetration of the GSP by such droplets could not take place (*cf.* Park and Rosner, 1988). Moreover, such small initial solute droplets also have characteristic evaporation times which are short on the time scale $(2a)^{-1}$. For example, in our N_2-diluted $CH_4(g)/O_2(g)$ CDF each water droplet of 0.5 μm diameter at T_{PSP} would have an evaporative lifetime of only *ca.* 3 μs, and a stopping time of only 0.75 μs, which should be compared to $(2a)^{-1} \approx$ 27 ms.

sacrifice in both particle synthesis controllability and one's ability to predict their performance as fine particle producers. The link with our present discussion and laminar CDF measurements is clearest if the relevant particle precursor kinetics are rapid enough for the turbulent reaction zone to be realistically viewed as an ensemble of quasi-laminar, stretched "flamelets". However, even when kinetic limitations (especially associated with the particle-producing reactions) preclude a self-consistent "flamelet" ensemble description it seems likely that there will remain an interesting Φ_{eff}-interval (on both sides of unity) within which particle thermophoretic effects in these complex "transient laminar flows" will have to be incorporated.

3.8 Implications for Imaging Turbulent Reacting Flows by Laser Sheet Light Scattering

Addition of small light-scattering particles or droplets (or particle precursors) to either the fuel stream or the oxidizer stream is sometimes used in connection with transient light scattering from a sheet laser light source as a strategy to repetitively "image" the instantaneous geometry of the flame surface. This is based on the assumptions that the particles are small enough to a) "follow" the turbulence, and b) evaporate (or sublime) *upon reaching the flame zone*[14]. However, our discussion above (Section 3.5) reveals that even though the first criterion may be amply satisfied there may be non-negligible systematic differences between the position at which the small particles (droplets) disappear (near PSP) and the flame "surface" itself (*i.e.* in CDF-notation: $|z_{PSP} - z_f|$ may be too large compared to $(\Delta z)_{rxn}$ (where, say, $(\Delta z)_{rxn} \equiv 2\cdot|(dT/dz)_{max}|/|(d^2T/dz^2)_f|$, and even the radius of curvature of the flame "surface". We conclude that the information obtained from such flame surface "imaging" techniques should be used without correction only if this "thermophoretic displacement criterion" is clearly met, in addition to the more obvious criterion that the characteristic particle "stopping time" (see, e.g., Rosner (1986, 1990), page 374ff) is small on the scale $\kappa_f/\bar{\varepsilon}$ or, even $(\bar{\varepsilon}/\nu)^{-1/2}$, characterizing the local turbulence. Of course, there will be no thermophoretic displacements in such nearly isothermal "slow" particle-forming systems as $HCl(g) + NH_3(g) \rightarrow NH_4Cl(s)$, as recently studied by Kennedy and Chevalier, 1991 using light scattering techniques, with an eye toward ultimately using this type of reaction for "marking regions of (a turbulent) flow where reaction took place."

3.9 Applications to Particle/Gas Separation

One possible class of practical applications of the phenomenon described above is the "thermophoretic gas cleaner", *i.e.* a gas/solid separator suited to the continuous removal of submicron particles from even heavily loaded dusty gas streams (Park and Rosner, 1987). Considering that our dust-free regions measured 1.25 and 2.89 mm in thickness, it is feasible that thin skimmer discs centered coaxially with the burner and placed in the vicinity of the particle stagnation plane(s) and gas stagnation plane would divide such steady axisymmetric stagnation-flows into a clean, particle-free (and heated) part and a dust-enriched portion, with potential practical applications in similar combustion environments.

4. CONCLUSIONS

To develop and demonstrate a tractable laboratory technique, and provide needed high temperature data on the thermophoretic properties of combustion generated fine particles

[14] Nishioka *et al.* (1991) have reported evidence of "thermophoretic focusing" of particles upstream of the tips of conical flames which have been particle-seeded.

(including aggregates), we have investigated experimentally the formation of a dust-free layer in seeded laminar counterflow diffusion flames due to the thermophoretic repulsion of particles near the diffusion flame "sheet". This phenomenon is shown to lead to a sharply defined, essentially particle-poor zone, easily detected using laser sheet light scattering techniques. By exploiting this particle separation phenomenon, we have determined the particle thermophoretic diffusivity, $(\alpha_T D)_p$, and compared it with single-sphere predictions from kinetic theory in the free-molecule limit. Experiments and calculations indicate quantitative agreement between our measurements and kinetic theory predictions for isolated primary particles in the case of $CH_4/O_2/N_2$ gaseous diffusion flames. Replacement of N_2 with He as diluent resulted in a much thicker and more easily measured particle-free layer, but yielded only qualitative agreement with the abovementioned theory, partly because of uncertainties in the local gas compositions in this disparate molecular weight flame and partly because of concurrent diffusiophoretic effects estimated to be as important as thermophoresis. Particle deposit growth on an axially mounted fine platinum wire confirmed the existence of the optically measured particle-free zone straddling the sharp diffusion flame, and also revealed a smearing of the particle stagnation planes, probably due, at least in part, to particle Brownian motion. We also show that in many laminar or turbulent particle-laden diffusion flames operated near-stoichiometric conditions (based on fuel and oxidizer compositions), including those used to synthesize valuable ultra-fine powders, particle thermophoretic velocities can be large enough compared to local gas velocities through the flame to produce appreciable effects on particle radiant emission and particle properties.

A practical application of the phase separation phenomenon observed, exploited, and described here could be in a "thermophoretic gas cleaner", well-suited to the continuous removal of submicron particles from even heavily loaded dusty gas streams to which heat must be added (Park and Rosner, 1987).

In conclusion, it should be recognized that in these experiments, and the accompanying analysis, we have deliberately focused attention on thermophoretic phenomena which are insensitive to "soot" particle size, composition and morphology. However, with the insights gained here, and the intriguing examples provided by the recent work of Katz *et al.* (1985, 1989, 1991), Zachariah *et al.* (1989, 1991), it would now be fruitful to use the well-defined and easily controlled environment provided by laminar counterflow diffusion flames (CDFs) to examine aspects of particle birth and evolution clearly beyond the stated scope of this paper—*i.e.* those factors determining how flame-synthesized fine particles will be "distributed" with respect to aggregate "size" (*e.g.* number of attached primary particles), primary particle size, chemical composition (stoichiometry) and morphology at each position in the flames. Such a level of understanding could then be translated into efficient flame reactor design and operating strategies for producing "engineered" fine particles—including the use of compact, high-output turbulent[15] flow reactors under non-premixed feed conditions.

ACKNOWLEDGEMENTS

The authors would like to thank Prof. M.D. Smooke, (ME Department, Yale University), for numerical calculations performed in the preliminary phase of this investigation, and Miss Piraye Yaras for helping in the experiments on He-diluted flames. We have also benefited from useful discussions and/or correspondence

[15] Some aspects of the evolution behavior of particle populations in quasi-one dimensional, statistically steady *turbulent* duct flows have been studied recently by Rosner and Tassopoulos (1991), and Xiong and Pratsinis (1991). However, regarding the time-averaged birth rate and growth of such particles, some of the simplifying assumptions underlying the predictions of Xiong and Pratsinis (1991) are not likely to be valid in *non-premixed* turbulent reactors of industrial interest.

with Drs. J. Katz, M. Zachariah, R.O. Fox and D.W. Mackowski. It is a pleasure to acknowledge the U.S. Air Force Office of Scientific Research (Grants # 89-0223 and 91-0170), the U.S. Department of Energy (Grants DE-FG22-86-PC90756 and DE FG22-90PC90099) and HTCRE Laboratory Industrial Affiliates (Du Pont, Shell, Union Carbide, GE) for the financial support that made this investigation and its ultimate publication possible.

REFERENCES

Annis, B.K. and Mason, E.A. (1975). Theory of Thermodiffusiophoresis of Spherical Aerosol Particles, *J. Aerosol Sci.* (Pergamon) **6**, 105-117.

Axelbaum, R.L., Flower, W.L. and Law, C.K. (1988). Dilution and Temperature Effects of Inert Addition on Soot Formation in a Counterflow Diffusion Flame. *Comb. Sci. Tech.* **61**, 51-73.

Bilger, R.W. (1988). The Structure of Turbulent Non-Premixed Flames. Proc. 22nd Symposium (International) on Combustion, Combustion Institute, Pittsburgh, PA, 475-488.

Bradley, D. (1986). The Effects of Electric Fields on Combustion Processes, in *Advanced Combustion Methods.* (F.J. Weinberg, ed.), Academic Press, London.

Castillo, J.L., Mackowski, D.W. and Rosner, D.E. (1990). Photophoretic Modification of the Transport of Absorbing Particles Across Combustion Gas Boundary Layers. *Prog. Energy Combust. Sci.* **16**, 253-260.

Chung, S-Y. and Katz, J.L. (1985). The Counterflow Diffusion Flame Burner: A New Tool for the Study of the Nucleation of Refractory Compounds. *Combust. Flame* **61** (3), 271-284.

Dixon-Lewis, G. (1990). Structure of Laminar Flames. *Proc. 23rd Symposium (International) on Combustion*, The Combustion Institute, Pittsburgh, PA, 305-324.

Dobbins, R.A. and Megaridis, C.M. (1987). Morphology of Flame-Generated Soot as Determined by Thermophoretic Sampling. *Langmuir* (ACS) **3**, 254-259.

Eisner, A.D. and Rosner, D.E. (1985). Experimental Studies of Soot Particle Thermophoresis in Non-Isothermal Combustion Gases Using Thermocouple Response Techniques. *Combust. Flame.* **61**, 153-166.

Eisner, A.D. and Rosner, D.E. (1986). Experimental and Theoretical Studies of Submicron Particle Thermophoresis in Combustion Gases. *PCH-PhysicoChem Hydrodyn.* (Pergamon) **7** (2/3), 91-100.

Fox, R.O. (1992) Fokker-Planck Closure for Turbulent Molecular Mixing: Passive Scalars, *Phys. Fluids A.* (in press)

Friedlander, S.K., Fernandez de la Mora, J. and Gökoğlu, S.A. (1988). Diffusive Leakage of Small Particles Across the Dust-Free Layer Near a Hot Wall. *J. Colloid Interface Sci.* **125**, 351-355.

Garcia-Ybarra, P. and Rosner, D.E. (1989). Thermophoretic Properties of Nonspherical Particles and Large Molecules. *AIChE J.* **35** (1), 139-147.

Gökoğlu, S.A. and Rosner, D.E. (1984). Correlation of Thermophoretically-Modified Small Particle Diffusional Deposition Rates in Forced Convection Systems with Variable Properties, Transpiration Cooling and/or Viscous Dissipation. *Int. J. Heat Mass Transfer* **27**, 639-645.

Gökoğlu, S.A. and Rosner, D.E. (1986). Prediction and Rational Correlation of Thermophoretically Reduced Particle Mass Transfer to Hot Surfaces Across Laminar or Turbulent Forced-Convection Gas Boundary Layers. *Chem. Engrg. Commun.* **44**, 107-119.

Gomez, A., Smooke, M.D. and Rosner, D.E. (1987a). Counterflow Diffusion Flames: A New Tool for Estimating Fine Particle Thermophoretic Diffusivities. Presented at Eastern States Section: Combustion Institute; 20th Fall Technical Meeting: Chemical and Physical Processes in Combustion; Nov. 2-6, 1987; National Bureau Stds., Gaithersburg, MD; also: Paper 26f, AIChE; 1987 Annual Meeting, New York City, NY.

Gomez, A., Smooke, M.D. and Rosner, D.E. (1988). Application of Counterflow Diffusion Flames to the Determination of Particle Thermophoretic Diffusivities. Poster: *22nd Symposium (Int.) on Combustion*, Seattle, WA.

Hahn, W.A., Wendt, J.O. and Tyson, T.J. (1981). Analysis of the Flat Laminar Opposed Jet Diffusion Flame with Finite Rate Detailed Chemical Kinetics. *Comb. Sci. Tech.* **27**, 1-17.

Hung, C-H and Katz, J.L. (1992). Formation of Mixed Oxide Powders in Flames. I. TiO_2-SiO_2. *J. Materials Res.* **7** (7) 1861-1869.

Hung, C-H, Miquel, P.F. and Katz, J.L. (1992). Formation of Mixed Oxide Powders in Flames. II. SiO_2-GeO_2 and Al_2O_3-TiO_2. *J. Materials Res.* **7** (7) 1870-1875.

Katz J.L. and Hung (1990). Initial Studies of Electric Field Effects on Ceramic Powder Formation in Flames. *Proc. 23rd Symposium (Int.) on Combustion*, Combustion Institute, Pittsburgh, PA, 1733-1738.

Katz, J.L. and Hung C-H. (1992). Ultrafine Refractory Particle Formation in Counterflow Diffusion Flames. *Comb. Sci. Tech.* **82**, 169-183.

Kennedy, I.M. (1982). Some Aspects of Seeding Flames with Refractory Oxide Particles. *Comb. Sci. Tech.* **27**, 247-251.

Kennedy, I.M. and Chevalier (1991). Aerosol Formation in an Isothermal Stagnation Flow. *Experiments in Fluids* (Springer Verlag) **11**, 87-92.

Kim, B.S., Travelho, J., Jagoda, J.I. and Zinn, B.T. (1984). Soot Production in an Opposed Flow Polymer Diffusion Flame. *Proc. 20th Symposium (International) on Combustion*, Combustion Institute, Pittsburgh PA, 1113-1120.

Law, C.K. (1988). Dynamics of Stretched Flames. *Proc. 22nd Symposium (International) on Combustion*, Combustion Institute, Pittsburgh, PA, 1381-1402.

Liñan, A. (1974). The Asymptotic Structure of Counterflow Diffusion Flames for Large Activation Energies. *Acta Astronautica* (Pergamon) **1**, 1007-1039.

Mackowski, D.W. (1990). Phoretic Behavior of Asymmetric Particles in Thermal Non-Equilibrium with the Gas: Two Sphere Aggregates. *J. Colloid Int. Sci.* **140** (1), 138-157.

Mackowski, D.W., Tassopoulos, M. and Rosner, D.E. (1991). Effect of Radiative Heat Transfer on the Coagulation Rates of Combustion-Generated Particulates. Presented at the Central States Section Meeting/The Combustion Institute, Nashville, TN, April 21-24, 1991; expanded version prepared for submission to *Aerosol Sci. Tech.* (1992).

Makel, D.B. and Kennedy, I.M. (1992). Experimental and Numerical Investigation of Soot Deposition in Laminar Stagnation Point Boundary Layers. *Proc. 23rd Symposium (International) on Combustion*, Combustion Institute, Pittsburgh, PA, 1551-1557.

Matsoukas, T. and Friedlander, S.K. (1991). Dynamics of Aerosol Agglomerate Formation, *J. Colloid Int. Sci.* **146** (2), 495-506.

Megaridis, C.M. and Dobbins, R.A. (1990). Morphological Description of Flame-Generated Materials. *Combust. Sci. Technol.* **71**, 95-109.

Metternich, M., Kollmann, W., Kennedy, I.M. and Chen J-Y. (1991). PDF Prediction of Sooting Turbulent Flames. AIAA Paper No. 91-0481, 29th Aerospace Sci. Mtg., Reno NV; see also, Proc. Heidelberg (Nov. 1991) Workshop: *Soot Modeling*, Springer-Verlag (in press).

Nishioka, M., Uchida, N. and Takeno, T. (1991). Thermophoretic Behavior of Submicron Particles in Diffusion Flames, *Proc. 13th ICODERS Meeting*, Nagoya (1991) (AIAA Series) in press.

Pandya, T.P. and Weinberg, F.J. (1964). The Structure of Flat Counterflow Diffusion Flames. *Proc. Roy. Soc. A.* **279**, 544-561.

Park, H.M. and Rosner, D.E. (1987). Thermophoretically-Induced Phase-Separation in Highly Mass-Loaded 'Dusty' Gas Mixtures. Yale Univ., HTCRE Lab. Public. No. 162.

Peters, N. (1991). Length Scales in Laminar and Turbulent Flames. *Numerical Approaches to Combustion Modeling* (E.S. Oran and J.P. Boris, eds.), Vol. 135, Progress in Aeronautics and Astronautics, AIAA (Washington D.C.), 155-182.

Pope, S.B. (1990). Computations of Turbulent Combustion: Progress and Challenges. *Proc. 23rd Symposium (International) on Combustion*, The Combustion Institute, Pittsburgh, PA, 591-612.

Pope, S.B. (1991). Combustion Modeling Using Probability Density Function Methods. *Numerical Approaches to Combustion Modeling* (E.S. Oran and J.P. Boris, eds.), Vol. 135, Progress in Aeronautics and Astronautics, AIAA (Washington D.C.), 349-364.

Roquemore, W.M., Tankin, R.S., Chiu, H.H. and Lottes, S.A. (1986). A Study of a Bluff-Body Combustor Using Laser Sheet Lighting. *Exp. Fluids.* **4**, 270-278.

Rosner, D.E. (1980). Thermal (Soret) Diffusion Effects on Interfacial Mass Transport Rates. *PCH PhysicoChem. Hydrodyn.(Pergamon)* **1**, 159-185.

Rosner, D.E. (1986). *Transport Processes in Chemically Reacting Flow Systems.* Butterworth-Heinemann, Stoneham, MA. (Third Printing, 1990)

Rosner, D.E. (1987). Mass Transfer Across Combustion Gas Thermal Boundary Layers—Power Production and Materials Processing Implications, in: *Heat Transfer in Fire and Combustion Systems*, ASME HTD Publication No. 45, 3-8.

Rosner, D.E. and Kim, S.S. (1984). Optical Experiments on Thermophoretically Augmented Submicron Particle Deposition from 'Dusty' High Temperature Gas Flows. *Chem. Eng. J.* (Elsevier) **29**, 147-157.

Rosner, D.E. and Park, H.M. (1988). Thermophoretically Augmented Mass, Momentum and Energy Transfer Rates in High Particle Mass-Loaded Laminar Forced Convection Systems. *Chem. Eng. Sci.* **43** (10), 2689-2704.

Rosner, D.E., Mackowski, D.W. and Garcia-Ybarra, P. (1991). Size- and Structure-Insensitivity of the Thermophoretic Transport of Aggregated 'Soot' Particles in Gases. *Combust. Sci. Technol.* **80**, 87-101.

Rosner, D.E., Mackowski, D.W., Tassopoulos, M., Castillo, J.L. and Garcia-Ybarra, P. (1992). Effects of Heat Transfer on the Dynamics and Transport of Small Particles Suspended in a Gas. *I&EC-Research* (ACS) **31**, 760-769.

Rosner, D.E. and Tassopoulos, M. (1991). Correction for Sampling Errors Due to Coagulation and Wall Losses in Laminar and Turbulent Tube Flow: Direct Solution of Canonical 'Inverse' Problem for Log-Normal Size Distributions. *J. Aerosol Sci.* **22** (7), 843-867.

Sick, V. (1990). Two-Dimensional Laser Diagnostics and Modeling of Counterflow Diffusion Flames. *Proc. 23rd Symposium (International) on Combustion, Combustion Institute*, Pittsburgh PA, 495-501.

Smooke, M.D., Puri, I.K. and Seshadri, K. (1986). A Comparison Between Numerical Calculations and Experimental Measurements of the Structure of a Counterflow Diffusion Flame Burning Diluted Methane

in Diluted Air. *Twenty-first Symposium (International) on Combustion*, Combustion Institute, Pittsburgh PA, 1783.

Smooke, M.D. (1991). Numerical Modeling of Laminar Diffusion Flames. Numerical Approaches to Combustion Modeling (E.S. Oran and J.P. Boris, eds.), Vol. 135, *Progress in Aeronautics and Astronautics*, AIAA (Washington D.C.), 183-223.

Smooke, M.D. (1992). Private Communication.

Talbot, L., Cheng, R.K., Schefer, R.W. and Willis, D.R. (1980). Thermophoresis of Particles in a Heated Boundary Layer. *J. Fluid. Mech.* **101**, 737-758.

Tsuji, H. (1982). Counterflow Diffusion Flames. *Progress Energy Comb. Sci.* **8**, 93-119.

Ulrich, G. (1984). Flame Synthesis of Fine Particles. *Chem. Eng. News. (ACS)* **62** (32), 22.

Vandsburger, U., Kennedy, I.M. and Glassman, I. (1984). Sooting Counterflow Diffusion Flames With Varying Velocity Gradients, *20th Symposium (International) on Combustion*, Combustion Institute, Pittsburgh PA, 1105.

Waldmann, L. and Schmitt, K.H. (1966). Thermophoresis and Diffusiophoresis of Aerosols, Chap. 6 in: *Aerosol Sci.* (C.N. Davies ed.), Academic Press, 137-162.

Witze, P.O. and Baritaud, T.A. (1986). Particle Seeding for Mie Scattering Measurements in Combustion Flows, Sandia Report SAND85-8912.

Xiong, Y. and Pratsinis, S.E. (1991). Gas Phase Production of Particles in Reactive Turbulent Flows. *J. Aerosol Sci.* **22** (5), 637-655.

Zachariah, M.R. (1991), Chemistry of Silane Oxidation and Pyrolysis During Particle Formation: Comparison With *In-Situ* Measurements (submitted).

Zachariah, M.R., Chin, D., Semerjian, H.G. and Katz, J.L. (1989). Silica Particle Synthesis in a Counterflow Diffusion Flame Reactor. *Combustion and Flame* **78**, 287-298.

Zachariah, M.R., Chin, D., Semerjian, H.G. and Katz, J.L. (1989). Dynamic Light Scattering and Angular Dissymmetry for the *In Situ* Measurement of Silicon Dioxide Particle Synthesis in Flames. *Appl. Opt.* **28**, 530-536.

Zachariah, M.R. and Joklik (1990). Multiphoton Ionization Spectroscopy Measurements of Si-Atoms During Vapor Phase Synthesis of Ceramic Particles; *J. Appl. Phys.* **68**, 311

Zachariah, M.R. and Semerjian, H.G. (1989). Simulation of Ceramic Particle Formation: Comparison with *In Situ* Measurements. *AIChE J.* **35** (12), 2003-2012.

Zachariah, M.R. and Huzarewicz, S. (1991), *J. Materials Res.* **6** (2) 264-269.

REPORT DOCUMENTATION PAGE

Form Approved
OMB No. 0704-0188

1. AGENCY USE ONLY (Leave blank)	2. REPORT DATE	3. REPORT TYPE AND DATES COVERED
	1993	Book chapter (Reprint)

4. TITLE AND SUBTITLE
RECENT STUDIES OF THE KINETICS OF SOLID BORON GASIFICATION BY $B_2O_3(g)$ AND THEIR CHEMICAL PROPULSION IMPLICATIONS

5. FUNDING NUMBERS
PE - 61102F
PR - 2308
SA - BS
G - AFOSR 91-0170

6. AUTHOR(S)
ALESSANDRO GOMEZ, DANIEL E. ROSNER AND RONI ZVULONI

7. PERFORMING ORGANIZATION NAME(S) AND ADDRESS(ES)
HIGH TEMPERATURE CHEMICAL REACTION ENGINEERING LABORATORY
YALE UNIVERSITY
BOX 2159, YALE STATION
NEW HAVEN, CONNECTICUT 06520 U.S.A.

8. PERFORMING ORGANIZATION REPORT NUMBER

9. SPONSORING/MONITORING AGENCY NAME(S) AND ADDRESS(ES)
AFOSR/NA
110 Duncan Avenue, Suite E115
Bolling AFB DC 20332-0001

10. SPONSORING/MONITORING AGENCY REPORT NUMBER

11. SUPPLEMENTARY NOTES
in *Proc. 2d Int. Sympos. on Special Topics in Chemical Propulsion*: (K.K.Kuo, R.Pein, eds) **Combustion of Boron-Based Solid Propellants and Solid Fuels**, pp 113-132. *CRC* Press (Boca Raton)

12a. DISTRIBUTION/AVAILABILITY STATEMENT
Approved for public release; distribution is unlimited

12b. DISTRIBUTION CODE

13. ABSTRACT (Maximum 200 words)

Interfacial kinetics are likely to play a rate-limiting role in the combustion of small boron particles and yet little is known about boron gasification by $B_2O_3(g)$, which may be important because of its formation from O_2 in the boundary layer near the gasifying surface. For these reasons, intrinsic kinetics of the high temperature $B_2O_3(g)/B(s)$ reaction were investigated utilizing newly designed flow reactor techniques, together with a 'real-time' (boron) element detection technique based on microwave-induced plasma emission spectroscopy. Known amounts of the gaseous reactant B_2O_3 were generated using a resistively heated Knudsen effusion source operating in a high velocity argon gas background. Reaction rate measurements on a joule-heated boron filament covered the surface temperature interval 1330-2050 K at B_2O_3 partial pressures between $6 \cdot 10^{-3}$ and $6 \cdot 10^{-2}$ Pa.

These kinetic data are used to discuss the expected sequence of rate-controlling processes for the combustion of an individual B(s) particle in air under typical ramjet conditions

14. SUBJECT TERMS
boron combustion, boron particle ignition, extinction; flow reactor, gasification kinetics, boric oxide vapor, plasma emission spectroscopy

15. NUMBER OF PAGES
11

16. PRICE CODE

17. SECURITY CLASSIFICATION OF REPORT	18. SECURITY CLASSIFICATION OF THIS PAGE	19. SECURITY CLASSIFICATION OF ABSTRACT	20. LIMITATION OF ABSTRACT
Unclassified	Unclassified	Unclassified	UL

from : pp. 113 – 132

Combustion of

Boron-Based Solid Propellants and Solid Fuels

Edited by

Kenneth K. Kuo

The Pennsylvania State University, USA

Associate Editor

Roland Pein

DLR, Germany

begell house

CRC

CRC Press 1993

Boca Raton Ann Arbor London Tokyo

RECENT STUDIES OF THE KINETICS OF SOLID BORON GASIFICATION BY $B_2O_3(g)$ AND THEIR CHEMICAL PROPULSION IMPLICATIONS

ALESSANDRO GOMEZ[1], DANIEL E. ROSNER[2] AND RONI ZVULONI[3]

High Temperature Chemical Reaction Engineering Laboratory
Yale University, New Haven CT 06520-2159 Y.S., U.S.A.

ABSTRACT

Interfacial kinetics are likely to play a rate-limiting role in the combustion of small boron particles and yet little is known about boron gasification by $B_2O_3(g)$, which may be important because of its formation from O_2 in the boundary layer near the gasifying surface. For these reasons, intrinsic kinetics of the high temperature $B_2O_3(g)/B(s)$ reaction were investigated utilizing newly designed flow reactor techniques, together with a 'real-time' (boron) element detection technique based on microwave-induced plasma emission spectroscopy. Known amounts of the gaseous reactant B_2O_3 were generated using a resistively heated Knudsen effusion source operating in a high velocity argon gas background. Reaction rate measurements on a joule-heated boron filament covered the surface temperature interval 1330-2050 K at B_2O_3 partial pressures between $6{\cdot}10^{-3}$ and $6{\cdot}10^{-2}$ Pa. Results revealed remarkably high reaction probabilities over a broad temperature range (*ca.* 1400-2000 K) with a maximum close to unity, at *ca.* 1950 K, much higher than that for the $O_2(g)/B(s)$ reaction and comparable to that previously observed (locally) for O-atom attack of boron. Transition conditions for 'passivation' of the $B_2O_3(g)/B(s)$ reaction were identified experimentally and found to be in qualitative agreement with quasi-equilibrium model predictions, which also indicate that the dominant product species in the "active" regime were $(BO)_2$ over the intermediate temperature regime, *ca.* 1050-1500 K, and BO in the high temperature regime, *ca.* 1500-2200 K. Mechanistic implications of these results include a high sticking (O-atom deposition) probability for B_2O_3 on solid boron, but with a fall-off above ca. 2000 K, causing ε to drop precipitously despite the stability of BO(g) at these temperatures. These kinetic data are used to discuss the expected sequence of rate-controlling processes for the combustion of individual B(s) particles in

[1] Assistant Professor, Department of Mechanical Engineering.

[2] Professor, Department of Chemical Engineering; Director HTCRE Laboratory.

[3] Doctoral Research Student, Department of Chemical Engineering; present address: Intel Corporation, Jerusalem, Israel.

air under typical ramjet conditions. While most previous boron particle combustion and extinction laboratory experiments have been performed in the regime of gas-phase *diffusion control*, under conditions of actual ramjet interest the *gas/solid kinetics* for the efficient B_2O_3(g)/B(s) reaction and the slower O_2(g)/B(s) reaction, as well as non-continuum transport effects, become rate-limiting.

1. INTRODUCTION

Elemental boron has been long recognized as a potentially very attractive jet propulsion fuel because of its high volumetric energy density, yet practical difficulties associated with particle ignition, combustion and oxide condensation problems still impede its exploitation. For most practical fuel formulations boron eventually burns as a solid particle at typical anticipated operating conditions (Glassman et al., 1985). Constraints on combustor residence times impose particle diameters sufficiently small for the burning to be *kinetically limited* during most, if not all, of the burning time. Nonetheless, probably because of advantages from an experimental standpoint, research in the late 1960s and early 1970s concentrated on *diffusion-controlled* combustion (Macek and Semple, 1969 and 1971; Mohan and Williams, 1972; King, 1972 and 1974), revealing only some of the features of boron particle combustion in such environments. Two stages were identified: an ignition stage, involving the removal of a pre-existing condensed B_2O_3 layer on the surface which must melt and ultimately evaporate for the underlying semi-metal to burn rapidly; a second stage of full fledged combustion, during which diffusion-limited quasi-steady surface oxidation of the bare boron particle takes place. The combustion stage presents similarities with solid carbon combustion since ambient O_2 molecules can react in the gas phase with boron-suboxides to form B_2O_3, which, in turn, may act as the main surface 'gasifier', i.e. B_2O_3 in B-gasification plays the same role as CO_2 in carbon gasification. Because of vapor phase "interception" by suboxide vapors generated at the surface, O_2 does not necessarily reach the particle surface. One of the reasons why the present study of B_2O_3 (g)/B(s) reaction kinetics was undertaken was to help understand this regime of boron combustion and what role interfacial kinetics would play at intermediate particle sizes. For still smaller particle sizes this picture is expected to break down since homogeneous kinetics begins to limit the production of B_2O_3(g) in the boundary layer and O_2(g) may be able to reach the surface and become the dominant surface gasifier. Moreover, heat and mass transfer to/from the particle exhibit new characteristics in the rarefied regime achieved when the particle diameter becomes comparable to the gas mean-free-path and the individual particle flow field is no longer continuum, in which case interfacial O_2(g)/B(s) kinetics will become decisive. While not emphasized in previous work on B(s) particle extinction, under kinetically controlled surface oxidation conditions,

B_2O_3(c) may be present on the boron particle surface as a continuous sub-microscopic layer or as 'patches', even at temperatures higher than the (equilibrium) condensation temperature. As the energy balance dictates lower particle temperatures, extinction due to surface repassivation may ensue. Only by experimentally studying the surface reaction kinetics can we reliably determine the conditions leading to 'bare' or 'covered' surface behavior in such non-equilibrium cases.

In addition to a propulsion motivation, a study of the intrinsic kinetics of the high temperature reaction of B_2O_3(g) with solid boron presents some challenging questions of kinetic nature. High temperature chemical reactions of refractory solids with comparatively 'simple' gaseous reactants like O_2, Cl_2, F_2 and, more recently, with their respective atoms, have been experimentally studied in the past (Rosner and Allendorf, 1968, 1969 and 1971). However, less is known or can be predicted about high temperature reactions of structurally more complicated molecules with the same refractory solids. The present system is interesting for comparative purposes precisely because as an oxygen "source" B_2O_3(g) is more complicated than the 'simple' O_2 or O reactants and yet it does not add new chemical elements to the basic B-O system. For "steric" reasons which impede chemisorption, B_2O_3 may not be an efficient O-atom source. On the other hand, B_2O_3, compared to diatomic molecules or atoms, has additional degrees of freedom and hence the ability to store energy in different modes upon interaction with solid boron might facilitate O-atom chemisorption. It would be interesting to check if in the B_2O_3-B system a dissociative adsorption step might control the observed gasification rate, similarly to the conclusions of earlier studies of reactions of refractory solids with simple diatomic gaseous reactants (Rosner and Allendorf, 1968 and 1971). One can argue that with more complex reactant molecules such as B_2O_3, where more then one bond must be broken in order to achieve an adsorbed oxygen atom , it is even more likely that adsorption is the rate-limiting step. By normalizing our boron gasification rate data using the impingement rate of B_2O_3(g) with the surface we effectively determine the probability that an incident B_2O_3(g) molecule (structurally OBOBO in a V configuration) successfully deposits the central O-atom under various conditions. If subsequent steps in the formation and desorption of boron suboxides were rapid, estimates of the gaseous *products* of this surface reaction could be made using a local thermochemical equilibrium assumption, i.e. quasi-equilibrium theory (Batty and Stickney, 1969).

Until now a lack of experimental data, especially for the less predictable surface kinetics, has precluded accurate predictions of boron particle combustion behavior in the kinetically limited, and possibly non-continuum regime, except for an indirect determination of some kinetic parameters

during ignition (Li et al., 1989). Our approach has been to obtain the necessary kinetic data using well-defined filament/flow reactor techniques (Rosner and Allendorf, 1969; Rosner, 1972) rather than actually burning boron particles. Experimental techniques, results, mechanistic and chemical implications of this study are discussed in greater detail elsewhere (Zvuloni et al., 1990 and 1991); this summary contribution draws heavily from these sources.

1.1 Criterion for the Establishment of Kinetic Control

Principles and experimental techniques for measuring the intrinsic kinetics of efficient gas/solid reactions at high reactant and carrier gas pressures without diffusional 'falsification' have been discussed previously by Rosner (1972). Low pressure Transverse Filament Flow Reactors were employed to achieve test environments appropriate for this condition. The following criterion must normally be fulfilled for the establishment of kinetic control (Rosner, 1972; Rosner and Nordine, 1976):

$$\frac{\varepsilon \cdot \bar{c} \cdot \delta}{4 \cdot D \cdot} << 1 \qquad (1)$$

where: ε is the reaction probability defined below, δ is the diffusion boundary layer thickness, $\bar{c}$ is the local mean thermal speed of gaseous reactant molecules and D the Fick diffusivity for the gaseous reactant in the prevailing gas mixture. The *reaction probability*, ε, is a dimensionless 'overall' rate constant defined here as :

$$\varepsilon \equiv \dot{Z}_{(B)} / \dot{Z}_i^* \qquad (2)$$

where $\dot{Z}_{(B)}$ is the net efflux of substrate boron atoms irrespective of speciation, emerging from the boron surface as a result of chemical reactions and $\dot{Z}_i^*$ is the arrival flux of the reactant "i" incident upon the surface (e.g., B_2O_3, O_2, ..). By assuming that the reactant gas is 'ideal' and in local Boltzmann equilibrium, the "Hertz-Knudsen" equation may be used to calculate $\dot{Z}_i^*$, that is

$$\dot{Z}_i^* = \frac{1}{4} \cdot \frac{p_{i,w}}{k_B \cdot T_{g,w}} \cdot \left(\frac{8 \cdot k_B \cdot T_{g,w}}{\pi \cdot m_i} \right)^{\frac{1}{2}} \qquad (3)$$

Here $p_{i,w}$ is the partial pressure of the gaseous reactant, $T_{g,w}$ is its temperature at the surface, m_i is its molecular mass and k_B the Boltzmann constant. For low density gases the inequality (1) is equivalent to:

$$\frac{1}{2} \cdot \frac{\varepsilon}{Kn\delta} << 1 \qquad (4)$$

where $Kn\delta \equiv \lambda/\delta$ is the Knudsen number based on the gas mean-free-path, λ, and diffusion boundary layer thickness. Note that if ε is sufficiently small there is no difficulty in satisfying (4) under continuum conditions. However, if the reaction probability, not known *a priori*, is close to unity, as found here, the sufficient condition (4) would not be satisfied even by operating at a pressure low enough to cause $Kn\delta = O(1)$. Under such conditions, however, the effective reactant diffusion distance is no longer δ, as in eq. (3), but $\delta - \lambda$, where λ is the thickness of the Knudsen sublayer. Then, if $Kn\delta < 1$, the necessary condition to be satisfied to study interfacial kinetics should be extended to read

$$\frac{1}{2} \cdot \frac{\varepsilon (1 - Kn\delta)}{Kn\delta} << 1 \qquad (5)$$

a condition that was honored in the present studies. Thus, the true kinetics of very high-efficiency heterogeneous reactions can be observed, but only under sufficiently 'non-continuum' gas dynamic conditions.

2. EXPERIMENTAL METHODS

2.1 Experimental Arrangement and Diagnostic Technique

On the basis of these considerations, as well as constraints dictated by the diagnostic technique described in (Zvuloni et al., 1991) and summarized below, experiments were performed in a flow reactor maintained at a total pressure of 0.5 Torr (66.7 Pa) (see Fig. 1). An amorphous boron filament (AVCO-Textron) of 0.14 μm initial diameter was resistively heated to the desired temperature by a regulated DC power supply. The filament brightness temperature at a wavelength of 0.65 μm was measured by an optical pyrometer and converted to the actual surface temperature by assuming a temperature-independent spectral emittance of 0.69. The specimen was mounted transversely at the outlet of a 1 cm diameter horizontal tube discharging an argon gas jet at 130 m/s. The jet entrained measurable amounts of $B_2O_3(g)$ obtained by steady effusion from an electrically heated platinum source 'boat', positioned upstream of the filament. The product stream was collected through a glass skimmer from the central, uniform temperature, section downstream of the filament, and ultimately met an opposing jet of metastable Ar atoms, Ar*, generated by a microwave plasma discharge. To detect the boron-content of the gaseous reaction products we applied Microwave Induced Plasma Emission Spectroscopy (MIPES) (Oner, 1985): the metastable Ar* collide with the reaction product molecules, break these molecules into their constituent atoms and excite the resulting atoms to high (electronic) energy levels. By solely detecting the emission intensity

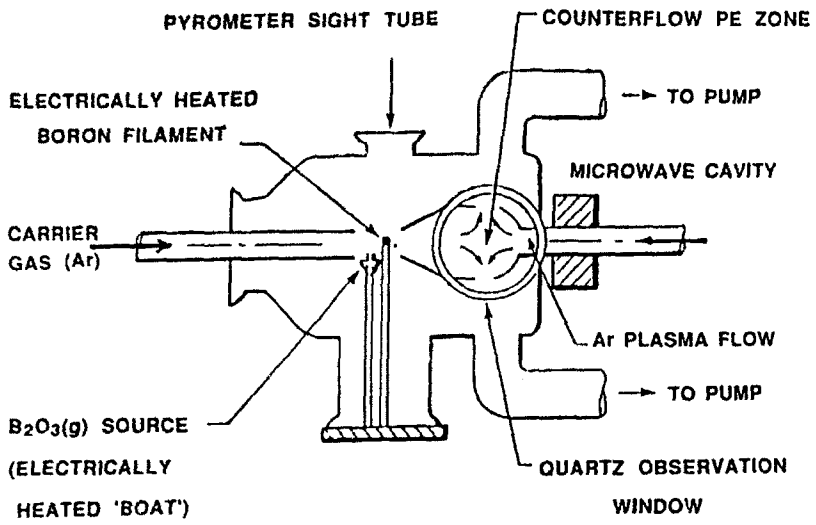

FIGURE 1. Flow reactor configuration (after: Zvuloni, 1990; and Zvuloni et al., 1991).

from the boron atoms in the ultraviolet, at 2497 Å, we could infer the elemental boron content of the mixture of gaseous products and determine gasification rates. High temperature structural instability of CVD-boron (Zvuloni, 1990) and the consequent likelihood of a transient increase in the apparent surface area available for reaction necessitated the use of a rapid detection technique such as MIPES to measure the surface reactions of interest here. The novel design of a counter-flow geometry for the downstream portion of the flow reactor had the advantage of being able to eliminate interferences associated with the condensation of reaction products on the reactor walls, their removal by the plasma 'active' Ar* and subsequent re-entrainment in the main stream.

The abovementioned continuous effusion source, constructed from a folded platinum sheet, generated $B_2O_3(g)$ via congruent evaporation of liquid B_2O_3 (Lamoreaux and Hildebrand, 1985) through a slit of 0.5 mm width and ca.

20 mm length. The boat was electrically heated to the desired temperature by a DC regulated power supply; the inner boat temperature was measured routinely with the pyrometer through the slit and corrected to account for an effective emissivity of 0.97, as determined by independent measurements using fine thermocouples.

2.2 *Calibration Techniques*

As discussed in greater detail elsewhere (Zvuloni et al., 1991), several tests were performed to assess the analytical capability of our approach for studying the rate of gas/solid reactions. The spectral signals of atomic boron from both sublimation of the boron filament and vaporization of B_2O_3 from the effusion source were measured over wide temperature ranges. A best fit when the logarithm of the measured emission intensity signals was plotted vs. the relevant reciprocal temperature yielded enthalpy of boron sublimation and B_2O_3 vaporization, respectively, which compared well to available literature values (ΔH_{subl}=132 Kcal/mole for boron (Paule and Margrave, 1963), and ΔH_{vap}=93 Kcal/mole for B_2O_3 (JANAF Tables, 1985). We also compared boron line emission signals coming from three rather different sources of boron atoms: (i) boron sublimation from the filament with an evaporation coefficient assumed equal to unity (Burns et al., 1963), (ii) B_2O_3 evaporation followed by effusion with an evaporation coefficient of 0.32 (Stolyarova et al., 1977) and (iii) calibrated flow rates of gaseous BF_3. The results, Fig. 2, not only prove the linearity of the output signals with respect to boron flux but, more importantly, also show that the plasma excitation efficiency was approximately the same for boron atoms irrespective of their origin. Finally, we gravimetrically measured the boron filament mass loss during sublimation and during reaction with $B_2O_3(g)$) to find directly a factor converting the output signal of the spectroscopic measurements during sublimation and during reaction to the independently measured mass flow rate of boron atoms emerging from the boron surface.

To relate the partial pressure of B_2O_3 at the filament location to its equilibrium pressure based on the 'boat' inner temperature we have measured directly the accumulation of condensed B_2O_3 'scale' on a cold boron filament over a known period of time and at a known 'boat' temperature. Allowing for a condensation coefficient of 0.32, equal to the reported evaporation coefficient (Stolyarova et al., 1977), we found very good agreement between these measurements and theoretical calculations accounting for both the non-ideal behavior of effusion sources and diffusion effects of the B_2O_3 entrained in the Ar main stream (Zvuloni, 1990; Zvuloni et al., 1991). Significantly, these experiments revealed also that a condensed layer deposited uniformly around the filament, confirming experimentally that the low Mach number near-field flow around the filament was indeed well out of the continuum regime, as required by the criterion stated in eq. 5.

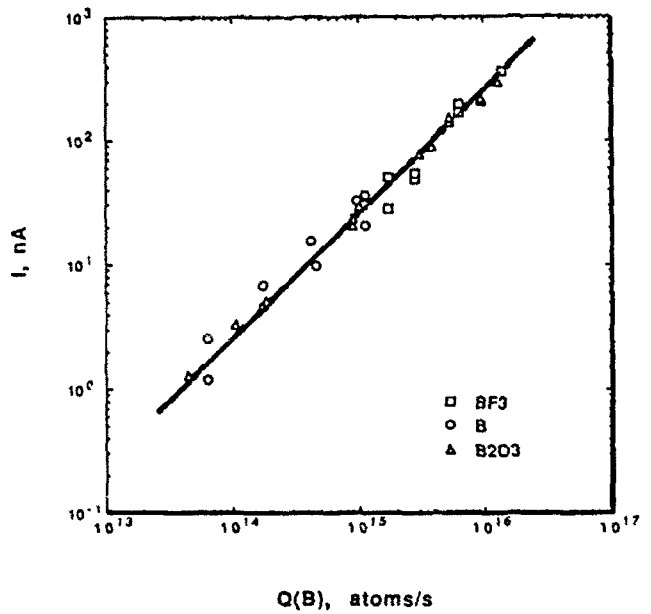

Figure 2 MIPES calibration: measured emission intensity for B sublimation, B_2O_3 vaporization and BF_3 (g) versus the calculated B-atom flow rate (per unit filament length) (after: Zvuloni, 1990; and Zvuloni et al., 1991).

Details of the determination of the temperature "jump" at the boron filament surface, between the gas temperature at the wall, $T_{g,w}$, needed in eq. 2, and the measured wall temperature, T_w, are given elsewhere (Zvuloni et al., 1991).

3. RESULTS AND DISCUSSION

Reaction rate results are presented here in terms of the above-defined *boron atom removal probability*, ε. This dimensionless presentation of our surface reaction rate data has the advantage of revealing explicitly the probability of boron gasification reaction for each molecule arriving onto the surface, irrespective of the identity of the desorbing boron-containing products, and thus gives better insight into the microscopic processes on the surface than alternate presentations using dimensional, empirical rate constants. If we assume here that every incident B_2O_3 molecule can ultimately gasify at most one B-atom from the surface, then ε cannot exceed unity. We return to this

point in discussing quasi-equilibrium predictions of the reaction product distribution.

Figure 3 shows our results for the surface reaction rate between solid boron and gaseous B_2O_3 as a function of the solid surface temperature. Reaction rates were measured over a surface temperature range of ca. 1330-2050 K, at an estimated partial pressure of 10^{-2} Pa. Our experimental results reveal the following behavior: (i) remarkably high reaction probabilities, ($\varepsilon \cong 0.5$), are inferred, exhibiting very low sensitivity to surface temperature over the broad range 1450-1800 K; (ii) at still higher surface temperatures the reaction probability rises to a maximum near 0.9 at 1950 K and then falls steeply; (iii) below about 1450 K we also observed a sharp reduction in the reaction probability. The obvious departures from simple Arrhenius behavior indicate that the experimentally measured surface reaction is not 'elementary' over this broad range of conditions. Our Arrhenius diagram also includes a straight line which is an estimate of what would be the contribution to the apparent reaction probability from the boron atom flux subliming into vacuum under the same conditions. At temperatures up to about 2000 K the contribution to the apparent reaction probability from boron sublimation is seen to be negligible; it becomes significant only in the higher temperature regime where the observed fall-off in chemical *reaction* probability occurs.

Of major interest and quite unforeseen are the extremely high reaction probabilities we have found for the B_2O_3(g)/B(s) reaction. The maximum reaction probability is similar to those found earlier for the O(g)/B(s) and O(g)/Me(s) systems, where Me stands for either Mo or W, and much higher than reaction probabilities reported for the corresponding O_2(g)/B(s) and also other O_2(g)/solid systems (Rosner and Allendorf, 1969; Zvuloni et al., 1990). Shown for comparison in Fig. 3 are also results of boron gasification by O_2; for the O_2-B system the reaction probability in the 'active' regime is *ca.* ε=0.2. The B_2O_3(g)/B(s) reaction is also very efficient over a broader temperature range than the abovementioned reactions. On the basis of our reasonable postulate as to the stoichiometry of the boron surface reaction with B_2O_3(g) and the definition of the reaction probability above, the sticking (O-atom deposition) probability, s, must satisfy the obvious condition $1 \geq s \geq \varepsilon$. The fact that we have found very high reaction probability therefore implies, at least for this regime, almost unity O-atom deposition probability; i.e., almost every arriving B_2O_3 molecule gives up one O-atom and ultimately delivers either one $(BO)_2$ molecule or two BO molecules to the gas phase (see below). Our experimental results thus indicate that the previously discussed steric effect is secondary and point to the dominance of energy transfer factors in the chemisorption of O originating from an incident B_2O_3 molecule compared to an incident "naked" O(g)-atom coming from the ambient.

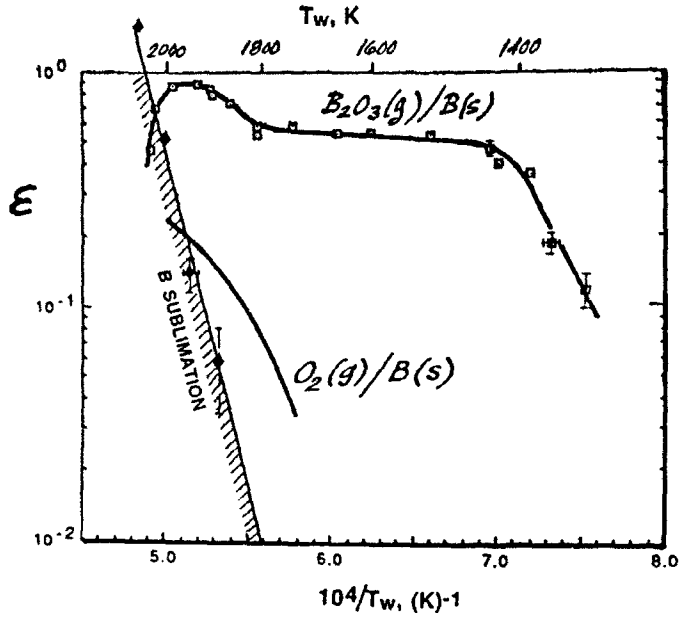

Figure 3. Boron atom removal probabilities for gasification of solid boron by $B_2O_3(g)$ and O_2 at reactant pressure of ca. 10^{-2} Pa (after: Zvuloni, 1990; and Zvuloni et al., 1991).

Figure 4 displays our results for the effect of reactant pressure, $p(B_2O_3)$ on the inferred reaction probability, ε, at two different surface temperatures. The reactant pressure was varied over more than two decades from about $2{\cdot}10^{-4}$ to $4{\cdot}10^{-2}$ Pa. As can be seen directly from the definition of the reaction probability, eqs. 2 and 3, if the overall surface reaction *rate* depends on the reactant pressure with 'order', n, then the *reaction probability*, ε, would be proportional to the n-1 power of the reactant pressure. Thus, from the local slope of the reaction probability data, the corresponding reaction order may be immediately deduced. We observe that measurements at T_w=1765 K, in the 'active' regime of almost constant reaction probability (low activation energy), give a linear relation on logarithmic scales with a slope of about 0.2, corresponding to a reaction order of ca. n=1.2. At T_w=1940 K, where the reaction probability maximum was observed, we estimated zero slope over the entire pressure range covered experimentally;

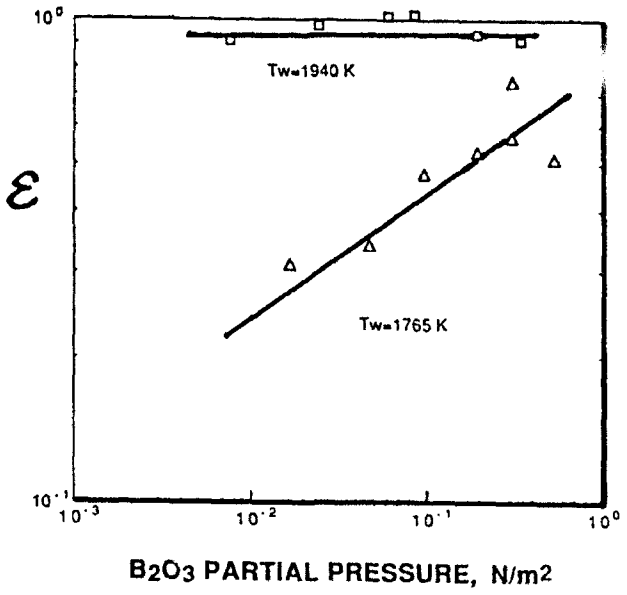

Figure 4. Dependence of the $B_2O_3(g)/B(s)$ reaction probability on the reactant $B_2O_3(g)$ partial pressure (after: Zvuloni, 1990; and Zvuloni et al., 1991).

i.e., this highest reaction probability regime is characterized by first order kinetics.

The possibility that O-atom deposition on a boron surface is the rate-controlling step as opposed to surface product formation and desorption suggested the use of a Quasi-Equilibrium (QE) model, similar to that developed by Batty and Stickney (1969), to estimate surface reaction product concentration trends. From the many possible gaseous reaction products: BO, BO_2 and $(BO)_2$ known in the literature (Lamoreaux and Hildebrand, 1985) one might expect multiple local maxima in the resulting ε vs. 1/T curve below the sublimation threshold since each product might become the dominant species in a distinct surface temperature interval, as was found in several other gas-solid reactions in the past (Rosner and Allendorf, 1971). QE model predictions for the reaction product distribution, Fig. 5, show the partial pressures dependencies of the different eligible boron oxide product species (BO(g), $BO_2(g)$, $(BO)_2(g)$ at surface temperatures between 900 K to 2200 K and in the range of the reactant $B_2O_3(g)$ pressures covered here, ca. 10^{-3} to

10^{-1} Pa, (assuming near unity sticking probability on the surface; see below). The following results are noteworthy: (i) the monomer BO(g) is the favored product for the surface reaction at the highest surface temperatures (ca. 1500-2200 K), the dimer $(BO)_2(g)$ is the favored product at intermediate surface temperatures (ca. 1050-1500 K), and the higher oxide $B_2O_3(g)$ is the favored "product" at low temperatures, ca. <1050 K; ii) near ε_{max}, BO is the dominant product, with only negligible mole fraction of $(BO)_2$; iii) $BO_2(g)$, a thermodynamically less stable species, was found to be negligible compared to both $(BO)_2(g)$ and BO(g) over the entire temperature range covered.

The QE predictions can help explain explain the high temperature decrease in reaction probability observed experimentally above ca. 2000 K. In principle, two alternatives are possible: either the reaction products (BO, $(BO)_2$)

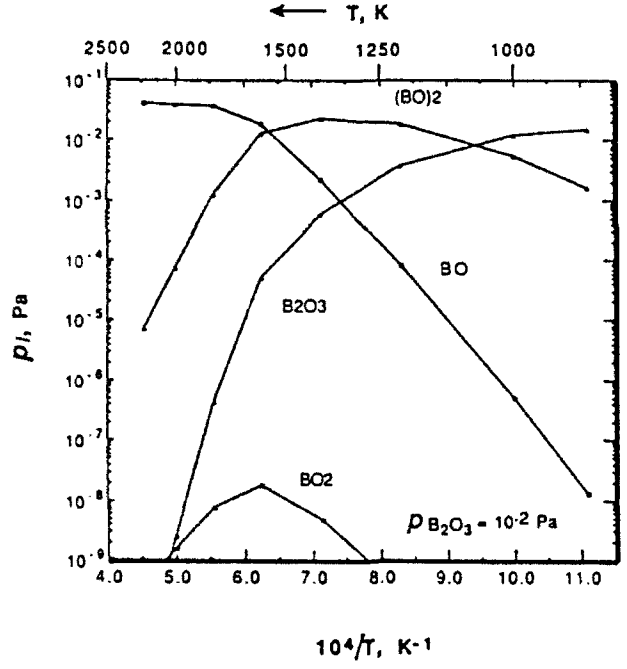

Figure 5. Quasi-equilibrium predictions of the surface reaction products for $B_2O_3(g)$ reacting with solid boron. Surface temperature dependence of the product partial pressures, for unity O-atom deposition probability (after: Zvuloni, 1990; and Zvuloni et al., 1991).

become thermally unstable; or the O-reagent cannot get on to the surface. Since our predictions, obtained on the basis of an assumed constant sticking probability, indicated that above 2000 K BO was still the dominant desorbing species, the cause of the high temperature fall in ε is probably a fall in s rather than the thermal desorption of unreacted *atomic* oxygen (O_2 is unstable under these conditions). For further details see (Zvuloni et al., 1991).

In Fig. 6 we show results for the 'active-to-passive' transition locus of the $B_2O_3(g)/B(s)$ reaction at different B_2O_3 pressures. This locus is of potential relevance in the extinction of boron particles, as discussed below, and is defined as the condition where the low-temperature ε–fall off occurs (e.g., ca. 1450 K in Fig. 3). It is seen to divide the $p(B_2O_3)$-T 'field' into two qualitatively different regimes. The 'active' regime is characterized by high reaction probability with very low apparent activation energy. On the other hand, the 'passive' regime is characterized by lower reaction probabilities and much higher activation energy (the transition was found to be more abrupt as $p(B_2O_3)$ is reduced and more abrupt than its counterpart for the $O_2(g)/B(s)$ reaction). When a condensed phase is formed on the boron surface at 'low' temperatures, conditions are beyond the the scope of simple QE model predictions. However the type of gaseous species favored under conditions found to exhibit condensed layer formation provide insight into the 'cause' of passivation. Thus, the rise in the QE-predicted $B_2O_3(g)$ pressure with falling temperature is qualitatively consistent with (ultimate) $B_2O_3(c)$ formation on the B surface suggested as a reason for the dramatic reduction in reaction probability at low temperatures. We also estimated the slope of the 'active-to-passive' transition locus based on this type of theoretical approach. By assuming that a 'passive' surface is established whenever condensible B_2O_3 is the dominant "product", it was found that QE predictions were in qualitative agreement with our experimental measurements. Linear slope of the ambient 'passivation' B_2O_3 pressure (logarithmic scale) vs. reciprocal surface temperature was inferred using different quantitative criteria to estimate when the B_2O_3 was a dominant "product". Both experiments and QE predictions show that the expected 'active-to-passive' transition temperature increases with B_2O_3 partial pressure; however, the predicted slope was slightly less than the one observed experimentally (ca. 130 Kcal/mole). We can use this 'active-to-passive' locus to assess possible boron particle extinction due to this cause, as discussed in (Zvuloni et al., 1990) and reviewed below. In the "passive" regime of the $B_2O_3(g)/B(s)$ reaction (in contrast to the $O_2(g)/B(s)$ reaction), the slope of the log ε vs. $1/T$ plot need bear no simple relation to $\Delta H_{subl.}$ of $B_2O_3(c)$. In this regime one can explain $B_2O_3(g)$ reactant facilitating boron filament loss by proposing that it forms a B_2O_3 condensate "solvent" layer which expedites one of the following two limiting cases: (i) boron atom dissolution and subsequent escape from a well-

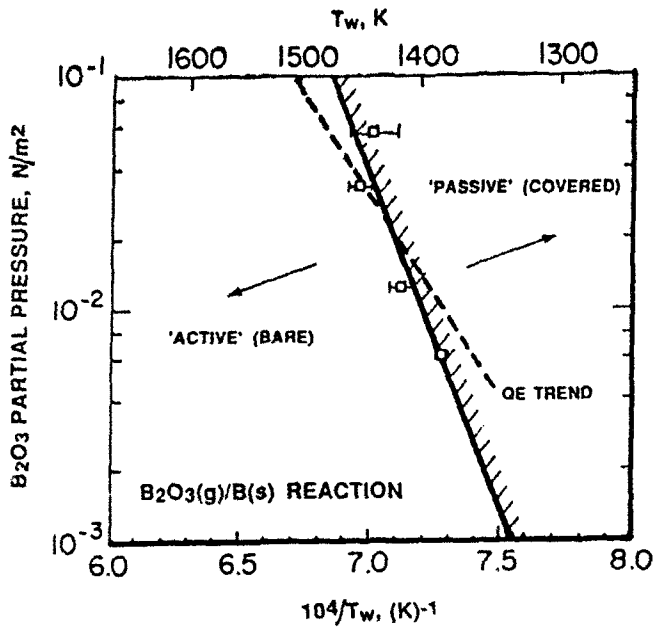

Figure 6. "Active-to-passive" transition locus. Solid line: experimental. Dashed line: from Quasi-Equilibrium theory (after Zvuloni et al., 1990 and 1991).

mixed steady-state condensed B_2O_3(c)-microlayer or (ii) boron atom dissolution and diffusion across a steady state quiescent B_2O_3(l) microlayer, and subsequent escape to the gas phase (Glassman et al., 1985).

4.1 Chemical Propulsion Implications

In the light of these new heterogeneous kinetic data we now return to the questions of boron particle combustion which motivated our experiments. To appreciate the relative importance of chemical reactions and transport processes in the combustion and extinction of a boron particle, we performed calculations summarized in Fig. 7 taken from (Zvuloni et al, 1990). The diagonal straight lines on the log-log plot of particle diameter versus total pressure define estimated locii of transition from the diffusion-controlled regime to the kinetically controlled regime for *surface* reactions of B_2O_3(g) and O_2(g) with solid boron and for the B_2O_3(g) homogeneous formation reaction. A typical gas temperature of 2000 K was chosen for these calculations. Also shown is the unity Knudsen number locus indicating the transition to non-continuum behavior. As illustrated below, a knowledge of

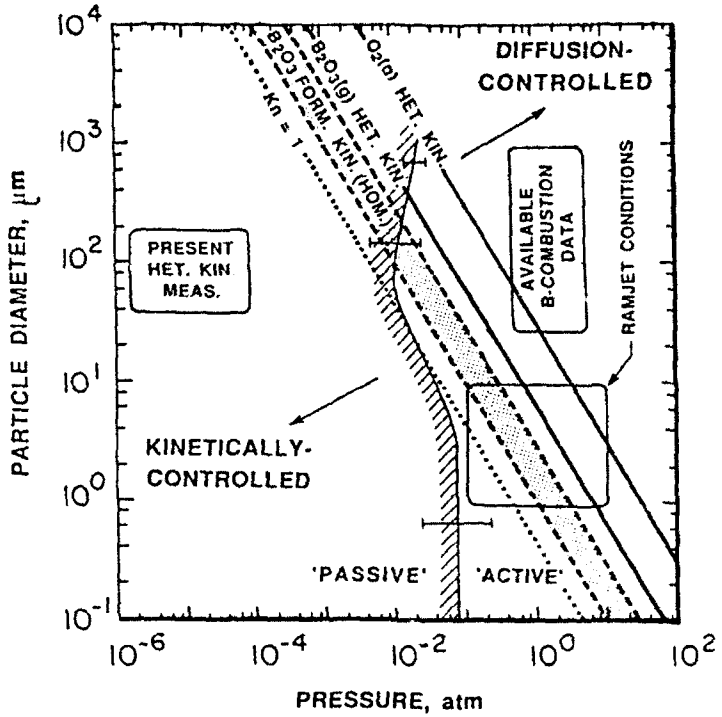

Figure 7. Boron particle combustion map (after: Zvuloni, 1990; and Zvuloni et al., 1990).

the relative position of these transitions helps understand what are likely to be the important gaseous species and rate-controlling mechanisms in the history of a burning particle. Separated by the diffusion-to-kinetics transition locii, large particles at high pressures experience diffusion-controlled combustion and small particles at low pressures lead to kinetically-controlled combustion, possibly in a free-molecular flow field. On the same graph we also present three domains of special interest: one pertains to most previous experimental boron particle combustion research and is essentially in the diffusion-controlled region; another domain reflects the combination of oxygen pressure and specimen size in which we have been measuring intrinsic gas/solid reaction kinetic data; and, finally, the domain of principal ramjet interest.

The approximate transition from the diffusion-controlled regime to the interface-kinetics controlled regime for *surface* reactions of $B_2O_3(g)$ and $O_2(g)$ with solid boron was estimated by assuming a reaction probability, ε, equal to 1 and 0.2, respectively, as indicated by the gas/solid kinetic measurements in Fig. 3; the diffusion layer thickness was estimated as d/2 for Fick diffusion of O_2 in air and a stoichiometrically determined fraction of this for B_2O_3 in air. On the other hand, the homogeneous kinetics band also shown in Fig. 7 covers the formation rate of B_2O_3 from boron suboxides, ranging from the highest possible bimolecular collision rate (left boundary) to an estimated overall rate. The latter was based on fragmentary experimental measurements (Di Giuseppe and Davidovits, 1987; Llewellyn et al., 1981) and theoretical estimates of rate constants appearing in (Yetter et al., 1989) for selected gaseous elementary reactions between boron-containing species and oxygen-containing species. Homogeneous formation of atomic oxygen in the B-O system was predicted to be negligible compared to $B_2O_3(g)$ formation (Yetter et al., 1989) and consequently is not considered further here.

It is instructive to evaluate the implications of these estimates by considering, for example, the fate of a boron particle of diminishing size at a constant total pressure of, say, one atmosphere corresponding to the midvalue of the domain of ramjet operations. Boron particles under about 7 μm diameter would undergo kinetically-limited combustion and the surface attack would be governed by the $B_2O_3(g)/B(s)$ reaction until the particle diameter reached perhaps 3 μm. Such a particle, then, would deliver as much as 92 % of its mass and energy under this type of rate control and $B_2O_3(g)$ would be the main B(s) gasifier in the kinetic regime, having been formed at an adequate rate in the gas phase diffusion boundary layer. Below the particle size at which homogeneous kinetics begins to limit the formation of $B_2O_3(g)$, the particle surface would be directly attacked by $O_2(g)$ with a consequent reduction in gasification rate because of its smaller reaction probability.

Another possibly important feature of these kinetically-controlled combustion processes is *extinction* due to the transition from 'active' to 'passive' behavior for the surface oxidation reaction. Since the overall oxidation reaction is exoergic, when the reaction rate falls less chemical energy is released and the particle surface temperature necessarily drops. This, in turn, leads to a further reduction in the reaction rate and the particle surface temperature, possibly causing extinction. We estimated the 'active-to-passive' locus, the curved boundary on the graph, based on data for the $O_2(g)/B(s)$ reaction, similar to those in Fig. 6 for the $B_2O_3(g)/B(s)$ reaction. Then, using a quasi-steady energy balance for an individual particle under the assumption of maximum radiation losses, we estimated particle temperatures as a function of particle diameter and total pressure (at T_g=2000 K and $p(O_2)/p$=0.20) and the

conditions under which passivation should occur due to the formation of a 'protective' $B_2O_3(c)$ layer. While this locus is independent of particle diameter in the free-molecular regime, in the continuum kinetically-controlled surface reaction regime the slope of the curve is determined by the solution of the energy balance and therefore is not known *a priori*. We found that in the continuum regime somewhat lower pressures are needed for extinction by passivation, i.e. a boron particle burning at atmospheric pressure undergoes heterogeneous reaction in the kinetically 'active' regime and would likely remain in this regime through its entire burning time. This implies that a successfully ignited particle in the environments considered here would not extinguish because of surface passivation by $B_2O_3(c)$, but such extinction remains a possibility at lower pressures.

5. CONCLUSIONS

Our recent experimental studies of the high temperature kinetics of the $B_2O_3(g)$-B(s) system have led to the following conclusions:

1. B_2O_3 is a remarkable gasifier of solid boron over a broad temperature range above 1400 K, with a reaction probability much higher than for O_2 and comparable to the maximum local value previously observed for O atom attack. Therefore, perhaps due to the availability of more energy dissipation channels as compared to simpler molecules, B_2O_3 exhibits a high O-atom deposition probability on "bare" solid boron;

2. The $B_2O_3(g)$-B(s) reaction is first order in the reactant B_2O_3 pressure near the highest observed reaction probability, and ca. n=1.2 order over much of the high temperature ε-'plateau', implying that the active regime ε-values observed here are only weakly dependent upon B_2O_3 pressure;

3. We identified experimentally transition conditions for surface 'passivation' in the $B_2O_3(g)/B(s)$ reaction and found qualitative agreement between experimental measurements and quasi-equilibrium model predictions;

4. Quasi-equilibrium model predictions indicate that the dominant reaction product species in the $B_2O_3(g)$-B(s) reaction were the monomer BO above about 1500 K, and the dimer $(BO)_2$ at intermediate temperatures (1050-1500 K).

Regarding chemical propulsion implications, we have shown that, with the help of these and previous experimental measurements for the relevant gas/solid reactions, it is possible to identify the chemical kinetic and physical phenomena likely to play a dominant role at each stage in the combustion history of a solid boron fuel particle. For this purpose a log-log plot of

particle diameter versus pressure is particularly helpful. We estimate that at atmospheric pressure boron particles under about 7 μm diameter would undergo kinetically-limited combustion and the surface attack would be governed by the $B_2O_3(g)/B(s)$ reaction for particle diameters down to perhaps 3 μm. Below this size, we estimate that the particle surface would be attacked mainly by $O_2(g)$ at a lower gasification rate. Under the prototypical conditions selected, the boron particle undergoes heterogeneous reaction in the kinetically 'active' regime and would likely remain in this regime through its entire burning time; however, extinction due to passivation appears to be possible at lower pressures.

6. ACKNOWLEDGEMENTS

Thanks are due to Drs. A. Fontijn, A. Gany, B. Halpern, P.C. Nordine, and R. Weber for their helpful comments. We are indebted to the U.S. Air Force Office of Scientific Research for providing financial support (under Grant AFOSR 89-0223).

7. REFERENCES

Batty, J. C., & Stickney, R.E. (1969) Quasi-equilibrium Treatment of Gas-Solid Reactions J. Chem. Phys., 51, 4475-4492.

Burns, R. P., Jason, A. J. & Inghram, M. (1967). Evaporation Coefficient of Boron. J. Chem. Phys., 46, 394-396.

Di Giuseppe, T. G., & Davidovits, P. (1981). Boron Atom Reactions. II. Rate Constants with O_2, SO_2, CO_2, and N_2O. J. Chem. Phys., 74, 3287-3291.

Glassman, I., Williams, F. A., & Antaki, P. (1985). A Physical and Chemical Interpretation of Boron Particle Combustion. Proc. 20th Symp. (Int.) on Combustion, The Combustion Institute, Pittsburgh, pp. 2057-2064

JANAF Thermochemical Tables,(3rd ed.), (1985).

King, M. K. (1972). Boron Ignition and Combustion in Air-Augmented Rocket Afterburners. Comb. Sci. and Techn., 5, 155-164.

King, M. K. (1974). Boron Particle Ignition in Hot Gas Streams. Comb. Sci. and Techn., 8, 255-273.

Lamoreaux, R. H. & Hildenbrand, D. L. (1985). Vaporization Behavior of Oxides. High Temp. Sci., 20, 37-49.

Li, S. C., Williams, F. A., & Takahashi, F. (1989). An Investigation of Combustion of Boron Suspensions. Proc. 22nd Symp. (Int.) on Combustion, The Combustion Institute, Pittsburgh, pp. 1951-1960.

Llewellyn, I. P., Fontijn, A., & Clyne, M. A. A. (1981). Kinetics of the Reaction BO +O_2 --> BO_2 + O. Chem. Phys. Letters, 84, 504-508.

Macek, A., & Semple, J. M. (1969). Combustion of Boron Particles at Atmospheric Pressure. Comb. Sci. and Techn., 1, 181-191.

Macek, A., & Semple, J. M. (1971). Combustion of Boron Particles at Elevated Pressures. Proc. 13th Symp. (Int.) on Combustion, The Combustion Institute, Pittsburgh, pp. 859-868.

Mohan, G., & Williams, F. A. (1972). Ignition and Combustion of Boron in O_2/Inert Atmospheres. AIAA Journal , 10, 776-783.

Oner, A. (1985). Application of MIPES to the Study of Gas/Solid Reactions. Ph.D. Dissertation, Yale University, Dept. of Chemical Engineering.

Paule, R. C., & Margrave, J. L. (1963). A Langmuir Determination of the Sublimation Pressure of Boron. J. Phys. Chem., 67, 1368-1370.

Rosner, D. E., & Allendorf, H. D. (1968). Kinetics of Elemental Boron Chlorination by Chlorine Atoms and Chlorine Molecules. J. Phys. Chem., 72, 4159-4162.

Rosner, D. E., & Allendorf, H. D. (1969). Kinetic Studies of the Attack of Refractory Materials by Oxygen Atoms and Chlorine Atoms. Proc. 3rd Int. Symp. on High Temperature Technology, Butterworths, London, pp. 707-719.

Rosner, D. E. and Allendorf, H. D. (1971) Kinetics of the Attack of Refractory Solids by Atomic and Molecular Fluorine. J. Phys. Chem, 75, 308-317.

Rosner, D. E. (1972). High Temperature Gas-Solid Reactions, Ann. Rev. of Material Sci., 2, 573-606.

Rosner, D. E., & Nordine, P. C. (1976). Mass Transport Requirements and a New Technique for Studying the Intrinsic Kinetics of High Temperature Gas/Liquid Reactions", in R. M. Fisher et al., (eds.), Physical Chemistry in Metallurgy, Proc. Darken Conf., (pp. 496-499) U.S. Steel Corp., Monroeville, PA

Stolyarova, V.L., et al. (1977). Determination of Evaporation Coefficient of Melts in the B_2O_3-GeO_2 System Using Mass Spectrometry. Fizika i Khimiya Stekla (Physics and Chemistry of Glass; Plenum, N.Y.), 3, 635-637.

Yetter, R. A., Cho, S. Y., Rabitz, H., Dryer, F. L., Brown, R. C., and Kolb, C. E. (1989). Chemical Kinetic Modeling and Sensitivity Analyses for Boron-Assisted Hydrocarbon Combustion. Proc. 22th. Symposium (Int.) on Combustion, The Combustion Institute, Pittsburgh, pp. 919-927.

Zvuloni, R., Gomez, A. and Rosner, D. E. (1990). High Temperature Kinetics of Solid Boron Gasification by its Higher Oxide $B_2O_3(g)$: Chemical Propulsion Implications", AIAA J. Propulsion and Power, in press.

Zvuloni, R. (1990). Flow Reactor Studies of the High Temperature Gasification Kinetics of Solid Boron and Carbon and their Chemical Propulsion Implications. Ph.D. Dissertation, Yale University, Dept. of Chemical Engineering.

Zvuloni, R., Rosner, D. E., Gomez, A. (1991). High Temperature Kinetics of Solid Boron Gasification by its Higher Oxide $B_2O_3(g)$: Flow Reactor Techniques, Rate Measurements and their Implications. Submitted to J. Phys. Chem..

YALE UNIVERSITY

HIGH TEMPERATURE CHEMICAL REACTION
ENGINEERING LABORATORY
YALE UNIVERSITY
BOX 2159, YALE STATION
NEW HAVEN, CONNECTICUT 06520 U.S.A.

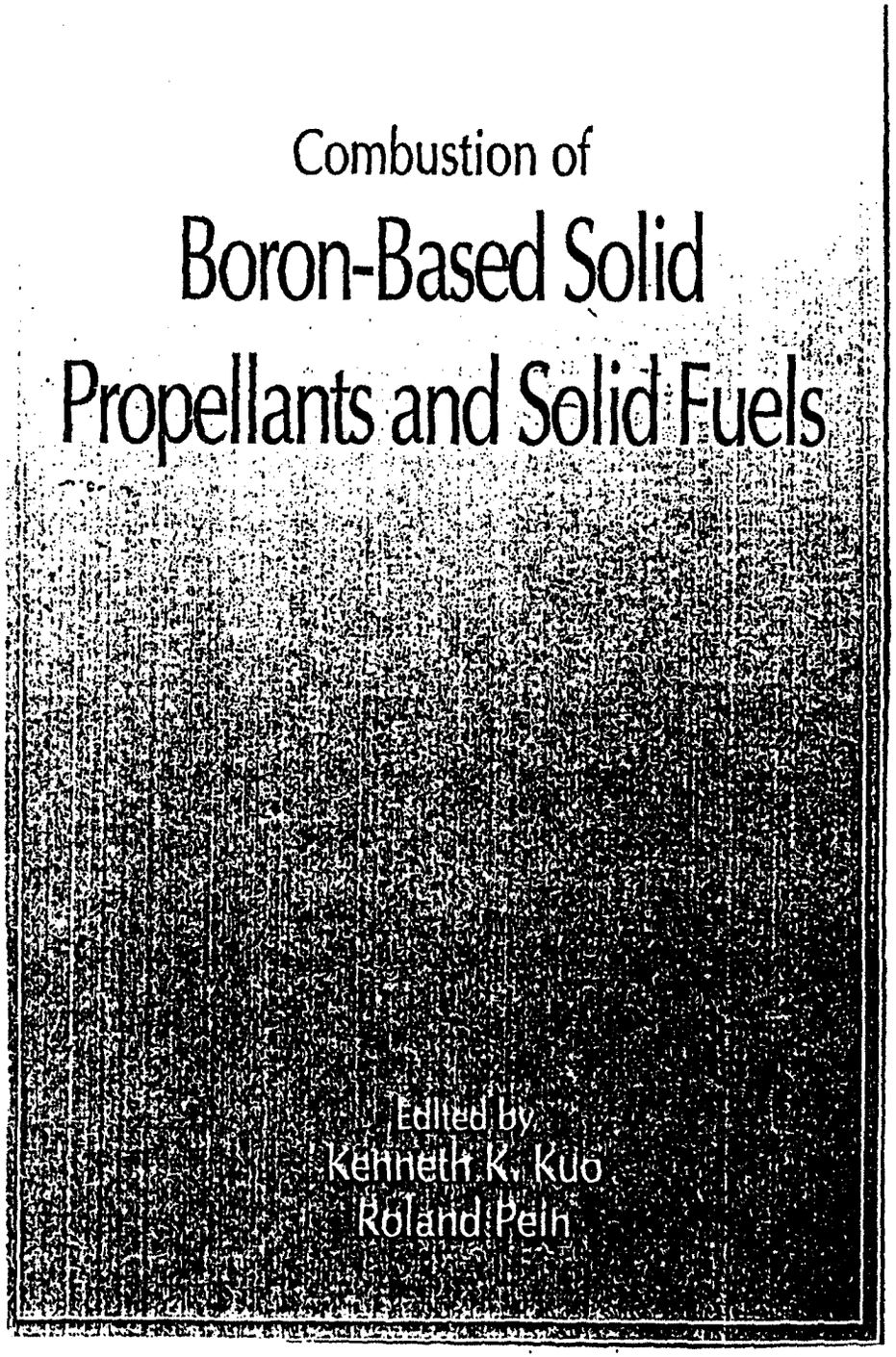

REPORT DOCUMENTATION PAGE

Form Approved
OMB No. 0704-0188

1. AGENCY USE ONLY (Leave blank)	2. REPORT DATE	3. REPORT TYPE AND DATES COVERED
	1992	Book chapter

4. TITLE AND SUBTITLE

DEPOSITION DYNAMICS OF COMBUSTION-GENERATED PARTICLES: SUMMARY OF RECENT STUDIES OF PARTICLE TRANSPORT MECHANISMS, CAPTURE RATES AND RESULTING DEPOSIT MICROSTRUCTURE/PROPERTIES

5. FUNDING NUMBERS

PE - 61102F
PR - 2308
SA - BS
G - AFOSR 91-0170

6. AUTHOR(S)

D. E. Rosner, A. G. Konstandopoulos, M. Tassopoulos, and D. W. Mackowski

7. PERFORMING ORGANIZATION NAME(S) AND ADDRESS(ES)

HIGH TEMPERATURE CHEMICAL REACTION ENGINEERING LABORATORY
YALE UNIVERSITY
BOX 2159, YALE STATION
NEW HAVEN, CONNECTICUT 06520 U.S.A.

8. PERFORMING ORGANIZATION REPORT NUMBER

9. SPONSORING/MONITORING AGENCY NAME(S) AND ADDRESS(ES)

AFOSR/NA
110 Duncan Avenue, Suite E115
Bolling AFB DC 20332-0001

10. SPONSORING/MONITORING AGENCY REPORT NUMBER

11. SUPPLEMENTARY NOTES

in *Proc. Engineering Foundation Conference*: Inorganic Transformations and Ash Deposition During Combustion, Engineering Foundation/ASME, New York (1992); pp. 585-606

12a. DISTRIBUTION/AVAILABILITY STATEMENT

Approved for public release; distribution is unlimited

12b. DISTRIBUTION CODE

13. ABSTRACT (Maximum 200 words)

We review here some of the principal results of our recent research directed towards understanding and predicting the *deposition dynamics of combustion-generated particles* in fossil-fuel power production technologies. In view of our previous review papers (Engineering Foundation Symposia, ASME-HTD and J. PCH; *loc.cit.*), which explicitly dealt with dense spherical particles, isolated targets and vapor-particle interactions prior to deposition, the specific topics emphasized in this overview are:

Brownian diffusion-, thermophoretic- and inertial-properties of *aggregated* particles

Effects of particle size *spectrum* and *morphology* on total deposition rates

Combined effects of *inertia* and *thermophoresis* for surfaces with streamwise curvature

Prediction and correlation of *inertial* particle capture by fluid-dynamically *interacting cylinders* in cross-flow

Micro-mechanical aspects of arriving *particle capture* and associated *deposit growth*

Computer simulation of particle deposition *mechanism/deposit microstructure /property interrelations*

14. SUBJECT TERMS

Key Words: Aerosols, Soot, Aggregated Particles, Gaseous Diffusion Flames, Thermophoresis, Brownian Diffusion, Flame Synthesis of Fine Particles, Aerosol Reaction Engineering

15. NUMBER OF PAGES

12

16. PRICE CODE

17. SECURITY CLASSIFICATION OF REPORT	18. SECURITY CLASSIFICATION OF THIS PAGE	19. SECURITY CLASSIFICATION OF ABSTRACT	20. LIMITATION OF ABSTRACT
Unclassified	Unclassified	Unclassified	UL

INORGANIC TRANSFORMATIONS AND ASH DEPOSITION DURING COMBUSTION

Proceedings of the
Engineering Foundation Conference On
Inorganic Transformations and Ash Deposition During Combustion
March 10-15, 1991
In Palm Coast, Florida

Edited By
Steven A. Benson
Energy and Environmental Research Center
University of North Dakota

1992
Published on Behalf of the
ENGINEERING FOUNDATION
by
THE AMERICAN SOCIETY OF MECHANICAL ENGINEERS
United Engineering Center • 345 East 47th street • New York, N.Y. 10017

YALE UNIVERSITY

DEPOSITION DYNAMICS OF COMBUSTION-GENERATED PARTICLES: SUMMARY OF RECENT STUDIES OF PARTICLE TRANSPORT MECHANISMS, CAPTURE RATES AND RESULTING DEPOSIT MICROSTRUCTURE/PROPERTIES

D. E. Rosner, A. G. Konstandopoulos, M. Tassopoulos,
and D. W. Mackowski
Department of Chemical Engineering
High Temperature Chemical Reaction Engineering Laboratory
Yale University
New Haven, Connecticut

ABSTRACT

We review here some of the principal results of our recent research directed towards understanding and predicting the *deposition dynamics of combustion-generated particles* in fossil-fuel power production technologies. In view of our previous review papers (Engineering Foundation Symposia, ASME-HTD and J. PCH; *loc.cit.*), which explicitly dealt with dense spherical particles, isolated targets and vapor-particle interactions prior to deposition, the specific topics emphasized in this overview are:

- Brownian diffusion-, thermophoretic- and inertial-properties of *aggregated* particles
- Effects of particle size *spectrum* and *morphology* on total deposition rates
- Combined effects of *inertia* and *thermophoresis* for surfaces with streamwise curvature
- Prediction and correlation of *inertial* particle capture by fluid-dynamically *interacting cylinders* in cross-flow
- Micro-mechanical aspects of arriving *particle capture* and associated *deposit growth*
- Computer simulation of particle deposition *mechanism/deposit microstructure /property interrelations*

While our most important findings are presented here, details on each of these studies and their immediate antecedents will be found in the cited references. Our emphasis throughout continues to be on developing more accurate general methods, and rational engineering correlations to predict heat exchanger (gas-side) fouling rates. We conclude with projections of these current studies into the forseeable future, and thoughts on the ultimate incorporation of these results into engineering design practice. Our results will also be seen to have implications for hot-gas clean-up devices, particle sampling systems, and soot-laden flame diagnostics.

1. INTRODUCTION, BACKGROUND

Progress has been made on several fronts in developing rational methods to predict and, ultimately control, fine particle deposition since the 1982 Engineering Foundation Conference: *Fouling of Heat Exchanger Surfaces*, in which we

summarized our theoretical results on submicron spherical particle *thermophoresis* and larger spherical particle *inertial impaction* on isolated cylindrical targets, and the related 1981 EF Conference: *Fouling and Slagging From Impurities in Combustion Gases* in which we described new optical techniques for laboratory studies of alkali vapor deposition. In the intervening years interactions between submicron particulate matter and mixed alkali-containing vapors have been clarified, based, in part, on "seeded" laboratory flat-flame burner/"flash"-evaporation experiments and ancillary theoretical studies of multiphase boundary layer behavior (see, *e.g.*, Rosner (1988) and Castillo and Rosner (1988)). In the present review of our more recent studies (Section 2) we instead focus on providing answers to the following specific *questions*:

Q1 If the suspended particles are non-spherical (e.g., as a result of primary particle *aggregation* without rapid coalescence) how does this affect their transport properties?

Q2 How can one conveniently predict the total deposition rates of suspended particles which are "distributed" with respect to particle *size*, and how sensitive are such predictions to inevitable uncertainties in particle *morphology*?

Q3 How do the mechanisms of thermophoresis and inertial drift "interact" for particle deposition from rapidly moving gases to curved (convex- and concave-) surfaces which are cooled or heated?

Q4 How does the *proximity* of adjacent collectors influence inertial impaction rates from high-velocity particle-laden gases?

Q5 What physical properties and conditions determine the *capture (sticking-) probability* when arriving particles impact on a microparticulate *deposit*?

Q6 What will be the *microstructure* and, hence, effective transport properties of *deposits* formed by the diffusive- or inertial-capture of suspended particles?

In what follows we briefly summarize our principal results and methodology in seeking answers to these, and closely related, questions. For additional information and important "details" the interested reader is directed to the archival publications explicitly cited in Section 2 and listed in Section 4. As in the past, a judicious blend of laboratory experiments, theory, numerical computation, and intuition is necessary to economically arrive at results and proposed methods which promise to improve the generality and accuracy of future ash-deposition-related design calculations for a wide variety of types of coal-fired equipment. Of course, especially from the perspective of power-plant designers, there remain important unanswered questions, and our methods are now being generalized to treat more complex situations of practical importance not only for fossil fuel power generation applications but for other technologies involving particle-laden hot gases. Some of these research extensions are indicated in Section 2, and generically summarized in Section 3, which concludes this paper. Other high-priority extensions will undoubtedly be identified as a result of information presented at this conference by participants representing the entire spectrum from engineering science to engineering practice. For brevity, we deliberately confine our attention here to recent fundamentally-oriented work carried

out in the Yale HTCRE Laboratory. Readers interested in a more comprehensive review of the recent vapor deposition- and particle deposition-literature are directed to, *e.g.*, Marner (1989). It is hoped that *this* EF-presentation and its supporting (cited) papers (Section 4) will facilitate the refinement and/or incorporation of some of the present ideas into design procedures of much greater generality and reliability, and help identify new directions where research results would have a significant impact on engineering practice.

2. RECENT RESEARCH AT YALE-HTCRE LAB

2.1 Brownian Diffusion-, Thermophoretic- and Inertial-Properties of Aggregated Particles: Dependence on Size and Morphology

While isolated, uniformly dense *spherical* particles form the natural starting point and "reference state" for particle transport properties (say, Brownian diffusivity, thermophoretic diffusivity, and particle "stopping-time") it is now known that in many combustion environments rapid *coagulation* rates and slow coalescence rates (due to high viscosity and/or low surface tension) lead to highly "aggregated" particles composed of dense "primary" spheres joined together in various morphologies (branched chains, nearly straight chains, quasi-spherical, fractal,...). Whatever the dominant particle deposition mechanism, it is necessary to examine the dependence of the relevant transport property on both the *number*, N, of primary spheres in such aggregates and their physical arrangement ("*morphology*"). Frequently, orientation-averaged values, hereafter denoted < >, will be of greatest engineering interest, but when dealing with highly asymmetrical aggregates it may be necessary to correct for systematic departures from random orientation which may be flow-field specific. Moreover, information is required over the entire Knudsen number regime, from cases where the local gas mean-free-path, l_g, is large compared to the radius of gyration, R_g, of the aggregate, to cases where the l_g is small on the scale of the aggregate primary particles.

Figure 2.1-1, taken from Rosner (1991), illustrates the size- and structure-sensitivity of the orientation-averaged Brownian diffusivity $\langle D \rangle_N$ of such aggregates in the near-continuum ($Kn_p \ll 1$) limit, where the normalization is based on D_1 (the Brownian diffusivity of a single *primary sphere* in the same environment). While immediately relevant to the prediction of particle deposition rates by convective-*diffusion* (see, e.g. Rosner 1989, 1991) this information is also relevant to capture by *inertial impaction* (Section 2.4) in view of the Einstein relation for the orientation-averaged particle stopping time:

$$\langle t_p \rangle_N = \frac{\langle D_p \rangle_N}{(k_B T / m_{p,N})} \qquad (2.1\text{-}1)$$

where, of course, $m_{p,N} = N m_{p,1}$. Of considerable practical and theoretical interest (Section 2.2) are the nominal *slopes* of these double-logarithmic "curves" (values shown in parentheses) and the large spread in $\langle D \rangle_N$-values at any particular value of N. Since convective-*diffusion* rates of particles are normally proportional to a power of <D> near 2/3 this translates to a considerable "structure-sensitivity" of deposition rates by this mechanism, and an even greater sensitivity of *inertial deposition* rates to particle morphology and size. In Section 2.2, summarizing the methods/results of Rosner (1991), we outline how these <D>-results can be used to predict total particle deposition rates when there is a *distribution* of suspended aggregate sizes, and even a distribution of particle morphologies.

In sharp contrast to the size- and structure-*sensitivity* of aggregate particle deposition rates by either convective-*diffusion* or *inertial* mechanisms, we have recently found (Rosner, García-Ybarra and Mackowski (1990)) that adequate

engineering estimates of *thermophoretically* depositing particles can often be made *without* accurate information on aggregate size and morphology. This is a consequence of an approximate cancellation of thermophoretic (propulsive-) force and gas-dynamic drag which renders the relevant diffusivity ratio: $\langle\alpha_T D\rangle_N/(\alpha_T D)_1$ remarkably *insensitive* to N and morphology, especially in the free-molecule limit, but also in the continuum limit. Thus, in the continuum limit, all calculated $\langle\alpha_T D\rangle_N$-values, which yield the aggregate drift velocities per unit -grad *ln* T_g, fell within about a 21% band straddling $(\alpha_T D)_1$, including straight chains and random quasi-spherical clusters, irrespective of the number of contained primary particles and even for primary particles which have a thermal conductivity only 10-times that of the prevailing gas.

While beyond the scope of this paper, it should also be noted that when the primary spheres are not identical in properties and/or size, small aggregates in a local temperature gradient can experience net *torques* which will tend to orient them relative to the local vector **grad** T_g (see, *e.g.* Rosner *et al.* (1991) and Mackowski (1990)) despite the randomizing tendency of Brownian rotation. Moreover, as discussed in these references, such particles can exhibit "anomalous" Brownian- and thermophoretic-diffusivities. Also described elsewhere are *photophoretic* effects on intermediate-size radiation-absorbing particles (small char particles and large organic soot aggregates) in the presence of high radiation heat fluxes; see, *e.g.*, Castillo *et. al.* (1990), and Mackowski(1989).

2.2 Effects of Suspended Particle Size Spectrum and Morphology on Total Deposition Rates

The total particle capture fraction, η_{cap}, and closely associated dimensionless overall mass transfer coefficient (Stanton number; Rosner(1986)), St_m are generally dependent on particle *size* (say, volume v) and, as will also be clear from Fig. 2.1-1 and Eq. (2.1-1), particle *morphology*. Qualitatively, this dependence is sketched in Fig. 2.2-1 along with the prevailing mainstream dimensionless particle size distribution (PSD-)function

$n(v)\bar{v}/N_p \equiv \psi$, where $n(v,...) \equiv dN_p/dv$ and N_p is the total particle number density. The left hand $St_m(v)$-branch, with negative slope, is typical of capture by convective-*diffusion*, but above some intermediate particle size (in the prevailing target environment) effects of particle *inertia* set in and $St_m(v)$ increases with particle volume, at least until particles rebound or total capture (η_{cap}=1) occurs. While upstream coagulation among suspended particles may help shape the PSD, particle number densities in ash-bearing fossil fuel combustion application are usually small enough to preclude appreciable coagulation *within the thin diffusion boundary layers* adjacent to solid targets. This implies that each particle size class deposits with "its own" mass transfer coefficient $St_m(v)$, uninfluenced by the presence of particles of other sizes. The total mass deposition rate per unit target area may then be written as an integral over all particle volumes (Rosner (1989)):

$$-\dot{m}_p'' = U\int_0^\infty St_m(v,...)\,\tilde{\rho}_p(v)\,v\cdot n(v,...)\,dv \qquad (2.2\text{-}1)$$

where $\tilde{\rho}_p$ is the intrinsic *density* (m_p/v) of a particle of volume v (often sufficiently constant to be removed from under the integral sign). We have recently shown (Rosner (1989), Rosner and Tassopoulos (1989)) that such calculations are dramatically simplified when the function $St_m(v)$ is a power-law and the PSD n(v) is "log-normal" (Gaussian in *ln* v), as is often the case. Moreover, it is instructive and appropriate to compare actual deposition rates to the easily computed "reference" mass

deposition rate, $-\dot{m}''_{p,ref}$, that would be predicted in the same environment if *all* particles had the mean particle volume $\bar{v}$, defined by ϕ_p/N_p, where ϕ_p is the actual total aerosol *volume fraction:*

$$\phi_p \equiv \int_0^\infty v\cdot n(v,...)\,dv = \frac{\rho\omega_p}{\tilde{\rho}_p} \qquad (2.2\text{-}2)$$

(which does not change due to coagulation).

We have found that, for the case of isothermal convective-diffusion across gas boundary layers, actual mass deposition rates from coagulation-aged populations of suspended particles will be a nearly constant fraction (*ca.* 0.92) of the abovementioned reference mass deposition rate, over a wide range of environmental conditions (Reynolds number, Knudsen number) and particle morphologies (Rosner (1991; 1989)). Table 2.2-1 summarizes our estimated values of this "constant" for a number of important combinations, including aggregates composed of equal-sized (volume v_1) primary particles. These results imply that the calculation of total mass deposition rates can often be reduced to the simpler calculation of $-\dot{m}''_{p,ref}(\bar{v})$, to which the abovementioned (nearly constant) correction factor is then applied.

We can now examine the size- and structure-sensitivity of particle deposition rates for polydispersed aggregate populations by using, say, the Kn_p<<1 results for $\langle D\rangle_N$ shown in Fig. 2.1-1 and well-known high Schmidt number results for $St_m(Re,Sc)$. For turbulent boundary layers this leads to the approximate size and morphology dependence:

Table 2.2-1 *Values*[a] *of* $[-\dot{m}_p''/-\dot{m}_p''(\bar{v})]$ *for Deposition From Coagulation-Aged Aggregated Particle Populations*[b] *(after Rosner(1989,1991))*

Aggregate Particle Morphology	Sc>>1 Convective-diffusion				Turbulent Eddy Impaction
	LBL		TBL		
	fm	c	fm	c	(c)
dense single spheres[d]	0.905	0.942	0.904	0.940	2.94
compact aggregates	?	0.936	?	0.934	2.62
fractal aggregates	0.925	0.922	0.933	0.921	1.79
linear chains[e]	0.914	0.918	0.919	0.917	1.47

a Thermophoretically-dominated deposition rate ratios (closer to unity) not reported here; present values are for negligible transport by non-convective mechanisms other than Brownian diffusion (numerical columns 1-4) or inertia (column 5)

b log-normal orientation averaged populations with $\sigma_g(fm)$=2.46 and $\sigma_g(c)$ =2.30 (see,*e.g.* Rosner and Tassopoulos(1989))

d Reference case; sintered single spheres with abovementioned σ_g-values for PSD

e For continuum cases not strictly a power-law (see Fig.2.1-1), however, values stated are for approximate power-law representation for $\langle D_p(N)\rangle$

$$\frac{\left[-\dot{m}\langle\bar{v}\rangle\right]_{actual}}{\left[-\dot{m}\langle\bar{v}\rangle\right]_{dense\ spheres}} = \frac{\left[St_m\langle\bar{v}\rangle\right]_{actual}}{\left[St_m\langle\bar{v}\rangle\right]_{dense\ spheres}} \approx \left\{\frac{\left(D\langle\bar{N}v_1\rangle\right)_{actual}}{\left(D\langle\bar{N}v_1\rangle\right)_{spheres}}\right\}^{0.7} \qquad (2.2\text{-}3)$$

This "scaling" relation, when combined with the data of Table 2.2-1 and Fig. 2.1-1, immediately allows estimates of *convective-diffusion* deposition rates from polydispersed aerosol populations of the aggregate morphologies considered, as they relate to the corresponding deposition rate if all of the suspended particles were isolated dense spheres of uniform volume $\bar{N}v_1$. Such calculations are in fact illustrated for a variety of simple simple fouling situations in Rosner (1991), including inertially-modified particle deposition ("eddy-impaction") from turbulent boundary layers. An interesting corollary of this recent research, and our abovementioned findings for

$\langle\alpha_T D\rangle_N$ (Section 2.1 and Rosner, Garcia-Ybarra and Mackowski (1990)), is that *thermophoretically*-dominated particle mass transfer rates will be remarkably *insensitive* to aggregate size and morphology --*i.e.*, for engineering predictions of *thermophoretically*- dominated particle mass transfer rates a knowledge of ϕ_p (or the corresponding *mass fraction* - ω_p (cf.Eq.(2.2-2)) alone will often suffice!

2.3 Combined Effects of Particle Inertia and Thermophoresis in Boundary Layer Flows with Streamwise Curvature

Frequently, a large portion of the particle size spectrum encountered in the effluents of power generation equipment (as well as hot gas clean-up technologies and industrial aerosol reactors) is in the range where *thermophoretic* and *inertial* effects dominate other deposition mechanisms (*e.g.* Brownian diffusion). The significant effects of thermophoresis on submicron particle deposition are by now well-studied both theoretically and experimentally (see, *e.g.*, Rosner (1985, 1986, 1988)). Similarly, the study of inertial impaction due to momentum non-equilibrium between the particle and the host gas-flow is a mature subject in aerosol science (Fuchs (1964); Friedlander (1977), Fernandez de la Mora and Rosner (1981)). Yet, little is known about the *interactions* of inertia and thermophoresis, especially for a class of practically important flows such as those over curved boundaries (*e.g.* gas turbine blades, heat exchanger tubes, duct bends). Particle-host gas flow *momentum equilibrium* is ordinarily assumed unless the particle Stokes number, *Stk* (ratio of particle relaxation time ,t_p, to the macroscopic characteristic timescale of the flow) is larger than at least the $O(10^{-1})$-values associated with the onset of inertial impaction.

Based on bench-top, high temperature boundary layer particle deposition experiments, using concave targets, and related theoretical calculations (Konstandopoulos and Rosner (1991a, 1991b)) we have shown that inertial effects on thermophoretic particle transport across boundary layers with streamwise curvature, in the small *Stk*-limit are controlled by the group $StkRe_x^{1/2}$ rather than *Stk* itself, in accord with previous related but largely unnoticed studies of inertial and interceptional capture by spheres and cylinders (Fernandez de la Mora (1986); Michael (1968)). Since, in boundary layers, $Re_x^{1/2}$ is usually a large number it is then possible for inertial effects to manifest themselves even for what were previously thought to be negligibly small *Stk*-values.

Our experimental set-up is based on a high speed/temperature jet generated by a micro-combustor, seeded with submicron *MgO* particles (Figure 2.3-1). The particles deposit on the concave side of a "cold", platinum circular arc-foil whose temperature is actively controlled. Deposition rates are inferred using a laser-light reflectivity technique, previously developed and used in this laboratory (Rosner and

Kim (1984)). Figure 2.3-2 shows our experimental results expressed in the dimensionless form:

$$St_m Re_x^{1/2} = \text{fct}\left(\frac{T_w}{T_e},\ Stk \cdot Re_x^{1/2}\right) \qquad (2.3\text{-}1)$$

suggested by an asymptotic theory ($Stk \ll 1$, $Re_x^{1/2} \gg 1$) of inertially modified thermophoresis (Konstandopoulos and Rosner (1991b)). In this functional equation, St_m is the mass transfer Stanton number, T_w the surface temperature and T_e the gas temperature at the outer edge of the boundary layer. The solid curves in Figure 2.3-2, are the corresponding theoretical predictions and are seen to be in good agreement with the data. Inertia, as quantified by $StkRe_x^{1/2}$, substantially increases the rates of thermophoretic transport to concave surfaces even when *Stk*-values are small enough (here of $O(10^{-2})$) for inertial effects to be conventionally (and incorrectly!) assumed negligible. Up to five-fold enhancements of deposition rates are obtained for a moderate cooling of the surface, *ca.* 30% below the mainstream. Similarly, our theoretical expectations for *convex* surfaces (not shown) lead to commensurate *reductions* of deposition rates to surfaces cooler than the mainstream. For surfaces kept at temperatures *higher* than the mainstream, the thickness of "particle-free" layers (Talbot *et al.* (1980), Park and Rosner (1987)) adjacent to the wall is also significantly affected by particle inertia. The thickness and diffusionally "smeared" structure of such layers, currently under study, is of interest since it may provide a basis for a convenient experimental procedure for measurement of thermophoretic and Brownian particle diffusivities (*cf.*, Gomez and Rosner (1990)).

These low-*Stk* inertial effects on thermophoretic (and other) deposition rates have important implications for accurate mass transfer predictions in aerosol deposition from flows over *curved* surfaces. Correlations derived from the theory of inertially modified thermophoretic transport outlined above, are now formulated and are expected to increase the reliability of such predictions. Interesting behavior is also expected at higher Stokes numbers and lower Reynolds numbers. These conditions are explored in an axisymmetric stagnation point flow, including high particle mass-loading effects, in Park and Rosner (1989).

2.4 Inertial Particle Capture by Cylinder Arrays in Cross-Flow

Inertial impaction of particles on an isolated circular cylinder target, especially at high *Re*, is now rather well understood. Classic studies in the aerosol literature (see, *e.g.*, Fuchs (1964)) have been extended to cover a larger range of parameters, and useful correlations for important quantities of interest have recently become available for routine engineering predictions (Israel and Rosner (1983), Wang (1986), Wessel and Righi (1988)). However, except for several singular special cases, little is yet known about the "proximity" effects of adjacent collectors on the amount and distribution of inertial impaction on any particular collector in an array. Such situations occur often in practice *e.g.*, in the entrance region of a heat exchanger tube bank. Choudhary and Gentry (1977) considered the two-cylinder problem using the method of images (MOI), while Ingham *et al.* (1990) focused on the infinite array problem (equivalent to a single cylinder centered in a straight channel) using the Boundary Element Method (BEM), to construct the flow field. Particle trajectories were then traced in these flow fields and the total capture efficiency, η_{cap} (if $s = 1$; see Section 2.5) was evaluated as a function of *Stk*. Results in both studies were presented only for a particular cylinder center-to-center spacing of 5.35 radii. We have also used the computationally efficient MOI to construct potential flow fields around cylinder assemblies and studied inertial impaction on them, with the following broader objectives:

1. To investigate how the number of collectors, N_{cyl} and their spacing alter the collection characteristics of a single cylinder in such an array.
2. To find appropriate ways to correlate the numerical results and provide an approximate, yet rational methodology for practical situations that would circumvent, or at least dramatically reduce, the need for further detailed computations of the type we have performed.

Our results for a straight column of cylinders in cross-flow shown in Figure 2.4-1 (Konstandopoulos *et al.* (1991)) support the conjecture (*cf.* Israel and Rosner (1983)) that an appropriately defined *effective* Stokes number, Stk_{eff} based on the dimensionless stagnation point fluid deceleration rate, $[du/dx]_0$:

$$Stk_{eff} \equiv Stk \cdot \left[\frac{du}{dx}\right]_0 \qquad (2.4\text{-}1)$$

can adequately describe the collection efficiency of the central cylinder in the column. This description, based on our present calculations for columns containing from three to an infinite number of cylinders, seems to be valid for other quantities of interest as well (*e.g.*, impact energies, particle concentration enrichment factors, *etc.*). Overall, it therefore now appears possible to estimate the collection efficiency of fluid-dynamically interacting cylinders in cross-flow from a knowledge of the stagnation point gradient (given in Konstandopoulos *et al.* (1991) as a function of number of cylinders and spacing) and the now well-known correlations for a single cylinder (Israel and Rosner (1983), Wang (1986), Wessel and Righi (1988)). Work in progress includes the study of high Reynolds number flow past "staggered" cylinder arrays.

2.5 Micro-Mechanical Aspects of Particle Capture and Deposit Growth

Deposit growth on collector surfaces is intimately associated with interaction of impacting particles, initially with the underlying surface, and later with the already deposited particles. The "sticking probability" π_s, of a *single* impact event is either 1 or 0, dictated by the specific contact physics. It is instructive to imagine that the abrupt transition from 1 to 0 occurs whenever some parameter λ, for example the impact velocity (Dahneke (1971), affecting the energetics of the collision reaches a critical value λ_{crit}, if all other parameters involved are kept constant. When considering an *ensemble* of impact events, however, it is convenient to introduce the notion of a "sticking coefficient" $s \equiv \langle \pi_s \rangle$, representing the overall fraction of impacting particles captured by the collector. In this way it is the ensemble averaging of the various impact events that gives rise to s-values *between* 1 and 0, with non-inertial transport mechanisms generally believed to result in perfect capture ($s = 1$). Similarly, when the collector surface is itself a particulate deposit, the concept of an "erosion coefficient" e, arises naturally, this coefficient being equal to the ensemble-averaged number of particles re-entrained from the surface per impaction event (see Rosner and Nagarajan, 1987). The coefficients s and e depend on many parameters (*e.g.* particle size, density, velocity, impact angle, charge, particle and collector material properties, *etc.*) as well as on the deposit morphology, which, in turn, is modified by the depositing particles. The possible existence of liquid phases on the deposition surface, or within the collecting particulate deposit, introduces additional dependencies on liquid phase distribution, viscosity, surface tension, density, *etc.* In addition, environmental variables such as local temperature are expected to influence many of the previously mentioned thermophysical parameters.

The two-way coupling between the fate of an incident particle and deposit microstructure makes the problem of predicting impacting particle capture on a deposit considerably more complex than the corresponding problem of particle capture by a

flat rigid surface, which in recent years has received renewed attention in the context of improved impactor performance (see Wall *et al.* (1990), Wall and John (1988) and references cited therein). While s for the latter problem can be evaluated deterministically by integrating over the *a priori* known parameter space, the same is not true for the former problem. The dynamic "randomness" introduced by the *evolving deposit microstructure* implies that even if all other parameters affecting particle capture were kept constant, the sticking fraction would still be a "random" variable, drifting in response to self-induced changes in the deposit morphology. Deposit microstructure is known to determine effective properties of engineering interest, presently also under investigation (see Section 2.6). Given the number of parameters involved and the technical difficulties of reliably measuring even only some of them under well-defined conditions, it is not surprising that very limited fundamental experimental knowledge exists about these phenomena. In our view, computer simulations provide a tractable route to study important aspects of the incident-particle/deposit interaction problem. While several purely algorithmic, deposit growth models have provided valuable insight to the structural and transport properties of particle packings (Section 2.6), they do not couple the collision outcome to the actual deposition physics. Hence, such models are unfit for our purposes of *computing*, rather than *prescribing* the collision outcome using *ad hoc* "rules".

Aiming at a micro-mechanical fundamental description of these coupled phenomena (Konstandopoulos and Rosner, 1991c), we have undertaken a program of computer simulations of deposit growth, patterned after the succesfull precedents of molecular dynamics (*e.g.* Hoover (1986), Alder and Wainwright (1956)) and Distinct Element Methods (DEM) for granular media (*e.g.* Cundall and Strack, (1977); Thornton and Barnes, (1986); Walton and Braun (1986); Werner and Haff, (1989)). Presently we have completed an investigation of what we term "frozen" deposits (Konstandopoulos and Tassopoulos, (1991), Tassopoulos and Konstandopoulos, (1991)), where each particle once deposited remains irreversibly in place due to stereological constraints and/or strong contact bonds with its neighbors. However in later collisions, those target particles which have been incorporated into the deposit, are assumed to present an "effective" inertial mass m_{eff} to subsequent incident particles, arising precisely from the fact that they are in contact with a number of their neighbors. Our first working hypothesis was to assume that m_{eff} depends only on the local microstructure and scales linearly with the target particle local coordination number Z:

$$m_{eff} = m(1 + C_m Z) \qquad (2.5\text{-}1)$$

where m is the actual particle mass and C_m a positive dimensionless control parameter. Physically interesting are small values of C_m, since as m_{eff} starts to become appreciably larger than m the limit of a rigid body is reached and the model becomes insensitive to C_m. This makes possible the calculation of bounds for the quantities of interest. The conjecture that the incident-target particle interaction can be described as a pseudo-binary collision using an effective inertial mass for the target particle is supported by the many-body, two-dimensional simulations of Werner (1987). Hence, based on this three-dimensional *kinetic* model of "frozen" deposit growth, the fate of each incident particle is determined extending a previously used (Chapman and Cowling (1960); Walton, (1989)) "rough" spheres (with friction coefficient μ) collision operator to include adhesion. This was accomplished introducing barriers on the kinetic (ΔU) and rotational ($E_\omega \Delta U$) energies for succesful particle rebound, calculated from contact mechanics theory using material properties appropriate for inorganic ash (*e.g. MgO*) particles. These simulations, implemented in the code FROZEN, can be animated in "real-time" on a computer screen. It should be

mentioned that we have recently relaxed the "frozen" deposit aspect and now allow all particles to move in response to their applied contact forces (Konstandopoulos and Rosner, 1991c). These latter, more elaborate DEM simulations, even incorporate additional contact forces arising from the presence of liquid pendular bridges among the deposit particles.

Figure 2.5-1 illustrates the temporal evolution (expressed in terms of number of deposited particles) of the sticking coefficient of "frozen" deposits at various dimensionless impact velocities. Note that velocities have been made dimensionless with $\sqrt{2\Delta U/m}$. A stationary state appears to set in at long times, suggesting that, so far as particle capture is concerned, the deposit morphology has also reached a stationary state (Section 2.6). The dependence of this stationary sticking coefficient on impact velocity is shown in Figure 2.5-2 for $\mu = 0.2$ and various values of E_ω and C_m. The results of these numerical "experiments" indicate the existence of a critical velocity below which all particles stick and above which sticking coefficients decay exponentially (Figure 2.5-2). Furthermore, the similar slope of all curves for a fixed value of C_m implies that a similarity transformation can remove the dependence on E_ω by normalizing the impact velocity in each experiment by its own critical velocity. Rather compact correlations can be then obtained for the dependence of s on impact velocity. Varying the angle of incidence in the range 0-65^0 relative to the outward normal (not shown) was found to produce only a slight decrease in s. We have also measured distributions characterizing relevant collision parameters (impact angle, m_{eff}, *etc.*) and the kinetics of particle capture and rebound (lifetimes of particles on the surface, mean travel distance, number of collisions before a particle comes to rest, *etc.*).

Such deposit growth models, together with highly selective experimental tests, promise to provide much needed, rational sticking "laws" that can be used to increase the reliability of engineering predictions for inertial particle deposition rates.

2.6 Relationships Between Deposition Mechanism and Resulting Deposit Microstructure/Effective Transport Properties

The important coupling between deposition mechanism and particulate deposit microstructure/effective transport properties has been until now poorly understood and only scarcely studied. In order to quantitatively treat these interrelated phenomena it is convenient to distinguish between two classes of arriving particles: (a) small "Brownian" particles (see Section 2.1), which are transferred by convective diffusion, possibly in the presence of some phoretic mechanism (thermophoresis, electrophoresis, *etc.*), and (b) larger particles which arrive at the target due to their inertia (non-negligible Stk; Sections 2.3, 2.4). The former, because of their low impact velocity, usually have unit sticking probability (see Section 2.5), so that deposit growth and hence microstructure evolution is primarily determined by the first contact event. Clearly, a higher probability of arriving at the deposit outer surface as opposed to penetrating deeper into the porous medium gives rise to more open, dendrite-like deposits. In Tassopoulos *et al.* (1989), we provided both theoretical and, using computer simulations, "experimental" evidence that the penetration depth of the arriving particle depends on the relative importance of deterministic- to diffusive-motion, as prescribed by a local Peclet number, Pe ($=VL_B/D_p$), where V is the phoretic velocity, L_B is the Brownian diffusion sublayer thickness and D_p is the particle diffusion coefficient. We found that the lower this Peclet number (diffusion more important), the more "open" is the resulting microstructure. This is shown in Figure 2.6-1, where we plot deposit porosity, ε, (open symbols) *vs.* Pe. For additional information, the interested reader is referred to the original paper, where we also present some indicative results on the effect of arriving particle morphology (dimers, trimers, ...) and orientation on the resulting deposit microstructure.

Larger particles, arriving at the target with higher velocities, may have a non-unity sticking coefficient (see Section 2.5), so that the subsequent motions of the incident and possibly target particles are determined by the actual deposition physics. When the particle kinetic energy upon impact is very high and/or the adhesive forces between the particles are weak, the deposits approach a *random loose packing* configuration irrespective of details of the particle trajectories and particle-particle interactions. Such deposits can be efficiently generated using appropriate off-lattice algorithmic models (see *e.g.*, Visscher and Bolsterli (1972); for a brief review, see also Tassopoulos and Rosner (1991a)). Similarly, the microstructures associated with "frozen" deposits (see Section 2.5), have been modelled using the code: FROZEN (Konstandopoulos and Tassopoulos (1991), Tassopoulos and Konstandopoulos (1991)). In Figure 2.6-1 (filled symbols) we show the effect of impact velocity on deposit porosity, assuming normal incidence and individual particle material properties typical of inorganic ash. The interplay between angle of incidence and impact velocity, and their effect on final deposit microstructure is qualitatively shown in Figure 2.6-2(a), (b), where we plot two 2D-deposits generated by FROZEN. All other parameters being the same $\left(\theta = 65°, E_\omega = 0, C_m = 2, \mu = 0.2\right)$, the incident particle dimensionless velocity is 2 for deposit (a) and 4 for (b). Note the absence of columnar structures in deposit (b), presumably due to the higher initial velocity of the arriving particles and their associated 'restructuring' motion after the first collision event with an already deposited particle. The resulting s-values are 0.53 and 0.15 respectively. Finally, it should be noted that, despite its computational demands, we are presently studying the microstructural properties of non-frozen deposits generated by Distinct Element Methods (Cundall and Strack (1979)).

In addition to typical structural descriptors (porosity, pore size distribution, surface roughness,...), the properties of the deposits generated are further quantified using orientation tensors and anisotropic correlation functions---quantities that readily provide theoretical estimates and bounds on the deposit effective transport properties. In parallel, we are extending and implementing Brownian motion simulation techniques to accurately determine the effective vapor/porous solid diffusivity tensor over the entire Knudsen number range (Tassopoulos and Rosner (1991a)) and the effective thermal conductivity tensor (Kim and Torquato (1990), Tassopoulos and Rosner (1991b)), incorporating the effects of contact resistance and/or liquid bridges. These "exact" simulation results can be also used to test the abovementioned theoretical estimates. In Figure 2.6-3 we plot the variation of the tortuosity factor, τ ($=\varepsilon D/D_{eff}$), with deposit porosity, ε, in the continuum limit, as "measured" by our Brownian motion simulations and as predicted by theoretical and semiempirical expressions (for details and other results, see the original paper).

3. CONCLUSIONS AND SIGNIFICANCE

Recent research described here has clarified a number of issues central to the understanding and prediction of suspended particle deposition rates from flowing hot gases, and the nature and properties of the resulting microparticulate deposits. Among the most noteworthy *conclusions and generalizations* of the studies described in greater detail in Section 2 (and the associated references, Section 4) are:

C1 Suspended particle aggregation (and resulting particle morphology and size) has a greater effect on the rate of inertial- and Brownian diffusive-capture of particles than on the rate of the thermophoretic capture of intermediate-sized particles from flowing gases (Rosner, *et.al.* (1990)).

C2 Capture rates from "coagulation-aged" polydispersed aerosols by the mechanisms of convective-diffusion and, especially, thermophoresis are close to those calculated if all such particles had the mean particle size (volume) ϕ_p/N_p. Correction factors for *convective-diffusion* are close to 0.92 for a surprisingly wide range of gas-dynamic and environmental conditions, and particle morphologies (Table 2.2-1 andRosner (1989,1991).

C3 Thermophoretically dominated capture rates are remarkably insensitive to particle-size and morphology --- so much so that useful engineering predictions of total (mass- or volume-) deposition rates can often be made from a knowledge of the total (mass- or volume-) fraction of such particles, irrespective of their size- and/or morphology-distribution (Rosner *et al.*, 1990).

C4 For high Reynolds number flows of particle-laden gases, smallness of the conventionally defined particle Stokes number, $t_p/(L/U)$, is no guarantee of the smallness of inertial effects on particle deposition rates, and their spatial distribution. For laminar boundary layer flow over targets with streamwise curvature (*e.g.* gas turbine blade surfaces, the forward regions of heat exchanger tubes in cross-flow) the governing parameter has been found to be $Stk \cdot Re_z^{1/2}$, which can be large enough for dramatic inertial effects even when $Stk \ll 1$ (Konstandopoulos and Rosner (1991b)).

C5 Recent laboratory experiments using a seeded microjet combustor and curved ribbon targets (Konstandopoulos and Rosner, (1991a)) demonstrate that the combined effects of thermophoretic- and inertial-particle drift toward a concave, "cold" target can substantially augment local particle deposition rates, in excellent accord with the predictions of two-phase laminar boundary layer theory (Konstandopoulos and Rosner (1991b)). On convex cooled surfaces, the theory can thus be used to predict the *competing* effects of thermophoretically-augmented capture and inertial drift *away* from the target.

C6 Our inertial impaction calculations for multiple-cylinder target configurations (simulating aerodynamic interference effects for neighboring cylinders in, say, the first column of a tube "bank") reveal that the principal effect of multiple target proximity is to change the local gas deceleration rates, thereby shifting the so-called "critical Stokes number" (see, *e.g.* Rosner and Israel (1983)). Thus, our numerical results for particle capture on individual cylinders in "banks" of from three up to an infinite number of flanking cylinders are well-correlated using the relevant particle Stokes number - *i.e.* basing the "flow time" on the *actual* (*not* isolated-target) gas deceleration rate in the vicinity of the forward stagnation point (line) (Section 2.4 and Konstandopoulos *et al.*, (1991)).

C7 Computer simulations provide a tractable route to study micromechanical aspects of incident particle capture and associated deposit growth. Using a recently formulated kinetic model of deposit growth (Konstandopoulos and Tassopoulos (1991)) we have examined how impact parameters (velocity, angle of incidence) affect the *sticking coefficient*, s , of particles impacting *on deposits*. Our numerical results indicate that increasing the input velocity beyond a critical value required for particle rebound, causes an exponential decrease in the sticking coefficient. However, varying the arriving particle angle of incidence in the range 0-65° produced only a slight decrease in s.

C8 On-lattice Monte-Carlo simulations have been successfully used to obtain qualitative information and scaling laws describing the effect of the arriving particle trajectories, as quantified by a local Peclet number, on *deposit microstructure* (Tassopoulos, *et al* (1989)). Detailed deposit morphologies have been studied using both "algorithmic" and kinetic models of varying complexity. The associated effective transport properties of the deposit have been accurately determined using Brownian Dynamics Simulations, (Tassopoulos and Rosner (1991a, 1991b)) including comparisons with particular theoretical and semiempirical expressions.

Despite the formidable complexities to be overcome in the design and operation of power plants utilizing a broad spectrum ash-bearing fuels these particular conclusions are indicative of the potentially useful *simplifications and generalizations* emerging from current fundamental research studies of suspended particle deposition mechanisms and their connection to microparticulate deposit formation. Our investigations continue in each of the specific areas summarized in Section 2, as well as new areas beyond the scope of this particular review, with the goal of ultimately providing engineering designers with better "tools" for making rational assessments of ash deposition phenomena in future, high-performance coal-fired equipment. It is hoped that this invited review, and the present EF Conference, accelerate this process *via* the requisite and timely exchange of R&D information.

ACKNOWLEDGEMENTS--The research summarized here was supported in large part by DOE-PETC under Grants DE-FG22-86-PC90756 (completed April 1990) and DE FG-22-90PC90099 (commencing Sept.1990), with significant inputs from AFOSR (under Grant 89-0223) and the present Yale HTCRE Laboratory *Industrial Affiliates* (Shell, SCM-Chemicals, DuPont, and Union Carbide Corporations). It is a pleasure to specifically acknowledge the contributions of Dr. M. Labowsky, whose formulation of the method of images enabled he calculations reported in Section 2.4, Prof. J. Fernandez de la Mora, who continues to contribute significantly to our understanding of inertial effects on other mechanisms of particle transport (cf. Section 2.3), Prof. A. Gomez for his counterflow flat-flame measurements of aggregate thermophoretic diffusivities, and Drs. J. Castillo and P. Garcia-Ybarra (U.N.E.D.-Madrid) for their analyses of multiphase boundary layer behavior and aggregate transport properties (Section 2.1), respectively. Dr. D W.Mackowski, formerly Postdoctoral Research Engineer, Yale HTCRE Laboratory, is currently Assistant Professor of Mechanical Engineering at Auburn University, Auburn, AL 38649-5341. Correspondence concerning this manuscript should be sent to Prof. Daniel E. Rosner, Director Yale HTCRE Laboratory, at the address given above the Abstract.

4.LITERATURE CITED

Alder, B. J. and Wainwright, T. E. (1959) "Studies in Molecular Dynamics. I. General Method", *J. Chem. Phys.*, **31**, pp. 459-466.

Castillo, J.L., and Rosner, D.E. (1988) "Non-equilibrium Theory of Surface Deposition from Particle-Laden, Dilute Condensible Vapor -Containing Streams, Allowing for Particle Thermophoresis and Vapor Scavenging within the Laminar Boundary Layer", *Int. J. Multiphase Flow*, **14** (1), pp. 99-120.

Castillo, J.L., Mackowski, D.W. and Rosner, D.E. (1990) "Photophoretic Contribution to the Transport of Absorbing Particles Across Combustion Gas Boundary Layers", *Prog. Energy and Combustion Science*, **16**, 253-260.

Chapman, S. and Cowling, T. G. (1960) **The Mathematical Theory of Non-Uniform Gases**, Cambridge University press, Cambridge.

Cundall, P. A. and Strack, O. D. L.(1979) "A Discrete Numerical Model for Granular Assemblies", *Geotechnique*, **29** (1), pp. 47-65.

Choudhary, K. R. and Gentry, J. W. (1977) "A Model for Particle Collection with Potential Flow Between Two Parallel Cylinders", *Canadian J. Chem. Engng.*, 55, pp. 403-407.

Dahneke, B. (1971), "The Capture of Aerosol Particles by Surfaces," *J. Colloid Interface Sci.*, 37 (2), p. 342.

Fernandez de la Mora, J. (1986) "Inertia and Interception in the Deposition of Particles from Boundary Layers", *Aerosol Sci. Tech.*, 5, pp. 261-266.

Fernandez de la Mora, J.and Rosner, D.E. (1981) "Inertial Deposition of Particles Revisited and Extended: Eulerian Approach to a Traditionally Lagrangian Problem", *J. PhysicoChemical Hydrodynamics (PCH)*, 2, 1-21

Fuchs, N. A. (1964) **The Mechanics of Aerosols**. Pergamon, New York.

Friedlander, S. K. (1977) **Smoke Dust and Haze: Fundamentals of Aerosol Behavior**, John Wiley and Sons, New York.

Gomez, A. and Rosner D. E. (1991) "Thermophoretic Effects on Particles in Counterflow Laminar Diffusion Flames", *AAAR 1990 Annual Meeting*, paper 6E.2, June 18-22, Philadelphia, PA. (prepared for submission).

Hoover W. G. (1986), **Molecular Dynamics**, Springer-Verlag, Berlin.

Ingham, D. B., Hildyard, M. L and Heggs, P.J.(1990) "The Particle Collection Efficiency of a Cascade of Cylinders", *Canadian J. Chem. Engng.*, 67, pp. 545-553.

Israel, R. and Rosner, D. E. (1983) "Use of a Generalized Stokes Number to Determine the Aerodynamic Capture Efficiency of Non-Stokesian Particles from a Compressible Gas Flow", *Aerosol Sci. Tech.*(AAAR) 9, pp. 29-60.

Kim, I. C. and Torquato, S. (1990), "Determination of the Effective Conductivity of Heterogeneous Media by Brownian Motion Simulation," *J. Appl. Phys.*, 68 (8), pp. 3892-3903.

Konstandopoulos, A. G. and Rosner, D. E. (1991a) "Inertial Effects on Thermophoretic Transport of Small Particles to Walls with Streamwise Curvature--I: Experiment",*AAAR 1990 Annual Meeting*, paper 7C.6, June 18-22, Philadelphia, PA. (prepared for submission to *Int. J. Heat Mass Transfer*).

Konstandopoulos, A. G. and Rosner, D. E. (1991b) "Inertial Effects on Thermophoretic Transport of Small Particles to Walls with Streamwise Curvature--II: Theory", (prepared for submission to *Int. J. Heat Mass Transfer*).

Konstandopoulos, A. G., Labowsky, M. and Rosner, D. E. (1991) "Inertial Deposition of Particles from Potential Flows past Cylinder Assemblies", *AAAR 1990 Annual Meeting*, paper 5E.6, June 18-22, 1990, Philadelphia, PA. (prepared for submission to *J. Aerosol Sci.*).

Konstandopoulos, A. G. and Rosner, D. E. (1991c) "A Micro-Mechanical Approach to Particle Capture and Deposit Growth" (in preparation).

Konstandopoulos, A. G. and Tassopoulos, M. (1991) "A Kinetic Model for Deposit Growth. Part I: Characterization of Sticking Probabilities", see also *AAAR 1990 Annual Meeting*, paper 6E.6, June 18-22, 1990, Philadelphia, PA. (prepared for submission to *J. Colloid Interface Sci.*).

Mackowski, D. W., (1990) "Phoretic Behavior of Asymmetric Particles in Thermal Nonequilibrium with the Gas: Two-Sphere Aggregates", *J. Colloid Interface Sci.*, 140 (1), pp. 138-157.

Mackowski, D. W., (1989),"Photophoresis of Aerosol Particles in the Free-Molecular and Slip-Flow Regimes", *Int. J. Heat Mass Transfer* , 32,(5),843-854.

Marner, W. J. (1989) "Progress in Gas-Side Fouling of Heat Transfer Surfaces" in **A. L. London Symposium on Compact Heat Exchangers**, pp. 421-489, Hemisphere, Washington.

Michael, D. H. (1968) "The Steady Motion of a Sphere in a Dusty Gas", *J. Fluid Mech.*, 31, pp. 175-192.

Park, H. M and Rosner, D.E.,(1987), "Thermophoretically Induced Phase-Separation in Highly Mass-Loaded 'Dusty' Gas Mixtures", Yale HTCRE Laboratory Publication No. 162; (prepared for submission to *Int. J. Heat Mass Transfer*)

Park, H. M and Rosner, D.E.,(1989),"Combined Inertial and Thermophoretic Effects on Particle Deposition Rates in Highly Loaded Dusty Gas Systems", *Chemical Engineering Science*, 44, (10) 2233-2244.

Rosner, D.E.(1986) **Transport Processes in Chemically Reacting Flow Systems**, Butterworth-Heinemann, Third Printing 1990.

Rosner, D.E.(1985),"Mass Transfer Across Combustion Gas Thermal Boundary Layers---Power Production and Materials Processing Implications", in **Heat Transfer in Fire and Combustion Systems**, HTD 45, ASME, NY, NY, pp 3-8

Rosner, D. E. and Kim, S. S.(1984) "Optical Experiments on Thermophoretically Augmented Submicron Particle Deposition from 'Dusty' High Temperature Gas Flows", *Chem. Engng. J.*, (Elsevier)29, pp. 147-157.

Rosner, D. E. (1988) "Experimental and Theoretical Studies of Inorganic Matter Deposition from Combustion Gases", *PhysicoChem. Hydrodyn. (B. Levich Memorial Issue)*, 10 (5-6), pp. 663-674.

Rosner, D.E. (1989) "Total Mass Deposition Rates from 'Polydispersed' Aerosols"; *AIChE J.* 35 (1) 164-167.

Rosner, D. E. (1991) "Structure-Sensitivity of Total Mass Deposition Rates from Streams Containing Coagulation-Aged Populations of Aggregated Primary Particles", (in preparation).

Rosner, D. E., Mackowski, D. W. and Garcia-Ybarra, P. (1990) "Size- and Structure-Insensitivity of the Thermophoretic Transport of Aggregated 'Soot' Particles in Gases", (submitted to *Comb. Sci. Tech.*).

Rosner, D. E. and Nagarajan R. (1987) "Toward a Mechanistic Theory of Net Deposit Growth from Ash-Laden Flowing Combustion Gases: Self-Regulated Sticking and Deposit Erosion in the Presence of Vapor 'Glue' ", *A.I.Ch.E. Symp. Ser.* 83 (257), pp. 289-296.

Rosner, D. E., Mackowski, D. W.,Tassopoulos, M., Castillo,J.,and Garcia-Ybarra, P. (1991), "Effects of Heat Transfer on the Dynamics and Transport of Small Particles in Gases", submitted to *IEC.-Research*

Rosner,D.E. and Tassopoulos,M, (1989) "Deposition Rates From Polydispersed Particle Populations of Arbitrary Spread", *AIChE J.* 35 (9), pp.1497-1508.

Tassopoulos, M. and Konstandopoulos, A. G. (1991) "A Kinetic Model for Deposit Growth. Part II: Characterization of Microstructure and Transport Properties", see also *AAAR 1990 Annual Meeting*, paper 6E.6, June 18-22, 1990, Philadelphia, PA.(prepared for submission to *J. Colloid Interface Sci.*).

Talbot, L., Cheng, R. K., Schefer, R. W., and Willis, D. R. (1980), "Thermophoresis of Particles in a Heated Boundary Layer", *J. Fluid Mechanics* , 101, 737-758.

Tassopoulos, M., O'Brien, J. A., and Rosner, D. E., (1989) "Simulation of Microstructure-Mechanism Relationships in Particle Deposition", *AIChE J.* 35 (6),967-980,

Tassopoulos, M. and Rosner, D.E. (1991a) "Simulation of Vapor Diffusion in Anisotropic Particulate Deposits", *Chem. Eng. Sci.*, in press.

Tassopoulos, M. and Rosner, D.E. (1991b) "Effective Thermal Conductivity of Anisotropic Particulate Deposits", (prepared for submission to *Int. J. Heat Mass Transfer*)

Thornton C. and Barnes D. J. (1986) "Computer Simulated Deformation of Compact Granular Assemblies", *Acta Mechanica*, 63, pp. 45-61.

Visscher, W.M. and Bolsterli (1972) "Random Packing of Equal and Unequal Spheres in Two and Three Dimensions", *Nature*, 239, pp. 504-507.
Wall, S. and John, W. (1988) "Impact Adhesion Theory Applied to Measurements of Particle Kinetic Energy Loss", *J. Aerosol Sci.*, 19 (7), p. 789.
Wall, S., John, W., Wang, H. W. and Goren, S. L. (1990) "Measurements of Kinetic Energy Loss for Particles Impacting Surfaces" *Aerosol Sci. Tech.*, (in press).
Walton, O. R. (1989) Personal communication, see also LLNL Granular Solids Flow *Project Quarterly Report UCID-20297-88-1, May 1988.*
Walton, O. R. and Braun, R. L. (1986) "Stress Calculations for Assemblies of Inelastic Spheres in Uniform Shear", *Acta Mechanica*, 63, pp. 73-86.
Wang, H. C. (1986) "Theoretical Adhesion Efficiency for Particles Impacting a Cylinder at High Reynolds Numbers", *J. Aerosol Sci.*, 17 (5), pp. 827-837.
Werner, B. T. (1987) **A Physical Model of Wind Blown Sand Transport**, PhD Thesis, Division of Physics, Mathematics and Astronomy, California Institute of Technology, Pasadena, California.
Werner, B. T. and Haff, P. K. (1988) "The Impact Process in Aeolian Saltation: Two Dimensional Simulations", *Sedimentology*, 35, pp. 189-196.
Wessel, R. A. and Righi, J. (1988) "Generalized Correlations for Inertial Impaction of Particles on a Circular Cylinder", *Aerosol Sci. Tech.*, 9, pp.29-60.

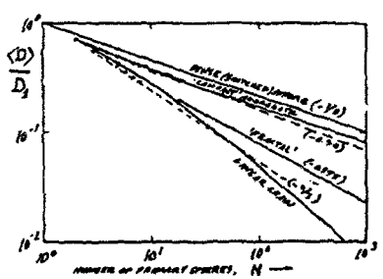

Figure 2.1-1 Orientation-averaged Brownian diffusivities of aggregates containing N primary spheres: Dependence on N and morphology in the continuum (Kn_p<<1) limit (after Rosner (1991)). (Normalization: Brownian diffusion coefficient, D_1, of primary sphere in same local environment)

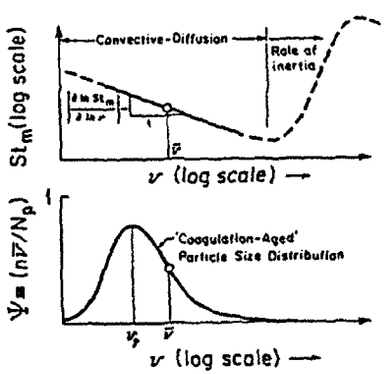

Figure 2.2-1 Behavior of the dimensionless particle mass transfer coefficient, St_m, and dimensionless aerosol particle size distribution function, ψ, as a function of suspended particle volume ,v (log-log coordinates) in a particular case of particle morphology/flow-field/target geometry (after Rosner (1989))

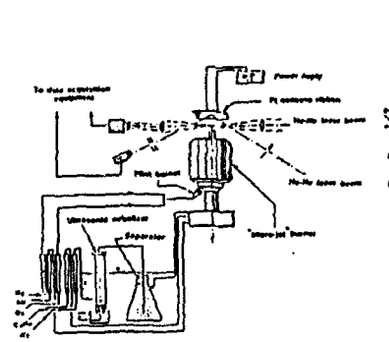

Figure 2.3-1 .Seeded microjet combustor apparatus (schematic) for optical reflectivity studies of inertially-modified thermophoretic deposition rates on solid target (platinum ribbon) with streamwise curvature (after Konstandopoulos and Rosner (1991a))

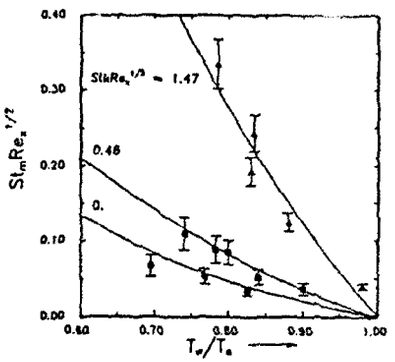

Figure 2.3-2. Experimental and theoretical particle deposition rate coefficient $St_m Re_x^{1/2}$ vs. temperature ratio T_w/T_e and the relevant particle relaxation time parameter $StkRe_x^{1/2}$ (after Konstandopoulos and Rosner(1991a)); Laminar BL flow, circular arc solid target.

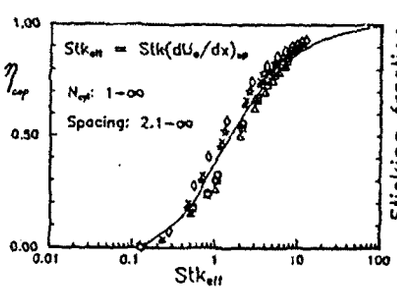

Figure 2.4-1 "Effective Stokes number" correlation of calculated inertial impaction fractions for high Reynolds number flow past a "column" of equidistant aerodynamically interfering circular cylinders in crossflow (after Konstandopoulos, *et al.* (1991))

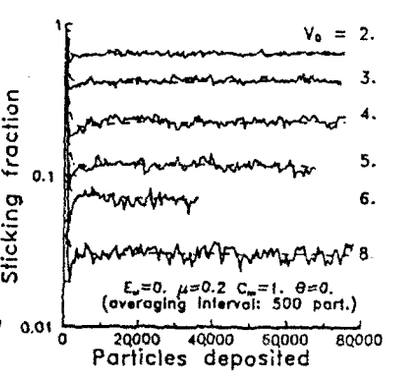

Figure 2.5-1 Example of sticking fraction evolution for different (dimensionless) impact velocities at normal incidence ($\theta = 0°$), computed using the code: FROZEN for indicated values of the model parameters (after Konstandopoulos and Tassopoulos (1991)).

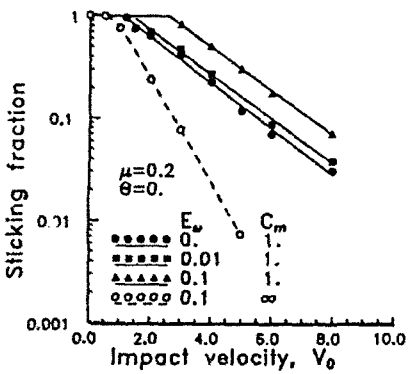

Figure 2.5-2 Exponential decay of stationary sticking fraction with incident (dimensionless) impact velocity at normal incidence ($\theta = 0^o$), computed using the code: FROZEN for indicated values of the model parameters (after Konstandopoulos and Tassopoulos (1991)).

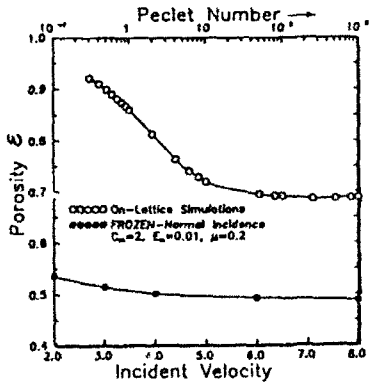

Figure 2.6-1 Predicted variation of deposit porosity with deposition conditions. Empty symbols: effect of Peclet number (Section 2.6). Data obtained using on-lattice simulations. Filled symbols: Effect of arriving particle V_0. Data obtained using the code FROZEN

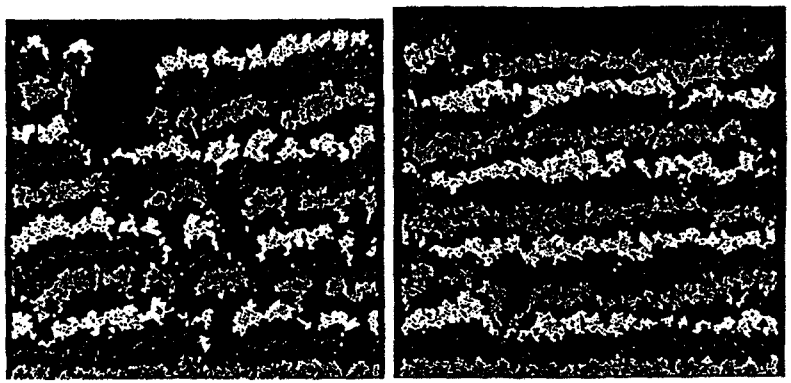

Figure 2.6-2 Effect of incident particle (dimensionless) impact velocity on 2-D deposit microstructure obtained with the code: FROZEN. Both deposits were generated by particles arriving at a 65° angle with respect to the target normal. The shading changes every 420 particles (approximately 4 mono-layers). For deposit (a) the impact velocity was 2 and for (b) 4. Resulting sticking fractions were 0.53 and 0.15 respectively.

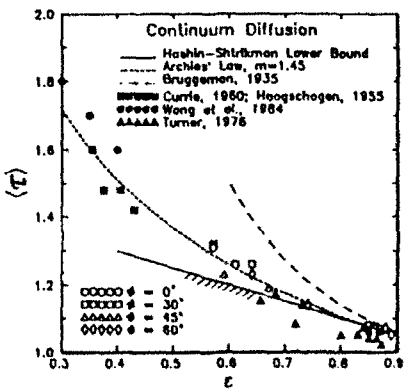

Figure 2.6-3 Predicted variation of deposit tortuosity factor for vapor diffusion (empty symbols) with deposit porosity in the continuum limit. Effect of the local deposit microstructure (as determined by the arriving particle angle of incidence); Filled symbols are experimental data points.

5. NOMENCLATURE

b	exponent describing dependence of St_m on particle volume v
C_m	positive dimensionless control parameter (Eq. (2.5-1))
D	Brownian diffusion coefficient for particle of volume v
d_p	particle diameter
e	erosion coefficient
$E_\omega \Delta U$	energy barrier to rolling motion of incident particle
k_B	Boltzmann constant
Kn_p	Knudsen number (based on prevailing gas mean-free path and particle diameter)
L_B	Brownian diffusion sublayer thickness
l_g	local gas mean-free-path
m, m_p	mass of particle of volume v
m_{eff}	effective inertial mass of struck "particle"
$-\dot{m}_p$	total mass deposition rate per unit target area
N	number of primary spheres in aggregate particle
n	size distribution function dN_p/dv
N_{cyl}	number of cylinders in array (column) of collectors
N_p	total suspended particle number density
Nu_m	mass transfer Nusselt (Sherwood) number (Rosner (1986))
Pe	Peclet number, VL_B/D_p
R	radius (of curvature) of target
Re	Reynolds number
R_g	radius of gyration of aggregate
s	sticking coefficient $(\equiv \langle \pi_s \rangle)$
Sc	particle Schmidt number, $(\mu/\rho)_{gas}/D_p$
Stk	Stokes' number, $t_p/t_{flow,ref}$
St_m	mass transfer Stanton number, $Nu_m/(ReSc)$ (Rosner (1986))
T	absolute temperature (Kelvins)
t	time
T_e	gas temperature at the outer edge of the boundary layer
T_g	gas temperature
t_p	particle stopping time in prevailing gas
T_w	surface temperature
U	velocity of carrier gas

u	local streamwise velocity (as multiple of U)
V	phoretic (drift) velocity of particle in gas phase
v	volume of spherical particle
v_g	geometric-mean particle volume in log-normal PSD $n(v,...)$
v_0	initial velocity of incident particle, in units of $\sqrt{2\Delta U/m}$
$\bar{v}$	mean particle volume, ϕ_p/N_p, of local aerosol
Z	local coordination number of target particle in deposit

Greek

α_T	thermal diffusion factor (dimensionless)
ΔU	energy well parameter responsible for incident particle trapping
ϵ	porosity (void fraction)
ϕ_p	total aerosol volume fraction
η_{cap}	total particle capture fraction
μ	friction coefficient
μ_{gas}	dynamic Newtonian viscosity of the carrier gas
π_s	sticking probability of a single impact event
θ	angle of particle incidence (relative to normal direction)
ρ	density
ρ_p	intrinsic density of a particle (m_p/v)
σ_g	geometric standard deviation of log-normal PSD $n(v,...)$ (see Rosner and Tassopoulos (1989))
τ	porous deposit "tortuosity"; $\epsilon D/D_{eff}$
ω_p	mass fraction of suspended particles
ψ	mainstream dimensionless particle size distribution (PSD-) function, $\bar{v}n(v)/N_p$

Subscripts

cap	pertaining to particle capture
e	pertaining to outer edge of the gaseous boundary layer
eff	effective value
g	pertaining to log-normal PSD (geometric)
gas, g	pertaining to carrier gas
max	maximum value

meas	measured
N	pertaining to aggregate composed of N primary spheres
o	pertaining to forward stagnation point (line)
o	pertaining to incident condition
p	particle(s)
ref	reference case (*e.g.*, evaluated at particle volume $\bar{v}$)
w	pertaining to the wall (surface)
x	pertaining to streamwise station x
1	pertaining to a primary sphere

Other

$(\cdot)$	mean value (*e.g.*, $\bar{v}= \phi_p/N_p$)
< >	orientation-averaged value (*e.g.*, $<t_p>$, $<D_p>$) or ensemble-averaged value ($<\pi_s>$)

Abbreviations

BEM	boundary element (numerical) method
c	continuum ($Kn_p<<1$)
DEM	distinct element method
fct	function
fm	free molecule ($Kn_p>>1$)
grad	spatial gradient operator
LBL	laminar boundary layer
MOI	method of images
ODE	ordinary differential equation
O( )	order of magnitude
PSD	particle size (volume) distribution
RHS	right hand side (of equation)
TBL	turbulent boundary layer

HIGH TEMPERATURE CHEMICAL REACTION ENGINEERING LABORATORY
YALE UNIVERSITY
BOX 2159, YALE STATION
NEW HAVEN, CONNECTICUT 06520 U.S.A.

Daniel E. Rosner
Selected Publications -'Thermophoretic' Mass Transport

101 "Thermal (Soret) Diffusion Effects on Interfacial Mass Transport Rates", *J. PhysicoChemical Hydrodynamics* (PCH) **1**, 159-185 (1980).

117 "Small Particle Transport Across Turbulent Non-Isothermal Boundary Layers", *ASME Trans.-J. Engrg. for Power* **104**, 885-894 (1982) (with J. Fernandez de la Mora).

122 "Correlation of Thermophoretically-Modified Small Particle Diffusional Deposition Rates in Forced Convection Systems with Variable Properties, Transpiration Cooling and/or Viscous Dissipation", *Int. J. Heat and Mass Transfer* **27**, 639-645 (1984) (with S.A.Gokoglu)

130 "Optical Experiments on Thermophoretically Augmented Submicron Particle Deposition from 'Dusty' High Temperature Gas Flows", *The Chemical Engrg. J.* (Elsevier) **29**, [3], 147-157 (1984) (with S.S. Kim).

131 "Thermophoretically Enhanced Mass Transport Rates to Solid and Transpiration-Cooled Walls Across Turbulent (Law-of-the-Wall) Boundary Layers", *I/EC Fundamentals* **24**, [2], 208-214 (1985) (with S.A. Gokoglu)

133 "Thermophoretically-Augmented Forced Convection Mass Transfer Rates to Solid Walls Across Non-Isothermal Laminar Boundary Layers", *A.I.A.A. J.* **24**, [1], 172-179 (1986) (with S.A. Gokoglu)

134 "Experimental Studies of Soot Particle Thermophoresis in Non-Isothermal Combustion Gases Using Thermocouple Response Techniques", *Combustion and Flame* **61**, 153-166 (1985) (with A.D. Eisner)

137 **Transport Processes in Chemically Reacting Flow Systems**, Butterworth-Heinemann Publishers, Stoneham, MA (1986), Third Printing Dec.1990).

140 "Thermophoretically Augmented Mass, Momentum and Energy Transfer Rates in High Particle Mass-Loaded Laminar Forced Convection Systems", *Chem. Engrg. Science* **43**, [10], 2689-2704 (1988) (with H.M.Park)

143 "Experimental and Theoretical Studies of Submicron Particle Thermophoresis in Combustion Gases", *J. PhysicoChemical Hydrodynamics* **7**, [2/3], 91-100, (1986) (with A.D. Eisner

144 "Prediction and Rational Correlation of Thermophoretically Reduced Particle Mass Transfer to Hot Surfaces Across Laminar or Turbulent Forced-Convection Gas Boundary Layers", *ChE Communications* **44**, 107-119, (June 1986) (with.A. Gokoglu).

146 "Mass Transfer Across Combustion Gas Thermal Boundary Layers — Power Production and Materials Processing Implications", in **Heat Transfer in Fire and Combustion Systems**, HTD 45, ASME, NY, 3-8 (1985)

148 "Nonequilibrium Theory of Surface Deposition from Particle-Laden, Dilute Condensible Vapor-Containing Stream, Allowing for Particle Thermophoresis and Vapor Scavenging within the Laminar Boundary Layer", *Int. J. Multiphase Flow* **14**, [1], 99-120, (1988) (with J.L. Castillo)

152 "Thermophoretic Properties of Nonspherical Particles and Large Molecules, *AIChE J* 35,139-147 (1989) (with P. Garcia-Ybarra)

161 "Combined Inertial and Thermophoretic Effects on Particle Deposition Rates in Highly Loaded Dusty Gas Systems", *Chemical Engrg. Science* **44**,(10),2233-2244,(1989) (with H.M. Park)

173 "Side-Wall Gas 'Creep' and Thermal Stress Convection' in Microgravity Experiments on Film Growth by Vapor Transport", *Physics Fluids A — Fluid Mechanics* **1**,(11),1761-1763,(1989)

176 "Effects of Heat Transfer on the Dynamics and Transport of Small Particles in Gases", **Proc. 9th Int. Heat Transfer Conference** (AIChE, ASME, ANS,...) , Hemisphere Pub. Corp., N.Y.(in press,1990) (with D.W.Mackowski, J.L.Castillo, P.García-Ybarra)